Die Embryonalentwicklung der Paradiesschnecke *Marisa cornuarietis* (Ampullariidae) unter dem Einfluss von Platin

Dissertation
der Mathematisch-Naturwissenschaftlichen Fakultät
der Eberhard Karls Universität Tübingen
zur Erlangung des Grades eines
Doktors der Naturwissenschaften
(Dr. rer. nat.)

vorgelegt von
Leonie Hannig geb. Marschner
aus Neuwied

Tübingen
2013

Tag der mündlichen Qualifikation:	17.12.2013
Dekan:	Prof. Dr. Wolfgang Rosenstiel
1. Berichterstatter:	Prof. Dr. Heinz-R. Köhler
2. Berichterstatter:	Prof. Dr. James Nebelsick

Inhaltsverzeichnis

Zusammenfassung

Hintergrund und Zielsetzung der Arbeit

Es existieren vielfältige technische Einsatzmöglichkeiten für Schwermetalle und viele davon führen zu einer Emission dieser Stoffe in die Umwelt: Korrosion in Trinkwasserleitungen führt zu einem Eintrag von Kupfer in Oberflächengewässer, Waschmittel enthalten unter anderem Zink und Blei, die über das Abwasser ebenfalls in Oberflächengewässer gelangen können und aus Bremsbelägen von Kraftfahrzeugen werden beim Bremsvorgang Kupfer, Zink, Blei, Chrom und Nickel in die Atmosphäre freigesetzt (Sörme und Lagerkvist, 2001). Eine andere Gruppe von Schwermetallen, die von Kraftfahrzeugen emittiert werden, sind die Platingruppenelemente (PGEs). Platin, Palladium und Rhodium werden in Autokatalysatoren eingesetzt und ihre Konzentration in der Umwelt ist seit Einführung der Katalysatortechnik beträchtlich angestiegen (Ek *et al.*, 2004). Die PGEs werden hierbei an Nanopartikel gebunden emittiert und zusammen mit den Autoabgasen an die Umgebungsluft abgegeben.

In die Luft freigesetzte Metalle können über weite Strecken in der Atmosphäre verteilt und transportiert werden (Marx und McGowan, 2010; Steinnes *et al.*, 1989). Trockene und feuchte Deposition führt zu einer Akkumulation der Schwermetalle in Gewässern und Böden. In schwermetallbelasteten Gebieten kann auch eine Anreicherung in Tieren und Pflanzen festgestellt werden (Kumar *et al.*, 2012; Nummelin *et al.*, 2007). In Gewässern reichern sich vielfach die Schwermetalle in Sedimenten an. Müller *et al.* (1977) beobachteten eine solche Anreicherung für Quecksilber, Kupfer, Zink, Chrom, Cobalt, Nickel, Blei und Cadmium in Sedimenten des Bodensees. Auch in aquatischen Organismen findet eine Akkumulation von Schwermetallen statt: Karibische Korallen reichern Schwermetalle aus Bootsanstrichen und Abwäs-

sern an (Berry *et al.*, 2013) und Schwermetalle aus der Goldgewinnung können in malaiischen Schnecken in für den Menschen nach Konsum dieser Tiere gesundheitlich bedenklichen Konzentrationen gefunden werden (Lau *et al.*, 1998).

Die direkten Wirkungen auf Organismen sind die am besten untersuchten Auswirkungen von Schwermetallen (Boyd, 2010). Schwermetalle sind an der Entstehung von Tumoren beteiligt (Snow, 1992) und können die Embryonalentwicklung von Organsimen stören. Bereits 1937 beschrieb Waterman eine Verlangsamung der Embryonalentwicklung von Seeigeln durch Nickelchlorid. Während der Embryonalentwicklung von Fischen kann Schwermetallbelastung zu Fehlbildungen und zum Absterben des Embryos führen (Hanna *et al.*, 1997). Ähnliche Wirkungen wurden auch bei Gastropoden beobachtet: Cadmium führt bei *Lymnaea stagnalis* zu verlangsamter Entwicklung und erhöhter Mortalität von Embryonen (Gomot, 1998) und bei der Paradiesschnecke *Marisa cornuarietis* konnten embryotoxische Wirkungen für verschiedene Schwermetalle nachgewiesen werden (Sawasdee und Köhler, 2009; 2010).

Wie für andere Schwermetalle konnte auch für die Platingruppenelemente eine Akkumulation in Tieren und Pflanzen beobachtet werden (Turner und Price, 2008). Um die Toxizität des Schwermetalls Platin genauer zu untersuchen, wurden Toxizitätstests mit der Paradiesschnecke *Marisa cornuarietis* durchgeführt (Osterauer *et al.*, 2009; 2010a; 2011). Während dieser Untersuchungen wurde beobachtet, dass die Exposition von *Marisa cornuarietis*-Embryonen gegenüber hohen Konzentrationen von Platin zu einem Ausbleiben der Bildung einer externen Schale und zu einer Umgestaltung des äußeren Erscheinungsbildes des Visceropalliums führt (Osterauer *et al.*, 2010b). Zwei Individuen von *M. cornuarietis* mit dieser Umgestaltung sind in Abb. 1 zu sehen (normal entwickelte Individuen sind weiter unten gezeigt). Ziel dieser Arbeit war es, dieses Platin^{2+}-induzierte Tiermodell zu verwenden, um die Torsion der Gastropoden zu untersuchen. Als Torsion wird eine während der Embryonalentwicklung aller Schnecken auftretende horizontale Rotation des Eingeweidesacks relativ zu Kopf und Fuß um 180° bezeichnet (Bieler, 1992), und es ist diese Rotation, die Schnecken von anderen Mollus-

ken unterscheidet (Ponder und Lindberg, 1997). Diese horizontale Rotation des Visceropalliums wird für verschiedene morphologische Eigenschaften der Schnecken verantwortlich gemacht: Sie soll die Ursache für die Positionierung von Mantelhöhle mit Kiemen und Anus vorne über dem Kopf und für die Überkreuzung der Pleurovisceralkonnektive sein (Streptoneurie oder Chiastoneurie, Abb. 2A) (Bieler, 1992; Haszprunar, 1988; Page, 2006; Raven, 1966). Die Torsion wurde häufig als zweiphasiger Prozess beschrieben, bei dem zunächst larvale Retraktormuskeln zu einer 90° Drehung führen und die weitere Rotation durch differentielles Wachstum ausgelöst wird (Haszprunar, 1988). Im Gegensatz dazu beobachteten Demian und Yousif (1973b) bei *Marisa*, dass die Torsion bei dieser Art ausschließlich von differentiellem Wachstum der beiden Seiten des Visceropalliums verursacht wird, bei dem das Gewebe der linken Seite des Eingeweidesacks den Eingeweidesack überwächst und hierbei den Mantel bildet, der die äußere Schale sekretiert. Auch Ergebnisse von Kurita und Wada (2011) deuten darauf hin, dass tatsächlich differentielles Wachstum die treibende Kraft hinter der Torsion der Gastropoden ist, eine Ansicht, die auch von Haszprunar (1988) geäußert wurde.

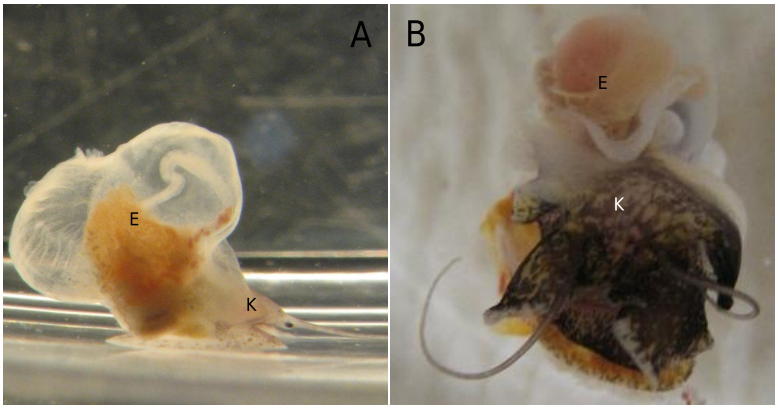

Abb. 1: Zwei Individuen von *M. cornuarietis*, bei denen die Bildung einer externen Schale durch Platin^{2+} verhindert wurde; A: ca. 5 Wochen nach der Eiablage; B: ca. 4 Monate alt; E, Eingeweidesack; K, Kopf

Gemäß der Haeckelschen Theorie der Rekapitulation phylogenetischer Prozesse durch die Ontogenie von Organismen stand am Anfang der Gastro-

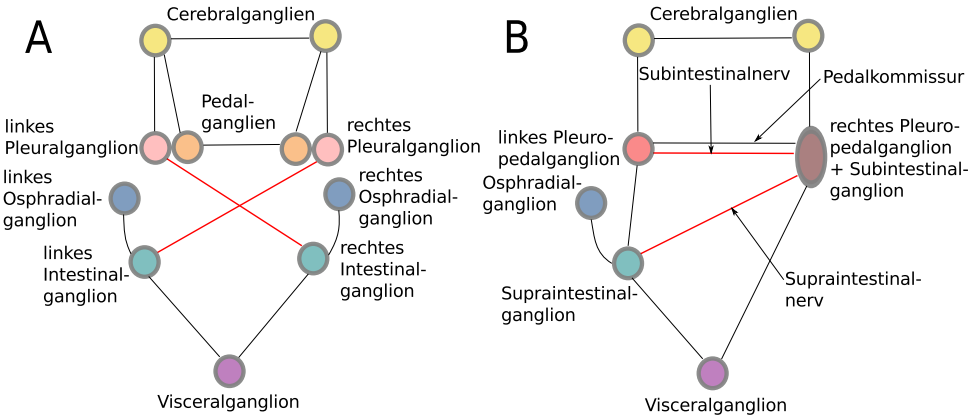

Abb. 2: Schematische Darstellungen der Nervensysteme von zwei Gastropodentaxa; A: Nervensystem der Vetigastropoda mit klassischer Streptoneurie (nach Haszprunar, 1988, verändert); B: Nervenystem der Ampullariidae mit Modifikationen (nach Demian und Yousif, 1975, verändert); die Pleurovisceralkonnektive sind rot eingefärbt

podenentwicklung ein sogenannter hypothetischer Ur-Mollusk, dessen Mantelhöhle, Anus und Kiemen am posterioren Körperende lagen und dessen Pleurovisceralkonnektive nicht überkreuzt waren (Page, 2006; Yonge, 1947). Aus diesem Ur-Mollusken haben sich nach der Theorie durch die Etablierung der Torsion Gastropoden entwickelt (Raven, 1966). Das Nervensystem von *Marisa* zeigt die für Schnecken typische Streptoneurie, jedoch mit einigen für die Ampullariidae spezifischen Modifikationen (Abb. 2B): Pleural- und Pedalganglien liegen dicht beieinander und verschmelzen zum Pleuropedalganglion (hypoathroides Nervensystem, Haszprunar, 1988), zusätzlich verschmilzt das Subintestinalganglion mit dem rechten Pleuropedalganglion (Demian und Yousif, 1975). Vor diesem Hintergrund wurden folgende zu testende Hypothesen formuliert:

1 Da bei gegenüber Platin^{2+} exponierten *M. cornuarietis*-Embryonen die während der normalen Embryonalentwicklung stattfindende Torsion unterbunden wird (Demian und Yousif, 1973b), zeigen die gegenüber Platin^{2+} exponierten Individuen keine der auf die Torsion zurückzuführenden morphologischen Merkmale.

2 Da bei gegenüber Platin^{2+} exponierten *M. cornuarietis*-Embryonen das differentielle Wachstum des schalenbildenden Gewebes und somit auch

die Bildung einer externen Schale unterbleibt, scheidet das schalenbildende Gewebe an einer anderen Position am Schneckenkörper Calciumcarbonat ab und es bildet sich eine andere Art der Schale.

Um auch die Frage zu beantworten, ob die Wirkung von Platin auf die Schalenbildung spezifisch für die Paradiesschnecke ist, wurden zusätzlich Embryotests mit der Posthornschnecke *Planorbarius corneus* durchgeführt.

Material und Methoden

Die Testorganismen *Marisa cornuarietis* und *Planorbarius corneus*

Die in dieser Arbeit untersuchten Arten *Marisa cornuarietis* und *Planorbarius corneus* sind in Abb. 3 dargestellt.

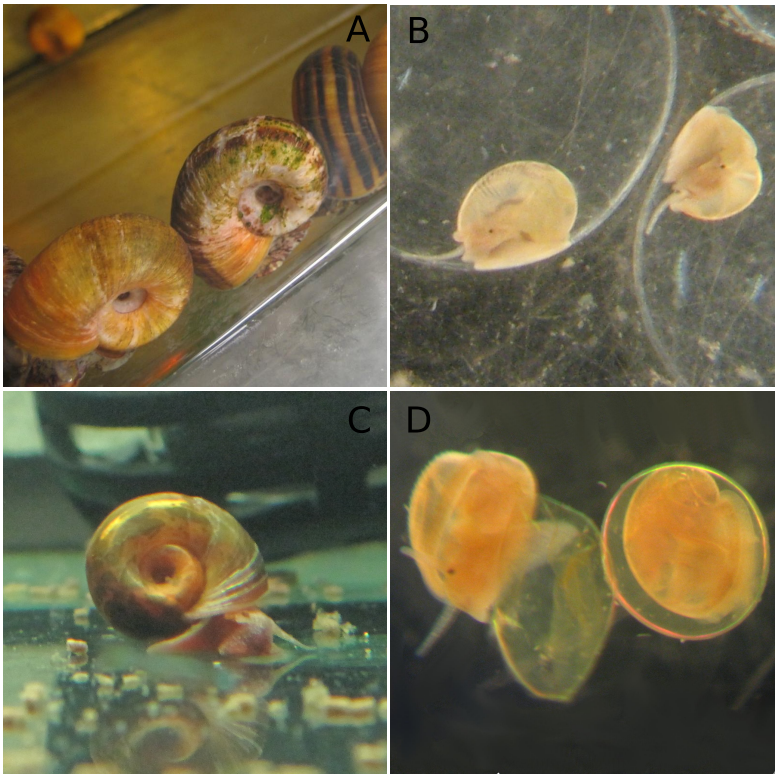

Fig. 3: Testorganismen *Marisa cornuarietis* und *Planorbarius corneus*; A: Adulte *Marisa cornuarietis* im Zuchtbecken; B: *Marisa cornuarietis*-Embryonen; C: Adulte *Planorbarius corneus*; D: *Planorbarius corneus*-Embryo in der Eihülle und geschlüpfte Jungschnecke

Marisa cornuarietis Systematische Einordnung von *Marisa cornuarietis* nach Bouchet und Rocroi (2005):

Stamm Mollusca
Klasse Gastropoda
Klade Caenogastropoda
Informelle Gruppe Architaenioglossa
Überfamilie Ampullarioidea
Familie Ampullariidae
Gattung *Marisa*
Art *M. cornuarietis* (Linné, 1758)

Die Paradiesschnecke *Marisa cornuarietis* ist eine getrenntgeschlechtliche, tropische Süßwasserschnecke mit planspiralem Gehäuse. Ihre Gelege heftet sie in Form von gelatinösen Eimassen von jeweils 20-80 Eiern unterhalb der Wasserlinie an Objekte an (Dillon, 2000; Schirling *et al.*, 2006). Die Embryonen entwickeln sich in ca 110 μm großen, zu Anfang undurchsichtigen Eiern, die später aufklaren (Demian und Yousif, 1973b). In Abhängigkeit von der Temperatur entwickeln die Embryonen sich innerhalb von 8 Tagen (25-30 °C) bis 18 Tagen (15-20 °C) bis zum Schlupf (Demian und Yousif, 1973b). *Marisa* gehört zu den prosobranchen Schnecken, deren Kiemen und Anus beide vor dem Herzen liegen. Zusätzlich besitzt die Paradiesschnecke auch eine Lunge, die sich kurz vor dem Schlupf aus dem Gewebe, das die Mantelhöhle auskleidet, bildet (Demian und Yousif, 1973d).

Hälterung Der ursprüngliche Zuchtansatz von *M. cornuarietis* entstammte der Zucht der Abteilung Aquatische Ökotoxikologie der Universität Frankfurt. Die Tiere wurden in Tübingen zunächst in vier 90 Liter Aquarien und einem 185 Liter Aquarium, später in 5 90 Liter Aquarien und zwei 185 Liter Aquarien gehalten. Die Becken wurden mit Leitungswasser, das ab Sommer 2012 mit einem Ionenfilter gefiltert wurde, gefüllt. Der Wasserwechsel fand einmal pro Woche statt, wobei stets die Hälfte des Wassers ausgetauscht wurde. Die Temperatur variierte zwischen 24 und 27 °C und der pH-Wert

zwischen 7 und 8. Die Leitfähigkeit wurde durch wöchentliche Zugabe von NaCl auf 800-1000 μS/cm eingestellt, die Carbonathärte lag zwischen 1 und 8° dH und wurde durch gelegentliche Zugabe von $CaCO_3$ reguliert. Der Hell-Dunkel-Rhythmus wurde auf 12:12 Stunden festgesetzt. Das Wasser in den Becken wurde kontinuierlich mit einem Außenfilter und später mit Filtermatten gereinigt und durch Ausströmsteine belüftet. Gefüttert wurde täglich einmal Fischfutter (Nutrafin MAX Hauptfutter, Hagen, Deutschland) und gelegentlich erhielten die Schnecken Karotten aus biologischem Anbau.

Planorbarius corneus Systematische Einordnung von *Planorbarius corneus* nach Bouchet und Rocroi (2005):

Stamm Mollusca
Klasse Gastropoda
Klade Heterobranchia
Informelle Gruppe Pulmonata
Überfamilie Planorboidea
Familie Planorbidae
Gattung *Planorbarius*
Art *P. corneus* (Linné, 1758)

Die Posthornschnecke gehört zu den aquatischen Lungenschnecken der Familie Planorbidae und kommt sehr häufig in Zentraleuropa vor (Jopp, 2006). Die Planorbidae heben sich von anderen Schnecken durch den Besitz von Hämoglobin ab, das ihr Blut rot erscheinen lässt (Engelhardt, 2008). Posthornschnecken sind Hermaphroditen und ernähren sich sapro- und phytophag. Typisch sind sie für Gewässer mit eher schwacher Strömung und mit einer dicken Schicht abgestorbenen biologischen Materials auf dem Grund, auf dem sie sich vorzugsweise aufhalten (Dillon, 2000; Engelhardt, 2008). Die befruchteten Eier sind gelblich gefärbt und klar. Sie werden in Form einer zähen, flachen und ovalen Masse abgegeben und an feste Objekte in Nähe der Wasseroberfläche geheftet, wobei die Eiablage eher nachts stattfindet (Dillon, 2000).

Hälterung Die Schnecken stammten aus einem Tümpel auf dem Spitzberg bei Tübingen und wurden in einer Klimakammer bei 20 °C in einem 30 Liter Aquarium gehalten. Gefüttert wurde Fischfutter (Nutrafin MAX Hauptfutter, Hagen, Deutschland) und gelegentlich frischer Salat oder frische Karotten aus biologischem Anbau. Das Aquarium wurde wöchentlich mit einem Schwamm gereinigt, wobei die Hälfte des Wassers mit abgestandenem Leitungswasser ausgetauscht wurde. Das Wasser wurde zusätzlich kontinuierlich durch einen Außenfilter gereinigt und belüftet.

Die Testsubstanz Platinchlorid

Verwendet wurde der Platinstandard von Ultra Scientific mit einer Konzentration von 1000 μg/L in einer Matrix von 98% Wasser und 2% HCl. Platin(II)Chlorid ist ein grau-grünes bis braunes Puder, unlöslich in Wasser, Alkohol und Ether, aber löslich in HCl (Perry, 1995). Platinsalze können Allergien auslösen (Migliore *et al.*, 2002).

Angewendete Techniken

Der Embryotest mit *Marisa cornuarietis* und *Planorbarius corneus* Die Embryotests mit *Marisa cornuarietis* wurden basierend auf dem von Schirling *et al.* (2006) entwickelten Protokoll durchgeführt und für die jeweiligen Fragestellungen angepasst. Am Tag vor dem Ansatz eines Versuchs wurden sämtliche Gelege aus den Aquarien entfernt. Am Tag des Versuchs wurden dann so viele frische Gelege entnommen, wie für die jeweiligen Experimente benötigt wurden. Die einzelnen Eier wurden mit einer Rasierklinge voneinander getrennt und je nach Fragestellung entweder nach Gelegen getrennt oder gemischt zu je 20-30 Eiern in Plastikpetrischalen gegeben. Die Plastikpetrischalen wurden mit der Testlösung bestehend aus einem Liter Aquarienwasser mit 200 μL Platinchloridstandard oder mit reinem Aquarienwasser als Kontrollmedium gefüllt. Die Petrischalen wurden in einem Wärmeschrank bei 26 °C und einem Hell-Dunkel-Rhythmus von 12:12 Stunden inkubiert und die Testlösungen wurden täglich gewechselt. Bei den Embryotests mit *Marisa* dauerte die Exposition 9 Tage. Die Tests mit *Planorbarius* dauerten 14 Tage

und wurden bei 20 °C durchgeführt. Da bei *P. corneus* nur wenige Gelege gewonnen werden konnten, wurden nur wenige Replikate mit unterschiedlich vielen Eiern angesetzt. Die Auswertung fand in den folgenden Tagen statt, wobei für *P. corneus* nur das Merkmal Schalenbildung ausgewertet wurde.

Diese Vorgehensweise wurde auch genutzt, um Embryonen für weitere Untersuchungen zu gewinnen, wobei die Embryonen in Abhängigkeit von der jeweiligen Fragestellung zu bestimmten Zeiten aus den Eiern entnommen oder die Eier bei höheren Temperaturen inkubiert wurden.

Rasterelektronenmikroskopie Zu den jeweils geplanten Zeitpunkten wurden die Embryonen mit zwei Kanülen aus den Eihüllen entfernt und in zweiprozentiger Glutardialdehydlösung (gelöst in 0.01 M Cacodylat-Puffer) fixiert. Die Embryonen wurden dann in Cacodylat-Puffer gespült, über Nacht in einprozentiger reduzierter Osmiumtetroxidlösung fixiert und in einer aufsteigenden Alkoholreihe entwässert. Die Schneckenembryonen wurden dann Kritisch-Punkt-getrocknet, auf Objekttische aufgeklebt und mit Gold besputtert. Die Untersuchung erfolgte in der Abteilung Evolutionsökologie der Invertebraten, Universität Tübingen (Prof. Dr. O. Betz) mit einem Rasterelektronenmikroskop.

Histologie Für die histologischen Untersuchungen der Embryonen wurden diese mit zwei Kanülen entnommen und in Bouin's Lösung oder in einer zweiprozentigen Glutardialdehydlösung (gelöst in 0.01 M Cacodylat-Puffer) fixiert. Danach wurden sie entweder in 70%igem Ethanol gewaschen und in einer aufsteigenden Ethanolreihe entwässert oder in Phosphatpuffer gespült und dann in der Ethanolreihe entwässert. Die Embryonen wurden in Technovit eingebettet, und es wurden Serienschnitte mit einem Mikrotom von 2-5 μm Dicke angefertigt. Die Schnitte wurden gefärbt (Hämatoxylin/Eosin-Färbung, Methylenblau-Färbung oder für Technovit angepasste Dreifachfärbung nach Mallory (Cason, 1950)) und mikroskopisch ausgewertet.

Für die histologischen Untersuchungen von adulten *Marisa cornuarietis* wurden Embryonen neun Tagen lang gegenüber Platin exponiert und dann in Aquarienwasser transferiert und aufgezogen. Zusätzlich wurden Kontrol-

lindividuen aufgezogen. Die adulten Schnecken wurden dann in einer zweiprozentigen Glutardialdehydlösung (gelöst in 0.01 M Cacodylat-Puffer) fixiert, in Cacodylat-Puffer gespült und in einem Ethanol-Ameisensäuregemisch entkalkt. Nach der Entwässerung in Ethanol wurden die Schnecken in Paraffin eingebettet. Mit einem Mikrotom (Leica SM 2000R) wurden Serienschnitte mit einer Dicke von 5 μm angefertigt und nach Cason (1950) gefärbt.

Immunhistochemie Die Embryonen wurden mit zwei Kanülen aus den Eihüllen entfernt und mit Eppendorf-Pipetten in kleine Glaspetrischalen mit Mineralwasser (Römerquelle medium, Göppingen, Deutschland) gegeben. Nach 10-15 Minuten wurden sie in Eppendorfgefäße mit 4% Paraformaldehyd mit 0,1% Triton X transferiert. Die Embryonen wurden über Nacht bei 6 °C fixiert und am nächsten Tag in Phosphatpuffer mit 0,1% Natriumazid gespült und 4 Stunden bei 6 °C im Blockierpuffer inkubiert. Die folgende Inkubation mit dem ersten Antikörper (rabbit-anti-Serotonin, 1:200) dauerte 48, 72 oder 96 Stunden und wurde ebenfalls bei 6 °C durchgeführt. Danach wurden die Proben in Phosphatpuffer mit 0,1% Natriumazid gespült und über 48, 72 oder 96 Stunden bei 6 °C mit dem zweiten Antikörper inkubiert (Alexa 488-konjugierter goat-anti-rabbit, IgG, 1:200). Dieser Schritt fand wie alle folgenden Schritte im Dunkeln statt, um ein Ausbleichen des an den zweiten Antikörper konjugierten Fluoreszenzfarbstoffs Alexa 488 zu verhindern. Nach der Inkubation mit dem zweiten Antikörper wurden die Embryonen in Phosphatpuffer gespült und in einer Clearinglösung (Sca*l*eB4, Hama *et al.*, 2011) transparent gemacht. Dies fand bei Raumtemperatur statt. Die Embryonen wurden mit einem confokalen Laserscanningmikroskop untersucht und die gewonnenen Daten wurden mit FIJI-ImageJ visualisiert und analysiert.

3D-Rekonstruktionen Für die Rekonstruktionen wurden die Schnitte der adulten Schnecken fotografiert und mit dem 3D-Rekonstruktionsprogramm Amira (Visage Imaging) ausgewertet. Es wurden 3D-Modelle generiert. Da kleine und dünne Strukturen bei Computermodellierungen verloren gehen können, wurden die Modelle mit den Originalschnitten verglichen und in den Schnitten präsente, jedoch in den Modellen fehlende Strukturen wurden per

Hand im Vektorgrafikprogramm Inkscape ergänzt. Für die Erstellung von 3D-Modellen des Nervensystems der Embryonen wurden die bei der Untersuchung entstandenden Daten in Amira geladen und die Modelle berechnet und gegebenenfalls manuell nachbearbeitet.

Stressproteinanalyse Die Embryonen wurden mit zwei Kanülen aus den Eihüllen entfernt und mit einer gewichtsspezifischen Menge Extraktionspuffer mit Ultraschall auf Eis homogenisiert und für 10 Minuten bei 20000g bei 4 °C abzentrifugiert. Die Gesamtproteinmenge wurde nach Bradford (1976) ermittelt und konstante Proteinmengen von 40 μg wurden mittels SDS-PAGE aufgetrennt und anschließend über Semi-dry Elektrotransfer auf Nitrocellulosemembranen übertragen. Die Nitrocellulosemembranen wurden zunächst mit einem ersten Antikörper gegen Hsp70 (monoklonaler Maus anti-human Hsp70 Antikörper) und dann mit einem zweiten, an Peroxidase konjugierten, Antikörper (Ziege anti-Maus IgG) inkubiert. Nach erfolgter Peroxidasefarbreaktion wurden die Banden densitometrisch ausgewertet.

Ergebnisse

Kapitel 1: Osterauer, R., Marschner, L., Betz, O., Gerberding, M., Sawasdee, B., Cloetens, P., Haus, N., Sures, B., Triebskorn, R., Köhler, H.-R., 2010. Turning snails into slugs: induced body plan changes and formation of an internal shell. *Evol. Dev.* 12, 474–483

Die Studie konnte zeigen, dass die Exposition von *Marisa cornuarietis* Embryonen gegenüber Platin^{2+} (200 μg/L $PtCl_2$) während ihrer Entwicklung zu einem zuverlässig reproduzierbaren Ausbleiben der Bildung einer äußeren Schale bei allen überlebenden Embryonen führt. Die exponierten Schnecken besitzen einen nackten Eingeweidesack und die Kiemen sind posterior vom Herzen auf dem Eingeweidesack positioniert. Anhand von Pulsexpositionen gegenüber Platin^{2+} wurde gezeigt, dass der für eine platininduzierte Fehlbildung empfindliche Zeitraum an den Tagen 4 und 5 der Embryonalentwick-

lung von *Marisa cornuarietis* liegt. Obwohl die meisten Experimente mit Aquarienwasser durchgeführt wurden, konnte die durch $Platin^{2+}$ ausgelöste „Schalenlosigkeit“ auch in eigens entwickeltem Kunstwasser zuverlässig induziert werden. Eine Kombination von $Platin^{2+}$ und äquimolaren $Calcium^{2+}$-Ionen in Form einer Zugabe von Calciumcarbonat zum Testmedium konnte jedoch die Häufigkeit „schalenloser“ Schnecken reduzieren und im Gegensatz zu niedrigeren Platinkonzentrationen die Bildung externer „Teilschalen“ induzieren. Die inhibierende Wirkung von $Platin^{2+}$ auf die Schalenbildung konnte auch bei der Lungenschnecke *Planorbarius corneus* beobachtet werden. Bei dieser Art führte die Exposition gegenüber 300, 400 und 500 μg/L $PtCl_2$ zu einem Ausbleiben der Bildung einer äußeren Schale. Bei *Planorbarius* blieb ebenfalls der Eingeweidesack nackt. Die Ergebnisse der rasterelektronenmikroskopischen Untersuchungen werden im Zusammenhang mit Kapitel 2 vorgestellt.

Kapitel 2: Marschner, L., Triebskorn, R., Köhler, H.-R., 2012. Arresting mantle formation and redirecting embryonic shell gland tissue by platinum^{2+} leads to body plan modifications in *Marisa cornuarietis* (Gastropoda, Ampullariidae). *J. Morphol.* 273, 830–841

Das Ziel dieser Arbeit war der Vergleich der Embryonalentwicklung von Individuen unter Kontrollbedingungen und gegenüber $Platin^{2+}$ exponierten Schnecken. Hierzu wurden rasterelektronenmikroskopische und histologische Untersuchungen von verschiedenen Entwicklungsstadien durchgeführt. Die gegenüber $Platin^{2+}$ exponierten Embryonen entwickeln sich zwar langsamer als die Kontrollen, sie durchlaufen aber die gleichen Entwicklungsstadien, bis sie in einem Alter von 4 Tagen Stadium VI (nach Demian und Yousif, 1973b) erreichen. Dieses Entwicklungsstadium ist dadurch gekennzeichnet, dass die linke Seite des Eingeweidesacks von Mantel, Schalendrüse und Mantelrand bedeckt ist. Im Folgenden wachsen diese Gewebe während der normalen Entwicklung über den Eingeweidesack in Richtung des Kopfes, wobei der gesamte Eingeweidesack mit Mantel und Schale bedeckt wird. Da das Gewebe auf der

rechen Seite des Eingeweidesacks weniger stark wächst, kommt es bei diesem Prozess zu einer horizontalen Drehung des Eingeweidesacks um ca. 180° und das Gewebe auf der rechten Seite des Eingeweidesacks wird in die entstehende Mantelhöhle eingefaltet.
Bei gegenüber $Platin^{2+}$ exponierten Embryonen wird zwar auch die linke Seite des Eingeweidesacks von dem Komplex aus Mantel, Schalendrüse und Mantelrand bedeckt (Stadium VI), es kommt aber nicht zu einer horizontalen Drehung des Eingeweidesacks, da in den erwähnten Geweben eine Proliferation der Zellen unterdrückt wird. Während sich die Embryonen der Kontrolle wie von Demian und Yousif (1973b) beschrieben entwickeln, findet in den gegenüber Platin exponierten Schneckenembryonen eine vertikale Rotation des Eingeweidesacks statt, durch die der Komplex aus Mantel, Schalendrüse und Mantelrand auf der ventralen Seite des Eingeweidesacks zu liegen kommt. Kopf und Fuß der exponierten Embryonen entwickeln sich wie bei Kontrollen, jedoch durch die Schwermetallbelastung bedingt langsamer als unter Kontrollbedingungen. Trotz ihrer veränderten Lage sekretieren Mantel und Schalendrüse Calciumcarbonat und es kommt zur Bildung einer internen Schale. Die Kiemen werden in den sich entwickelnden Embryonen auf der rechten dorso-lateralen Seite des Eingeweidesacks angelegt und bei Individuen unter Kontrollbedingungn im Zuge der horizontalen Rotation des Eingeweidesacks nach craniad verlagert und zusammen mit dem Gewebe auf der rechten Seite des Eingeweidesacks in die Mantelhöhle eingefaltet. Bei gegenüber $Platin^{2+}$ exponierten Embryonen verbleiben die Kiemen zunächst auf der rechten dorso-lateralen Eingeweidesackseite, bevor sie im Zuge der vertikalen Rotation auf die linke dorso-laterale Seite verlagert werden. Die rasterelektronenmikroskopischen und histologischen Untersuchungen zeigten, dass sich trotz des Ausbleibens der horizontalen Drehung des Eingeweidesacks Darm und Anus genauso entwickeln wie bei Individuen unter Kontrollbedingungen.

Kapitel 3: Marschner, L., Staniek, J., Schuster, S., Triebskorn, R., Köhler, H.- R., 2013. External and internal shell formation in the ramshorn snail *Marisa cornuarietis* are extremes in a continuum of gradual variation in development. *BMC Dev. Biol.* 13, 22.

Im Zuge dieser Studie wurden Embryonen gegenüber $Platin^{2+}$ und leicht erhöhten Temperaturen exponiert und in einem Zeitraum zwischen 3 und 17 Tagen nach der Eiablage untersucht. Eine Erhöhung der Temperatur während der Platinexposition um $2 - 4\,°C$ führt zu einer sehr hohen morphologischen Variation innerhalb der exponierten Individuengruppe: Normal entwickelte Schnecken, Individuen mit interner Schale und Tiere mit „Teilschalen“, bei denen unterschiedlich große Teile des Eingeweidesacks von dieser Schale bedeckt sind, während ein Teil des oberen Eingeweidesacks nackt bleibt, treten unter diesen Bedingungen parallel auf. Die Embryonalentwicklung dieser Schnecken mit „Teilschalen“ wurde rasterelektronenmikroskopisch und histologisch untersucht und mit der Entwicklung von Kontrollen und bei $26\,°C$ gegenüber $Platin^{2+}$ exponierten Embryonen mit interner Schalenbildung verglichen. Zusätzlich wurden histologische Schnitte von adulten Individuen, die sich unter Kontrollbedingungen entwickelt hatten, und exponierten Schnecken mit „Teilschalen“ angefertigt.

Die genaueren Untersuchungen der Entwicklung von Mantel, Schalendrüse und Mantelrand in gegenüber $Platin^{2+}$ exponierten Embryonen zeigten, dass zwar Schalendrüse und Mantelrand nach Erreichen von Stadium VI nicht mehr wachsen, das Mantelgewebe jedoch weiter proliferiert. Da ein Überwachsen des Eingeweidesacks durch den Mantel durch den starren Ring aus Schalendrüse und Mantelrand blockiert wird, wächst das Mantelgewebe in das Innere der Schnecke und legt sich um die Mitteldarmdrüse, wobei eine Lücke („Mantellücke“) zwischen dem inneren Teil des Mantelgewebes und dem äußeren Teil („Mantelfalte“) entsteht. Zwischen diesen beiden Teilen des Mantelgewebes liegt die innere Schale, die aus vom Mantel und der Schalendrüse abgegebenen Schalenmaterial besteht.

Bei gegenüber $Platin^{2+}$ und bei erhöhter Temperatur exponierten Embryonen kommt es zunächst ebenfalls zu einer vertikalen Rotation des Ein-

geweidesacks, durch die der schalenbildende Komplex auf die Unterseite des Eingeweidesacks gelangt. Auch bei diesen Embryonen wächst das Mantelgewebe weiter, während Schalendrüse und Mantelrand nicht mehr proliferieren. Dieser Wachstumsstop ist jedoch nur temporär, wobei seine Dauer variabel ist. Nach dieser Phase der Inaktivität beginnt das Wachstum von Schalendrüse und Mantelrand erneut, und das Mantelgewebe wächst von ventral nach dorsal über den Eingeweidesack. Durch histologische Schnitte konnte nachgewiesen werden, dass in Abhängigkeit von der Dauer des Wachsstumsstopps ein Teil des Mantelgewebes ins Innere der Schnecke verlagert wird und eine „Mantellücke“ und eine „Mantelfalte“ entstehen. Nach dem Wiederbeginn des Wachstums von Schalendrüse und Mantelrand werden „Mantellücke“ und „Mantelfalte“ im Zuge des Auswachsens des Mantels über den Eingeweidesack in Richtung Kopf geschoben, wobei es zu einer leichten Windung der „Teilschale“ kommt. Die resultierenden Schnecken haben eine teils interne, von der „Mantelfalte“ bedeckte, und eine teils externe Schale. Die Schalendrüse der gegenüber Platin^{2+} bzw. der gegenüber Platin^{2+} und erhöhten Temperaturen exponierten Schnecken liegt auf der Innenseite der „Mantelfalte“ und zeigt daher nach innen und nicht nach außen wie bei unter Kontrollbedingungen aufgezogenen Individuen.

Kapitel 4: Hannig, L., Schwarz, S., Köhler, H.-R. No torsion required for streptoneury in the ampullariid snail *Marisa cornuarietis*. Wird eingereicht bei PNAS

In dieser Studie wurde das Nervensystem von gegenüber Platin^{2+} exponierten *Marisa cornuarietis* mit dem von nicht exponierten Kontrollen verglichen. Die Untersuchung der adulten, mehrere Wochen alten Schnecken, welche gegenüber Platin^{2+} exponiert wurden, zeigte, dass das Nervensystem dieser Individuen trotz des Ausbleibens einer horizontalen Rotation des Eingeweidesacks (Torsion) denselben Aufbau zeigt wie in Kontrollen und dass auch eine Überkreuzung der Pleurovisceralkonnektive (Streptoneurie, Chiastoneurie) vorhanden ist. Dreidimensionale Modelle dieser Individuen zeigen auch, dass die Abwesenheit einer externen Schale zu einem unkontrollierten

Wachstum des Columellamuskels führt, was wiederum starke Verformungen der inneren Organe, insbesondere des Odontophors und des Nervensystems, verursacht.

Immunhistochemische Untersuchungen von unter Kontrollbedingungen gehaltenen Embryonen zeigen deutlich die von Demian and Yousif (1975) beschriebene Struktur des Nervensystems von *Marisa cornuarietis*. Die 3D-Modelle des Nervensystems der gegenüber Platin^{2+} exponierten Embryonen zeigen ansatzweise ebenfalls einen ähnlichen Aufbau wie bei den Kontrollen.

Kapitel 5: Hannig, L., Köhler, HR. Quantifikation der Hsp70-Level von bei unter Normalbedingungen gehaltenen sowie gegenüber Platin^{2+} exponierten Embryonen von *Marisa cornuarietis* bei 26 °C und 29 °C. Unveröffentlichte Daten

Stressproteine werden durch proteotoxischen Stress, wie z.B. erhöhte Temperaturen, induziert und sind dafür bekannt, dass sie Signaltransduktionswege während der Embryonalentwicklung stabilisieren können. In diesem Versuch wurde getestet, ob die Exposition von *M. cornuarietis*-Embryonen gegenüber Platin^{2+} bei gleichzeitiger leichter Erhöhung der Temperatur zu einer solchen Stabilisierung der Embryonalentwicklung führen kann und ob eine temperaturinduzierte Erhöhung des Hsp-Levels die Wirkung, die Platin^{2+} unter Normalbedingungen hat, ausgleichen kann. Quantitative Untersuchungen des Hsp70-Levels ermittelten den höchsten Gehalt, der in dieser Studie nachgewiesen wurde, für die bei 26 °C (Kontrolltemperatur) gegenüber Platin^{2+} exponierten Embryonen und den zweithöchsten Gehalt für die Kontrollen bei 29 °C. Die Embryonen aus der Kontrolle bei 26 °C zeigten einen wesentlich niedrigeren Hsp70-Level als die beiden anderen Gruppen und der niedrigste Wert trat bei den bei 29 °C gegenüber Platin^{2+} exponierten Embryonen auf. Die Ergebnisse zeigen, dass eine Temperaturerhöhung mit gleichzeitiger Platin^{2+}-Exposition nicht zu einer Überexpression von eventuell protektiv wirkendem Hsp70 führt. Das Auftreten der „Teilschalen“ und die Wiederaufnahme des Wachstums von Mantelrand und Schalendrüse bei erhöhter Temperatur muss also eine andere Ursache haben.

Diskussion

Die im Rahmen dieser Doktorarbeit durchgeführten Untersuchungen zeigten, dass eine Exposition von *Marisa cornuarietis* und *Planorbarius corneus* gegenüber $Platin^{2+}$ während der Embryonalentwicklung zu einem Ausbleiben der Bildung einer externen Schale führt. Dass diese morphologische Umgestaltung in zwei verschiedenen Schneckenarten, die phylogenetisch weit voneinander entfernten Taxa angehören, ausgelöst werden konnte, zeigt, dass die Wirkung von $Platin^{2+}$ auf die Schalenbildung nicht artspezifisch ist, sondern dass diesem Effekt ein basaler Mechanismus zu Grunde liegen muss.

Für die Paradiesschnecke konnte gezeigt werden, dass $Platin^{2+}$ das differentielle Wachstum von Mantelrand und Schalendrüse inhibiert, während der Mantel selbst weiterwächst. Ohne dieses differentielle Wachstum kommt es nicht zu einer Bildung einer externen Schale und die normalerweise im Alter von 82 h nach der Befruchtung beginnende horizontale Drehung des Eingeweidesacks (ontogenetische Torsion, Demian und Yousif, 1973b) bleibt ebenfalls aus. Statt dieser horizontalen Drehung kommt es zu einer vertikalen Drehung des Eingeweidesacks, durch die der schalenbildende Komplex, bestehend aus Mantel, Mantelrand und Schalendrüse, auf die ventrale Seite des Eingeweidesacks verlagert wird. Hierbei wird Schalenmaterial in das Körperinnere der Schnecke abgegeben und es bildet sich eine interne Schale (Hypothese 2). Obgleich die horizontale Rotation des Eingeweidesacks unter Platineinfluss nicht stattfindet, besitzen die „schalenlosen“ Schnecken ein „normal“ entwickeltes und durch Streptoneurie gekennzeichnetes Nervensystem sowie einen cranial liegenden Anus, die Kiemen jedoch liegen caudal auf dem Eingeweidesack statt vorne über dem Kopf. Versuche mit leicht erhöhter Temperatur konnten zeigen, dass eine Temperaturerhöhung die Wirkung von $Platin^{2+}$ abmildern und das differentielle Wachstum von Schalendrüse und Mantelrand nach einer Phase der Inaktivität wieder einsetzt. Die bei höheren Temperaturen gegenüber Platin exponierten Schnecken besitzen eine Schale, die zum Teil auf dem Mantel liegt und zum Teil vom Mantel bedeckt ist.

Schalenreduktion und -internalisierung wird innerhalb der Mollusken durch verschiedene Mechanismen erreicht: Bei Spezies aus manchen Gruppen (z.B.

Naticidae) entwickelt sich eine externe Schale, die in der weiteren Entwicklung von Mantel und/oder Fußgewebe überwachsen wird (Ponder *et al.*, 2008). Bei pulmonaten Landnacktschnecken hingegen entwickelt sich die interne Schale in einem Schalensack unterhalb der dorsalen Mantelregion (Simpson, 1901; Künkel, 1916). Im Gegensatz zu den gegenüber $Platin^{2+}$ exponierten Schnecken mit internalisierter Schale und Mantel besitzen diese Nacktschnecken jedoch einen externen Mantel.

Es gibt jedoch neben den gegenüber $Platin^{2+}$ exponierten Paradiesschnecken noch weitere Mollusken, bei denen die Schale gleichzeitig auf dem Mantel liegt und von ihm bedeckt wird. Bei rezenten höheren Cephalopoden (Coleoidea) wird Calciumcarbonat sowohl von innen als auch von außen an die interne Schale angelagert und wie in den umgestalteten Paradiesschnecken und den Gastropoden, in denen die Schale vom Mantel überwachsen wird, ist ein Teil des schalenbildenden Gewebes nach innen und nicht nach außen gerichtet (Bandel, 1989).

Die im Rahmen der vorliegenden Doktorarbeit gemachten Beobachtungen zeigen deutlich, dass eine Entwicklung hin zu einer internen Schale nicht graduell erfolgen muss, sondern im Gegenteil hierzu in einem einzigen Schritt passieren und durch einen einzigen Auslöser initiiert werden kann.

Der Mechanismus, über den $Platin^{2+}$ die Bildung einer externen Schale verhindert, ist noch unbekannt, jedoch wurde in den durchgeführten Studien deutlich, dass $Platin^{2+}$ spezifisch nur das differentielle Wachstum von Schalendrüse und Mantelrand inhibiert. Das Mantelgewebe selbst ist von der Wirkung nicht direkt betroffen. Durch die Inhibition des Wachstums der den Mantel umgebenden Gewebe wird dieser jedoch in der Folge der Platinexposition in das Körperinnere der Schnecke verlagert, wo sich die interne Schale bildet.

Ein möglicher Wirkmechanismus, über den $Platin^{2+}$ das Wachstum spezifischer Gewebe hemmen könnte, ist eine Interaktion mit Stressproteinen. Stressproteine werden durch proteotoxischen Stress, wie er z.B. durch Schwermetalle oder Temperaturerhöhung ausgelöst werden kann, induziert (Gupta *et al.*, 2010). Desweiteren haben Stressproteine jedoch auch wichtige Stabilisierungsfunktionen während der Embryonalentwicklung von Organismen (Ru-

therford und Lindquist, 1998; Queitsch *et al.*, 2002). Um zu testen, ob eine temperaturbedingte Induktion des Stressproteins Hsp70 zu den bei höheren Temperaturen beobachteten Individuen mit „Teilschalen"-Bildung führt, wurden die Stressproteingehalte von gegenüber $Platin^{2+}$ exponierten Embryonen bei zwei verschiedenen Temperaturen miteinander verglichen. Diese Untersuchungen zeigten jedoch, dass die Embryonen, die gleichzeitig gegenüber $Platin^{2+}$ und erhöhten Temperaturen exponiert waren und bei denen das Wachstum von Schalendrüse und Mantelrand nur kurz unterbrochen war, den niedrigsten Hsp70-Gehalt aufwiesen und nicht wie erwartet den höchsten. Diese Beobachtungen machen zumindest eine direkte Interaktion zwischen Platin und Hsp70 unwahrscheinlich. Es besteht jedoch die Möglichkeit, dass andere, jedoch in der vorliegenden Arbeit nicht untersuchte, temperaturinduzierte Stressproteine mit Platin interagieren.

Neben Stressproteinen können auch Metallothioneine durch erhöhte Temperaturen induziert werden (Piano *et al.*, 2004; Serafim *et al.*, 2002). Eine Erhöhung des Metallothioneingehalts und damit eine verbesserte Entgiftung des Platins könnte ebenfalls zu der Abschwächung des Platineffekts bei höheren Temperaturen führen. Dieser Theorie steht jedoch entgegen, dass niedrigere Platinkonzentrationen nicht zu einer Ausbildung von „Teilschalen" führen, sondern dass eine Exposition gegenüber verschiedenen Platinkonzentrationen bei der nicht erhöhten Temperatur von 26 °C entweder in einem vollständigen Ausbleiben einer externen Schale oder der Bildung einer vollständig normalen Schale resultiert (Osterauer *et al.*, 2009). Untersuchungen des Metallothioneingehalts in unterschiedlich exponierten Embryonen wurden allerdings noch nicht vorgenommen.

Wachstum von Geweben wird häufig durch Wachstumsfaktoren induziert (Wolpert, 2011). Die Windung der Schneckenschale entsteht durch ein differentielles Wachstum verschiedener Teile des Mantelgewebes (Shimizu *et al.*, 2013). Grande und Patel (2008) beobachteten, dass eine chemische Inhibition des Wachstumsfaktors Nodal, der an der Entwicklung der Chiralität bei Schnecken beteiligt ist, zu einem Verlust der Chiralität und damit auch zu einem Verlust der Schalenwindung führen kann.

Nederbragt *et al.* (2002) untersuchten die Expression der beiden Hox-Gene

engrailed und *dpp-BMP2/4* bei *Patella vulgata* und stellten die Hypothese auf, dass die beiden Gene zusammen eine Kompartimentgrenze zwischen dem schalensekretierenden und dem die Schale umgebenden Gewebe erzeugen. Weitere Untersuchungen der Expression von *dpp-BMP2/4*, das für seine Rolle bei der Festlegung der dorsoventralen Körperachse bei Vertebraten und Insekten bekannt ist (Arendt und Nübler-Jung, 1997), zeigten, dass möglicherweise *dpp-BMP2/4* direkt am differentiellen Wachstum des Mantels beteiligt ist. Shimizu *et al.* (2013) untersuchten die Expression von *dpp-BMP2/4* bei gewundenen und ungewundenen Mollusken und beobachteten einen asymmetrischen Gradienten des Hox-Genes, der mit der Richtung der Schalenwindung korresponiert. Die Autoren stellten die Vermutung auf, dass *dpp-BMP2/4* das differentielle Mantelwachstum induziert. Da $Platin^{2+}$ auf das differentielle Wachstum des Mantels wirkt, sollte eine mögliche Interaktion zwischen dem Edelmetall und dem Hox-Gen *dpp-BMP2/4* bei der Paradiesschnecke zukünftig untersucht werden.

Die bedeutsamste Frage bei der Betrachtung der durch $Platin^{2+}$ in der Körperform umgestalteten Schnecken ist jedoch die Frage nach der Torsion.

Der Vorgang der Torsion selbst scheint innerhalb der verschiedenen Gastropodengruppen variabel zu sein. Häufig wird ein zweiphasiger Prozess beobachtet, bei dem der erste Teil der Rotation des Visceropalliums durch Muskelkontraktionen und der zweite Teil durch differentielles Wachstum verursacht wird (Haszprunar, 1988). Page (2002) konnte jedoch zeigen, dass die Torsion bei Vetigastropoden auch stattfindet, wenn eine Verbindung zwischen den larvalen Retraktormuskeln und dem Protoconch chemisch verhindert wird, und Demian und Yousif (1973b) beschrieben für *Marisa cornuarietis* die Torsion als vollständig durch differentielles Wachstum ausgelösten Vorgang. Kurita und Wada (2011) beobachteten, dass eine chemische Inhibierung von Wachstumsfaktor β Signalwegen (inklusive Nodal) durch den Inhibitor SB-431542 die Torsion bei der Napfschnecke *Nipponacmea fuscoviridis* verhindern kann. Es existieren also in den verschiedenen Gastropodengruppen verschiedene Wege der Realisierung der ontogenetischen Torsion (Jenner, 2006).

Betrachtet man die Entwicklung von *Marisa cornuarietis* unter dem Ein-

fluss von Platin^{2+}, so stellt man fest, dass während der Embryonalentwicklung der Individuen mit interner Schale keine horizontale Rotation des Eingeweidesacks sichtbar ist und stattdessen eine vertikale Rotation um 90° stattfindet. Diese Schnecken zeigen also keine Torsion, während bei Kontrollen sehr deutlich eine solche Drehung, ausgelöst durch das differentielle Wachstum des Mantelgewebes auf der linken Seite des Eingeweidesacks, zu sehen ist (Demian und Yousif, 1973b). Trotzdem besitzen die durch Platin^{2+} umgestalteten Schnecken einen Anus, der vorne über dem Kopf liegt und eine Überkreuzung der Pleurovisceralkonnektive (Streptoneurie, Chiastoneurie). Die Kiemen liegen jedoch am posterioren Körperende, wie es bei einem Mollusken ohne Torsion zu erwarten ist. Die Paradiesschnecken mit interner Schale zeigen also gleichzeitig Merkmale von „rotierten“ Gastropoden und „unrotierten“ Mollusken. Die während dieser Arbeit erhaltenen Ergebnisse widersprechen also in großen Teilen der eingangs aufgestellte Hypothese 1. Abb. 4 enthält Darstellungen, in denen die mit der Torsion assoziierten morphologischen Merkmale der verschiedenen Expositionsgruppen miteinander verglichen werden.

Nach der gängigen Theorie sollten die Schnecken, bei denen eine Torsion ausbleibt, keine morphologischen Merkmale aufweisen, die auf die Torsion zurückgeführt werden. Dass sie dies dennoch tun, zeigt, dass die Embryonalentwicklung und insbesondere die Entwicklung von Mantelhöhle mit Anus und Kiemen und des Nervensystems komplizierter und nicht unbedingt von einem einzelnen Entwicklungsvorgang (Rotation des Visceropalliums) beeinflusst ist.

Tatsächlich sind die hier vorliegenden Beobachtungen nicht die einzigen Hinweise darauf, dass die klassische Theorie der Torsion kritisch überdacht werden sollte. Page (1997) beobachtete, dass Teile des Mantelgewebes bei *Haliotis kamtschatkana* nicht synchron mit anderen Teilen des Visceropalliums rotieren. Weitere ähnliche Beobachtungen beschreibt sie in ihrem Review von 2006 über die ontogenetische Torsion, in welchem sie eine Asymmetrie-Theorie als Alternative zur klassischen Theorie der Torsion vorschlägt: Nach Page steht am Beginn der Gastropodenentwicklung kein Mollusk mit einer posterioren Mantelhöhle, sondern ein Mollusk mit zwei lateralen Mantelhöh-

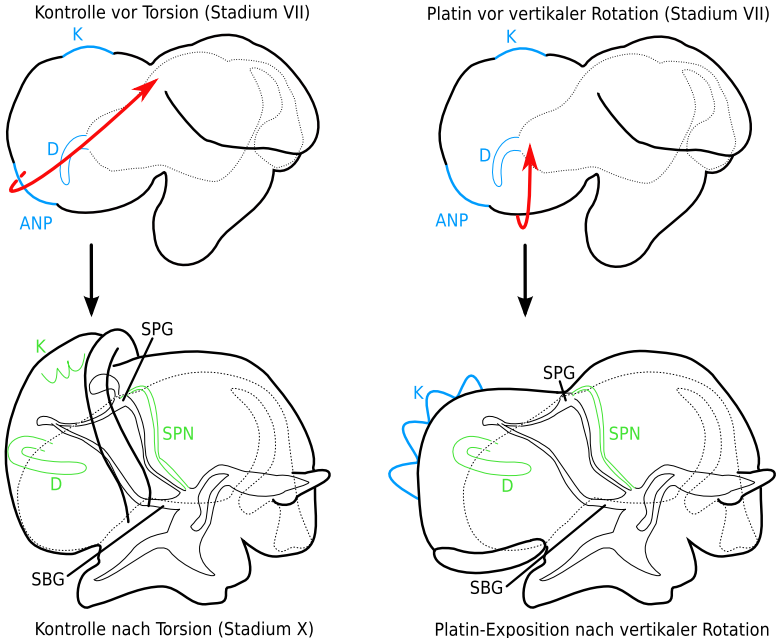

Abb. 4: Vergleich der mit Torsion assoziierten morphologischen Merkmale bei Embryonen der Kontrolle (links) und gegenüber Platin exponierten Embryonen (rechts) vor der Torsion bzw. der vertikalen Rotation (oben) und danach (unten) nach Demian und Yousif (1973b; 1975); Ansicht von rechts, Organe im prätorsionalen Zustand sind blau, Organe im posttorsionalen Zustand sind grün eingefärbt, die roten Pfeile bezeichnen die jeweiligen Rotationsrichtungen; ANP: Analplattenzellen; D: Darm; K: Kiemen; SBG: Subintestinalganglion; SPG: Supraintestinalganglion; SPN: Supraintestinalnerv

len, von denen eine verloren geht und die übriggebliebene Mantelhöhle sich von lateral nach craniad verlagert, wobei es zur Streptoneurie kommt. Sie wird dabei unterstützt von Jenner (2006), der zu dem Schluss kommt, dass die Theorie einer einheitlichen Rotation des gesamten Visceropalliums um 180° gegen den Uhrzeigersinn tatsächlich nur durch sehr wenige Untersuchungen gestützt wird und dass die alternative Theorie von Page möglicherweise eine plausiblere Erklärung als die Torsionstheorie für die Entstehung der Gastropoden sein könnte.

Welche Theorie die evolutiven Vorgänge an der Basis der Entwicklung der Gastropoden besser beschreibt, lässt sich auf der Grundlage der vorliegenden Arbeit nicht entscheiden. Es lässt sich jedoch der Schluss ziehen, dass, zumindest für die Paradiesschnecke *Marisa cornuarietis*, die Embryonalent-

wicklung nicht so verläuft, wie es die Theorie der Torsion impliziert. Im Falle sich „normal“ entwickelnder *Marisa*-Embryonen werden die Kiemen im Zuge des stärkeren Wachstums des Gewebes auf der linken Seite des Eingeweidesacks, durch das es zu der horizontalen Drehung kommt, nach vorne über den Kopf verlagert. Zumindest die Position der Kiemen wird durch die Torsion bestimmt. Anus und Nervensystem entwickeln sich jedoch unter Einfluss von Platin^{2+} auch ohne die Torsion „normal“ und erreichen einen Zustand, der dem post-torsionalen Zustand gleicht. Diese Beobachtungen führen zu dem Schluss, dass die Entwicklung von Anus und Nervensystem unabhängig von der horizontalen Rotation des Eingeweidesacks selbst ist und sogar trotz einer vertikalen Rotation des Visceropalliums „normal“ verläuft.

Auf der Grundlage der vorliegenden Ergebnisse lässt sich vermuten, dass Platin mit einem Signal interagiert, das das differentielle Wachstum von Mantelrand und Schalendrüse im Zuge der Torsion steuert. Kurita und Wada (2011) fanden bei der Napfschnecke *Nipponacmea fuscoviridis*, ähnlich wie Shimizu *et al.* (2013) bei ihrer Untersuchung der Schalenwindung, asymmetrische Gradienten von Wachstumsfaktoren, die mit der differentiellen Zellproliferation im Zuge der Torsion korrespondierten. Sie identifizierten Wachstumsfaktor β Signalwege, zu denen auch die Signalwege von Nodal und *decapentaplegic* (*dpp*) gehören, als Ursache für die Torsion bei der Napfschnecke, und es besteht die Möglichkeit, dass dies auch für andere Schneckengruppen, in denen die Torsion durch differentielles Wachstum ausgelöst wird, gilt. Vor diesem Hintergrund wäre eine Interaktion zwischen Platin^{2+} und einem der Wachstumsfaktor β Signalwege, vielleicht sogar mit *dpp-BMP2/4*, eine plausible Möglichkeit, wie diese Edelmetallionen die horizontale Rotation des Visceropalliums bei *M. cornuarietis* und die Bildung einer externen Schale bei *Marisa cornuarietis* und *Planorbarius corneus* verhindern können.

Schlussfolgerung

Mit dem beschriebenen Modellsystem existiert zum ersten Mal die Möglichkeit, die Rotation des Visceropalliums, welche als indikativ für den Prozess der Torsion angesehen wird, während der Ontogenese von Gastropoden ex-

perimentell zu unterbinden. Die im Rahmen dieser Doktorarbeit durchgeführten Studien haben gezeigt, dass der Übergang von einer externen Schale zu einer internen Schale bei Gastropoden nicht graduell verlaufen muss, sondern auch in einem einzigen Schritt vonstatten gehen kann. Es wurde auch gezeigt, dass die klassische Lehrbuchtheorie der Etablierung des Schneckenbauplans durch ontogenetische Torsion zumindest bei der Paradiesschnecke nicht zutrifft. Die Arbeit unterstützt damit andere Studien, die zwar eine Rotation des Eingeweidesacks nicht experimentell verhindern konnten, in denen jedoch in die gleiche Interpretationsrichtung deutende Beobachtungen gemacht wurden. Die Arbeit zeigt, dass eine Notwendigkeit besteht, die klassiche Torsionstheorie auf der Basis neuer Erkenntnisse zu reevaluieren und anzupassen.

Der Wirkmechanismus von Platin^{2+} bei *M. cornuarietis* wurde noch nicht identifiziert, jedoch wurden Hinweise gefunden, dass die Internalisierung der Schale möglicherweise auf eine Interaktion von Platin^{2+} mit das Mantelwachstum kontrollierenden biochemischen Signalwegen zurückzuführen ist. Künftigen Studien sollten daher Untersuchungen dieser Wachstumsfaktoren beinhalten.

Literatur

Arendt, D. und Nübler-Jung, K. (1997). Dorsal or ventral: Similarities in fate maps and gastrulation patterns in annelids, arthropods and chordates. *Mechanisms of Development*, 61(1–2):7–21.

Bandel, K. (1989). Cephalopod shell structure and general mechanisms of shell formation. *Short Courses in Geology*, 5:97–115.

Berry, K. L. E., Seemann, J., Dellwig, O., Struck, U., Wild, C., und Leinfelder, R. R. (2013). Sources and spatial distribution of heavy metals in scleractinian coral tissues and sediments from the Bocas del Toro Archipelago, Panama. *Environmental Monitoring and Assessment*.

Bieler, R. (1992). Gastropod Phylogeny and Systematics. *Annual Review of Ecology and Systematics*, 23:311–338.

Bouchet, P. und Rocroi, J. P. (2005). Classification and nomenclator of gastropod families. *Malacologia*, 47(1/2):397 pp.

Boyd, R. S. (2010). Heavy metal pollutants and chemical ecology: Exploring new frontiers. *Journal of Chemical Ecology*, 36(1):46–58.

Bradford, M. M. (1976). A rapid and sensitive method for the quantitation of microgram quantities of protein utilizing the principle of protein-dye binding. *Analytical Biochemistry*, 72(1–2):248–254.

Cason, J. E. (1950). A rapid one-step Mallory-Heidenhain stain for connective tissue. *Biotechnic & Histochemistry*, 25(4):225–226.

Demian, E. S. und Yousif, F. (1973a). Embryonic development and organogenesis in the snail *Marisa cornuarietis* (Mesogastropoda: Ampullariidae). I. General outlines of development. *Malacologia*, 12(1):123–150.

Demian, E. S. und Yousif, F. (1973b). Embryonic development and organogenesis in the snail *Marisa cornuarietis* (Mesogastropoda: Ampullariidae). IV. Development of the shell gland, mantle and respiratory organs. *Malacologia*, 12(2):195–211.

Demian, E. S. und Yousif, F. (1975). Embryonic development and organogenesis in the snail *Marisa cornuarietis* (Mesogastropoda: Ampullariidae). V. Development of the nervous system. *Malacologia*, 15(1):29–42.

Dillon, R. T. (2000). *The ecology of freshwater molluscs*. Cambridge University Press, Cambridge; New York.

Ek, K. H., Morrison, G. M., und Rauch, S. (2004). Environmental routes for platinum group elements to biological materials — a review. *Science of The Total Environment*, 334–335:21–38.

Engelhardt, W. (2008). *Was lebt in Tümpel, Bach und Weiher?: Pflanzen und Tiere unserer Gewässer; [über 400 Arten]*. Kosmos, Stuttgart.

Gomot, A. (1998). Toxic effects of cadmium on reproduction, development, and hatching in the freshwater snail *Lymnaea stagnalis* for water quality monitoring. *Ecotoxicology and Environmental Safety*, 41(3):288–297.

Grande, C. und Patel, N. H. (2008). Nodal signalling is involved in left–right asymmetry in snails. *Nature*, 457(7232):1007–1011.

Gupta, S. C., Sharma, A., Mishra, M., Mishra, R. K., und Chowdhuri, D. K. (2010). Heat shock proteins in toxicology: How close and how far? *Life Sciences*, 86(11–12):377–384.

Hama, H., Kurokawa, H., Kawano, H., Ando, R., Shimogori, T., Noda, H., Fukami, K., Sakaue-Sawano, A., und Miyawaki, A. (2011). Scale: a chemical approach for fluorescence imaging and reconstruction of transparent mouse brain. *Nature Neuroscience*, 14(11):1481–1488.

Hanna, L. A., Peters, J. M., Wiley, L. M., Clegg, M. S., und Keen, C. L. (1997). Comparative effects of essential and nonessential metals on preimplantation mouse embryo development in vitro. *Toxicology*, 116(1-3):123–131.

Haszprunar, G. (1988). On the origin and evolution of major gastropod groups, with special reference to the Streptoneura. *Journal of Molluscan Studies*, 54(4):367–441.

Jenner, R. A. (2006). Challenging received wisdoms: Some contributions of the new microscopy to the new animal phylogeny. *Integrative and Comparative Biology*, 46(2):93–103.

Jopp, F. (2006). Comparative studies on the dispersal of the great ramshorn (*Planorbarius corneus* L.): A modelling approach. *Limnologica - Ecology and Management of Inland Waters*, 36(1):17–25.

Kumar, N., Bauddh, K., Dwivedi, N., Barman, S. C., und Singh, D. P. (2012). Accumulation of metals in selected macrophytes grown in mixture of drain water and tannery effluent and their phytoremediation potential. *Journal of environmental biology / Academy of Environmental Biology, India*, 33(5):923–927.

Kurita, Y. und Wada, H. (2011). Evidence that gastropod torsion is driven by asymmetric cell proliferation activated by TGF-beta signalling. *Biology letters*, 7(5):759–762.

Künkel, K. (1916). *Zur Biologie der Lungenschnecken: Ergebnisse vieljähriger Züchtungen und Experimente*. Winter, Heidelberg.

Lau, S., Mohamed, M., Tan Chi Yen, A., und Su'ut, S. (1998). Accumulation of heavy metals in freshwater molluscs. *Science of The Total Environment*, 214(1–3):113–121.

Marx, S. K. und McGowan, H. A. (2010). Long-distance transport of urban and industrial metals and their incorporation into the environment: sources, transport pathways and historical trends. In Zereini, F. und Wiseman, C. L. S., editors, *Urban Airborne Particulate Matter: Origin, Chemistry, Fate and Health Impacts*. Springer.

Migliore, L., Frenzilli, G., Nesti, C., Fortaner, S., und Sabbioni, E. (2002). Cytogenetic and oxidative damage induced in human lymphocytes by platinum, rhodium and palladium compounds. *Mutagenesis*, 17(5):411–417.

Müller, G., Grimmer, G., und Böhnke, H. (1977). Sedimentary record of heavy metals and polycyclic aromatic hydrocarbons in Lake Constance. *Naturwissenschaften*, 64(8):427–431.

Nederbragt, A. J., van Loon, A. E., und Dictus, W. J. (2002). Expression of *Patella vulgata* orthologs of engrailed and dpp-BMP2/4 in adjacent domains during molluscan shell development suggests a conserved compartment boundary mechanism. *Developmental Biology*, 246(2):341–355.

Nummelin, M., Lodenius, M., Tulisalo, E., Hirvonen, H., und Alanko, T. (2007). Predatory insects as bioindicators of heavy metal pollution. *Environmental Pollution*, 145(1):339–347.

Osterauer, R., Faßbender, C., Braunbeck, T., und Köhler, H.-R. (2011). Genotoxicity of platinum in embryos of zebrafish (*Danio rerio*) and ramshorn snail (*Marisa cornuarietis*). *Science of The Total Environment*, 409(11):2114–2119.

Osterauer, R., Haus, N., Sures, B., und Köhler, H.-R. (2009). Uptake of platinum by zebrafish (*Danio rerio*) and ramshorn snail (*Marisa cornuarietis*) and resulting effects on early embryogenesis. *Chemosphere*, 77(7):975–982.

Osterauer, R., Köhler, H.-R., und Triebskorn, R. (2010a). Histopathological alterations and induction of Hsp70 in ramshorn snail (*Marisa cornuarietis*) and zebrafish (*Danio rerio*) embryos after exposure to $PtCl_2$. *Aquatic Toxicology*, 99(1):100–107.

Osterauer, R., Marschner, L., Betz, O., Gerberding, M., Sawasdee, B., Cloetens, P., Haus, N., Sures, B., Triebskorn, R., und Köhler, H.-R. (2010b). Turning snails into slugs: induced body plan changes and formation of an internal shell. *Evolution & Development*, 12(5):474–483.

Page, L. R. (1997). Ontogenetic torsion and protoconch form in the archaeogastropod *Haliotis kamtschatkana*: evolutionary implications. *Acta Zoologica*, 78(3):227–245.

Page, L. R. (2002). Ontogenetic torsion in two basal gastropods occurs without shell attachments for larval retractor muscles. *Evolution & Development*, 4(3):212–222.

Page, L. R. (2006). Modern insights on gastropod development: Reevaluation of the evolution of a novel body plan. *Integrative and Comparative Biology*, 46(2):134 –143.

Perry, D. L., editor (1995). *Handbook of inorganic compounds*. CRC Pr., Boca Raton [u.a.].

Piano, A., Valbonesi, P., und Fabbri, E. (2004). Expression of cytoprotective proteins, heat shock protein 70and metallothioneins, in tissues of *Ostrea edulis* exposed to heat andheavy metals. *Cell Stress & Chaperones*, 9(2).

Ponder, W. F., Colgan, D. J., Healy, J. M., Nützel, A., Simone, L. R. L., und Strong, E. E. (2008). Caenogastropoda. In Ponder, W. F. und Lindberg, D. R., editors, *Phylogeny and evolution of the Mollusca*. University of California Press, Berkeley.

Ponder, W. F. und Lindberg, D. R. (1997). Towards a phylogeny of gastropod molluscs: an analysis using morphological characters. *Zoological Journal of the Linnean Society*, 119(2):83–265.

Queitsch, C., Sangster, T. A., und Lindquist, S. (2002). Hsp90 as a capacitor of phenotypic variation. *Nature*, 417(6889):618–624.

Raven, C. P. (1966). *Morphogenesis - The analysis of molluscan development*. Pergamon Press, Oxford.

Rutherford, S. L. und Lindquist, S. (1998). Hsp90 as a capacitor for morphological evolution. *Nature*, 396(6709):336–342.

Sawasdee, B. und Köhler, H.-R. (2009). Embryo toxicity of pesticides and heavy metals to the ramshorn snail, *Marisa cornuarietis* (Prosobranchia). *Chemosphere*, 75(11):1539–1547.

Sawasdee, B. und Köhler, H.-R. (2010). Metal sensitivity of the embryonic development of the ramshorn snail *Marisa cornuarietis* (Prosobranchia). *Ecotoxicology*.

Schirling, M., Bohlen, A., Triebskorn, R., und Köhler, H.-R. (2006). An invertebrate embryo test with the apple snail *Marisa cornuarietis* to assess effects of potential developmental and endocrine disruptors. *Chemosphere*, 64(10):1730–1738.

Serafim, M., Company, R., Bebianno, M., und Langston, W. (2002). Effect of temperature and size on metallothionein synthesis in the gill of *Mytilus galloprovincialis* exposed to cadmium. *Marine Environmental Research*, 54(3–5):361–365.

Shimizu, K., Iijima, M., Setiamarga, D. H., Sarashina, I., Kudoh, T., Asami, T., Gittenberger, E., und Endo, K. (2013). Left-right asymmetric expression of dpp in the mantle of gastropods correlates with asymmetric shell coiling. *EvoDevo*, 4(1):1–7.

Simpson, G. B. (1901). *Anatomy and physiology of Polygyra albolabris and Limax maximus and embryology of Limax maximus*. Albany: University of the State of New York.

Snow, E. T. (1992). Metal carcinogenesis: mechanistic implications. *Pharmacology & Therapeutics*, 53(1):31–65.

Steinnes, E., Solberg, W., Petersen, H. M., und Wren, C. D. (1989). Heavy metal pollution by long range atmospheric transport in natural soils of southern norway. *Water, Air, and Soil Pollution*, 45(3-4):207–218.

Sörme, L., Bergbäck, B., und Lohm, U. (2001). Century perspective of heavy metal use in urban areas. A case study in Stockholm. *Water, Air and Soil Pollution: Focus*, 1(3-4):197–211.

Turner, A. und Price, S. (2008). Bioaccessibility of platinum group elements in automotive catalytic converter particulates. *Environmental Science & Technology*, 42(24):9443–9448.

Waterman, A. J. (1937). Effect of salts of heavy metals on development of the sea urchin, *Arbacia punctulata*. *Biological Bulletin*, 73(3):401.

Wolpert, L. (2011). *Principles of development*. Oxford University Press, New York; Oxford.

Yonge, C. M. (1947). The pallial organs in the aspidobranch Gastropoda and their evolution throughout the Mollusca. *Philosophical Transactions of the Royal Society of London. Series B, Biological Sciences*, 232:443–518.

Kapitel 1:Turning snails into slugs: induced body plan changes and formation of an internal shell[1]

Raphaela Osterauer[a], Leonie Marschner[a], Oliver Betz[b], Matthias Gerberding[c], Banthita Sawasdee[a], Peter Cloetens[d], Nadine Haus[e], Bernd Sures[e], Rita Triebskorn[a,f], Heinz-R. Köhler[a]

[a] *Animal Physiological Ecology Department, Institute of Evolution and Ecology, University of Tübingen, Konrad-Adenauer-Str. 20, D-72072 Tübingen, Germany*

[b] *Department of Evolutionary Biology of Invertebrates, Institute of Evolution and Ecology, University of Tübingen, Auf der Morgenstelle 28E, 72076 Tübingen, Germany*

[c] *Institute of Zoology, University of Hohenheim, Garbenstr. 30, 70599 Stuttgart, Germany*

[d] *European Synchrotron Radiation Facility, B.P. 220, RF-38043 Grenoble, France*

[e] *Department of Applied Zoology/Hydrobiology, Institute of Biology, University of Duisburg-Essen, Universitätsstr. 5, 45141 Essen, Germany*

[f] *Transfer Center for Ecotoxicology and Ecophysiology, Blumenstrasse 13, 72108 Rottenburg, Germany*

Abstract

The archetypal body plan of conchiferan molluscs is characterized by an external calcareous shell, though internalization of shells has evolved independently in a number of molluscan clades, including gastropod families. In gastropods, the developmental process of torsion is regarded as a hallmark that is associated with a new anatomical configuration. This configuration

[1]Evolution and Development, 2010, 12: 474–483, ©Wiley-Blackwell

is present in extant prosobranch gastropod species, which predominantly bear external shells. Here, we show that short-term exposure to platinum during development uncouples at least two of the processes associated with torsion of the freshwater snail *Marisa cornuarietis*. That is, the anus of the treated snails is located anteriorly, but the gill and the designated mantle tissue remains in a posterior location, thus preventing the formation of an external shell. In contrast to the prosobranchian archetype, platinum treatment results in the formation of a posterior gill and a cone-shaped internal shell, which persists across the lifetime. This first finding of artificially induced snail-slug conversion was also seen in the pulmonate snail *Planorbarius corneus* and demonstrates that selective alteration of embryonic key processes can result in fundamental changes of an existing body plan and – if altered regulation is inherited – may give rise to a new one.

Introduction

It is commonly assumed that the first mollusc-like animals in the early Cambrian were shell-less and only protected by a cuticle with aragonitic spicules or scales (Scheltema and Schander, 2006). Later a calcified shell evolved in the conchiferan clade, which includes the extant Tryblidiida, Gastropoda, Bivalvia, Scaphopoda, and Cephalopoda. Secondary reduction and internalization of the shell has evolved repeatedly and independently in several gastropod taxa (Vitrinidae, Arionidae, Limacidae, Nudibranchia, Velutinidae, Titiscaniidae, Fissurellidae), notably in the cephalopods (except for Nautilus), and most likely for greater motility (Furbish and Furbish, 1984). The ontogeny of internal shells has been described in detail for a selection of gastropod species (Furbish and Furbish, 1984; Page, 2000). Even though mechanisms of shell internalization vary between different evolutionary lines, always the interactions between mantle and shell growth have been shown to be modified in the early individual ontogeny.

Extant species of the paraphyletic and globally distributed group of prosobranch gastropods (nonheterobranch gastropods) mostly develop an outer shell (except for, e.g., a few species of Velutinidae, Titiscaniidae, Fissurelli-

dae). Their ontogeny also includes the process of torsion, which is crucial for the anatomical configuration of these snails. Torsion is defined as a process in gastropod ontogenesis that rotates the visceral body 180° relative to the larval headfoot region. As a consequence the digestive tract is U-shaped and the anus is located anteriorly, the mantle cavity is located anteriorly over the back of the head, and the gills are located anteriorly in front of the heart. This process is the key character defining the gastropod class.

It is generally thought that torsion involves a counterclockwise simultaneous movement of the outgrowing mantle, the shell, and the visceral sac, and – following Ernst Haeckel's theory of ontogeny recapitulating phylogeny – that this developmental process recapitulates evolutionary events at the rise of prosobranch gastropods.

In growing snails, the mineralization of the teleoconch takes place at the peripheral edge of the mantle fold and over the entire inner surface of the shell in order to increase shell thickness. Usually, invagination of the dorsal epithelium first occurs to form the shell gland, followed by shell field evagination and the migration of shell material-secreting cells toward the mantle edge (Kniprath, 1981; Waller, 1981). The shell gland originates at the aboral end of the embryo, later shifts to the left and forms the mantle (Demian and Yousif, 1973a). The helical growth of the shell occurs in parallel to the onset of the counterclockwise movement of the outgrowing mantle due to the process of torsion. The mantle overgrows the visceral sac in the right dorso-lateral direction and opens to the anterior, forming the mantle cavity sheltering the organs such as the gill(s).

The mollusc shell consists of an organic matrix and calcium carbonate ($CaCO_3$), which is formed from calcium and bicarbonate ions present in the extrapallidal fluid (Rousseau *et al.*, 2003). Catalyzing the reaction $CO_2 + H_2O \rightleftharpoons HCO^{3-} + H^+$ and being responsible for reversible hydration of CO_2, the enzyme carbonic anhydrase (CA) is associated with tissues involved in calcification and mineralization processes such as the formation of the embryonic shell (Costlow, 1959; Maren, 1967; Wilbur and Saleuddin, 1983; Takaichi *et al.*, 2003).

The course of anatomical modifications during embryonic development of

the prosobranch freshwater snail, *Marisa cornuarietis* (Ampullariidae), is well documented (Demian and Yousif, 1973a–d, 1975). Earlier studies revealed its embryos to be particularly sensitive to metals (Schirling *et al.*, 2006; Sawasdee and Köhler, 2009). Because of increasing importance of platinum group elements in ecotoxicology resulting from their use in automobile catalytic converters, we tested the effect of platinum (Pt) on the embryogenesis of this gonochoric species. Because we found that exposure to Pt separates the process of torsion from mantle cavity formation and therefore prevents the formation of an external shell in *M. cornuarietis* we used different methological approaches to study this effect. To investigate the variability of this effect we also tested other metals like the physicochemical similar element palladium (Pd) and the alkaline metal lithium (Li) on embryos of *M. cornuarietis*. Furthermore, we also tested the effect of Pt on the pulmonate snail *Planorbarius corneus* to compare effects on different snail species.

Materials and methods

Test animals

Test animals used in the present study were the freshwater snails *M. cornuarietis* (Ampullariidae, prosobranch gastropod) and *P. corneus* (Planorbidae, pulmonate). Origin and maintenance of the lab stock culture of the gonochoric species *M. cornuarietis* were described in Osterauer *et al.* (2009).

The breeding stock of the hermaphroditic snail *P. corneus* was gathered in a pond near Tübingen. *P. corneus* were kept in 30 L aquaria containing oxygenized tap water in the following conditions: temperature: $20 \pm 1\,^{\circ}\mathrm{C}$, pH: 8, conductivity: 800 μS/cm, and 12 h/12 h light/dark regime. To ensure optimal water quality, the water of the aquaria was exchanged every week. The snails were fed once a day with commercially available artificial diet (Nutrafin Max flakes, Hagen, Germany) and casually with fresh carrots or lettuce.

Exposure experiments

Test substances used in the present study were $PtCl_2$ (Ultra Scientific, Wesel, Germany), $PdCl_2$ (Sigma-Aldrich, München, Germany), LiCl ($\geq$ 99%, Fluka, Buchs, Switzerland), and, in combination with $PtCl_2$, $CaCl_2$ (Merck, Darmstadt, Germany). For both, exposure and pulse experiments, single eggs were separated from the egg masses laid during the night and distributed to Petri dishes containing the respective substance or the control medium which was tap water taken from the snail aquaria. The described effects occurred independently of using either tap/aquaria water or reconstituted water after the OECD Test Guideline 203 (1992), modified for *M. cornuarietis*, as a solvent. Concentrations used for chronic exposure (from the day of fertilization until hatch) were 100 and 200 μg/L $PtCl_2$, 50, 100, and 500 μg/L $PdCl_2$, 2.5 and 3 mg/L LiCl for *M. cornuarietis*, and 300, 400, and 500 μg/L $PtCl_2$ for *P. corneus*. For the pulse exposure experiments, *M. cornuarietis* eggs were exposed to 200 μg/L $PtCl_2$ for either 1 (at days 3, 4, 5, or 6 postfertilization) or 2 days (at days 3+4, 4+5, 5+6, 6+7, or 7+8 postfertilization) and subsequently returned to tap/aquaria water again. Furthermore, binary combinations of $PtCl_2$ (200 μg/L) and $CaCl_2 \times 2H_2O$ (0.54 g/L) in which $Pt2^+$and Ca^{2+} concentrations were equimolar, were tested on *M. cornuarietis* (exposure from the day of fertilization until hatch). Negative controls were exposed to tap/aquaria water, positive controls were exposed to 200 μg/L $PtCl_2$ during the whole study.

For all experiments, exposure media were exchanged daily. Throughout the exposure period, embryos were kept at 26 °C in a climate chamber and were only removed for monitoring their development using a stereomicroscope. The numbers of snails without external shell were counted at day 9 postfertilization (dpf) in chronic exposure experiments and at day 11 postfertilization in pulse experiments. To study the postembryonic development of *M. cornuarietis*, hatched snails either were continuously exposed to 100 or 200 μg/L $PtCl_2$ or 200 μg/L $PtCl_2$ plus 0.54 g/L $CaCl_2$ x $2H_2O$ or returned to tap/aquaria water but, in any case, hatched snails were fed with equal portions of commercially available artificial diet (Nutrafin Max, Hagen, Ger-

many) *ad libitum* once a day. The chronic exposure experiments with *M. cornuarietis* embryos and Pt, Pd, and Li were conducted with nine replicate groups (à 20 individuals), the pulse experiments and the exposure experiments with Pt plus Ca with four replicate groups (except for control and Pt-control in the first run of the 2-day pulses with eight replicate groups) (à 20 individuals) and the exposure experiments with *P. corneus* with two replicate groups at 300 μg/L $PtCl_2$ (à 13 individuals) and at 400 μg/L $PtCl_2$ (à 6 and 11 individuals) and, due to limitations in egg production, 1 group of four individuals at 500 μg/L $PtCl_2$. The Pt-induced internalization of the shell in the investigated gastropod species was found to be highly reproducible and allowed us to induce the described body plan modifications *ad libitum* ever since.

Reconstituted water composition for *M. cornuarietis*

Reconstituted water consisted of double-distilled water supplemented with KCl (17.94 mg/L), $MgSO_4 \times 7\ H_20$ (0.19 g/L), $NaHCO_3$ (98.42 mg/L), $CaCl_2 \times 2H_2O$ (0.45 g/L), and NaCl (0.43 mg/L).

Histology

Whole embryos of *M. cornuarietis* at the age of 26 dpf that had been exposed to 200 μg/L $PtCl_2$ throughout were fixed in Bouin's solution for 1 week. Detailed information on the histological techniques is given in Osterauer *et al.* (2010). Histological methodology was based on Triebskorn *et al.* (2005).

Analysis of platinum in *M. cornuarietis* and in the exposure media

After 26 dpf of exposure to 100 or 200 μg/L $PtCl_2$ or 200 μg/L $PtCl_2$ + 0.54 g/L $CaCl_2 \times 2H_2O$ (equimolar Pt^{2+} and Ca^{2+} concentrations), *M. cornuarietis* were frozen in liquid nitrogen and stored at $-20\,^{\circ}C$. Depending on the estimated Pt concentrations, quantity of bioaccumulated Pt in the organisms was measured with adsorptive cathodic stripping voltammetry (ACSV) after digestion via high-pressure ashing according to Zimmermann

et al. (2001, 2003) or with electrothermal atomic spectrometry (ET-AAS) after microwave-assisted digestion according to Sures *et al.* (1995). $PtCl_2$ concentrations above 100 μg/L were analyzed by ET-AAS, while lower concentrations were analyzed by ACSV. For controls and *M. cornuarietis* exposed to 100 μg/L $PtCl_2$ the replicate number n was 8, for *M. cornuarietis* exposed to 200 μg/L PtCl2 n=9, for *M. cornuarietis* exposed to 200 μg/L $PtCl_2$ plus equimolar Ca n=5. Depending on the estimated Pt concentrations in the exposure medium for *M. cornuarietis*, concentrations of Pt were measured with inductive coupled plasma mass spectrometry (ICP-MS, Perkin Elmer model Elan 5000, PerkinElmer Inc., Wellesley, MA, USA) or with ET-AAS (Perkin Elmer model 4100ZL). $PtCl_2$ concentrations above 100 μg/L were analyzed by ET-AAS, while lower concentrations were analyzed with ICP-MS. Each sample was analyzed in triplicate. Detailed descriptions of analytical procedures for ACSV and ICP-MS have been published by Osterauer *et al.* (2009).

Electrothermal atomic absorption spectrometry (ET-AAS)

Tissue samples of about 20 mg fresh weight each were digested by adding 1.8 mL HNO_3 (65 vol.%, subboiled) into 100 mL perfluoralkoxy vessels. Using a microwave digestion oven (CEM Model MDS-2000, 650 $\pm$ 50 W; Spectralab Scientific Inc., Toronto, ON, Canada) samples were digested according to the description of Sures *et al.* (1995). The resulting solution was filled up to 2 mL with bidistilled water. Analytical measurements were conducted with an atomic absorption spectrophotometer (Perkin Elmer Model 4100ZL). Therefore, 20 μL of each sample, priorily diluted with bidistilled water, were injected into a pyrolytic graphite furnace tube with L'vov platform by an autosampler AS 70. Operation parameters and further procedural descriptions have been published by Zimmermann *et al.* (2003). The detection limit for Pt in the tissue samples was defined to be threefold the standard deviation of the measurements of procedural blanks. For the average sample weight of 25 mg for *M. cornuarietis* it was found to be 62 ng/g.

For Pt analysis in the exposure medium 0.5 mL of the medium were topped

up to 1 mL with bidistilled water and analysed as described above. The detection limit for Pt was defined threefold the standard deviation of the measurements of blanks and was found to be 1.6 μg/L.

Carbonic anhydrase activity

M. cornuarietis at the age of 10 dpf (control animals and animals treated with 200 μg/L $PtCl_2$) were homogenized in 60 μL phosphate buffer (25 mM, pH 7.4). Homogenates were centrifuged for 5 min at 2000 $\times$ g and 4 °C according to the protocol of Giraud (1981). The supernatant served as enzyme source. The ΔpH method of measuring CA activity was conducted according to the description of Henry (1991) and Vitale *et al.* (1999). For activity measurement 7.5 mL reaction medium (mannitol, 225 mM; saccharose, 75 mM and tris-phosphate, 10 mM at pH 7.4), 50 μL supernatant and 1 mL of CO_2 containing sparkling mineral water (Selters, Löhnberg, Germany) were mixed and the pH-drop was measured for 25 s with a high-precision pH meter (WTW ph 391, WTW, Weilheim, Germany). A linear regression of pH data against time was calculated and the estimated slope was adopted as the catalyzed reaction ($b_{catalyzed}$). For control measurements, phosphate buffer was used instead of enzyme containing supernatant and the same procedure was performed. Total protein content was determined according to Bradford (1976). To determine the specific CA activity the formula according to Burnett *et al.* (1981) was used: SCA = ($b_{catalyzed}$ / $b_{noncatalyzed}$ –1)/mg of total protein. Five snails per sample and 3 replicates were used. All preparations were conducted at low temperature (vessels were kept on ice).

Diamino-benzidine (DAB) staining of mantle edge tissue

DAB staining usually is used as negative control for antibody labelling procedures. In other experiments we found DAB to specifically stain the mantle edge of developing *M. cornuarietis* embryos. Different stages of control embryos and embryos exposed to 200 μg/L $PtCl_2$ (day 3, 3.5, 4, 5 and 6 post fertilization) were mechanically removed from the chorion and fixed in 3.7% formaldehyde in phosphate-buffered saline (PBS) for 30 min. After washing

for 4 × 5 min with PTw (PBS with 0.01% Tween 20, Roth, Karlsruhe, Germany) embryos were incubated with PTw+N (PTw with 5% Goat Serum, Jackson ImmunoResearch, West Grove, PA, USA) overnight at 4 °C.

For horseradish peroxidase (HRP) reaction embryos were washed with PTw for 4 x 5 min and 4 x 15 min and afterwards incubated in 0.3 mg/mL DAB solution for 20 min. The reaction was started by adding H_2O_2 to a final concentration of 0.03%. When the brown signal became visible, as could be visually detected under a stereomicroscope, reaction was stopped by washing 2 × 5 min with PTw. Finally, embryos were mounted in a 50% glycerol/DAPI (4',6-diamidino-2-phenylindole) mix. For visual analysis and photography were used a light microscope and a stereomicroscope (both Zeiss, Jena, Germany).

Synchrotron X-ray phase contrast tomography and holotomography

Whole intact embryos of *M. cornuarietis* exposed to 100 μg/L $PtCl_2$ for 26 dpf were fixed in 100% ethanol overnight, critical point dried (CPD 020, Balzers, Wiesbaden, Germany) and mounted on specimen holder stubs. X-ray tomography was conducted at beamline ID19 (ESRF, Grenoble, France) at an energy of 20.0 keV. Measurements were performed at three different sample-detector distances, i.e. 16 mm, 100 mm, and 841 mm. The effective pixel resolution amounted to 5.05 μm. Otherwise, instrument settings and further data treatments were done according to the description of Heethoff and Cloetens (2008). Due to limitations in beam time, measurements were conducted with a single animal each of the Pt treated group and of the control group.

Scanning electron microscopy

Embryos of *M. cornuarietis* of different age and exposure (100 or 200 μg/L $PtCl_2$, and controls) were fixed overnight in 2% glutaraldehyde in 0.01 M cacodylate buffer at pH 7.4. Subsequently, the organisms were washed three times with 0.01 M cacodylate buffer and stored in 1% osmium tetroxide

overnight. The next day, the specimens were dehydrated in an ascending series of ethanol dilutions. After critical point drying they were fixed on specimen holder stubs, sputter-coated with gold, and viewed with a scanning electron microscop (SEM) (Cambridge Stereoscan 250 Mk2, Cambridge Scientific, Cambridge, UK).

Statistical analyses

Normally distributed data (Shapiro-Wilk test, JMP 4.0, SAS Systems, USA) were tested with the parametric one-way t-test (JMP 4.0, SAS Systems, USA) to detect significant differences between the treatment group and the control. Data not corresponding to normal distribution were tested using the nonparametric distribution-independent Wilcoxon's test (JMP 4.0, SAS Systems, USA) to detect significant differences between the respective treatment groups and the control group. The alpha level was set at 0.05. Differences were considered to be significant for $p \leq 0.05$ $(*)$ and highly significant for $p \leq 0.01$ $(**)$, and $p \leq 0.001$ $(***)$.

Results

Platinum accumulation and induced body plan changes in *M. cornuarietis*

To quantify Pt accumulation snails were exposed to 100 or 200 μg/L $PtCl_2$2 for the first 26 dpf. Chemical analytical data already have been partly published by Osterauer *et al.* (2009), and showed exposure of *M. cornuarietis* embryos (within the egg) and juveniles to result in exceptionally high Pt concentrations in the animals: 74.2 $\pm$ 5.3 μg/L Pt in the medium (nominal concentration of 100 μg/L $PtCl_2$ corresponding to 73.4 μg/L Pt) led to 53.7 $\pm$ 19.2 μg/g Pt wet weight in the animals (bioaccumulation factor 724) and 163.4 $\pm$ 2.7 μg/L Pt (nominal concentration of 200 μg/L $PtCl_2$ corresponding to 146.8 μg/L Pt) resulted in a tissue concentration of 90.3 $\pm$ 9.9 μg/g Pt wet weight (bioaccumulation factor 553), both indicating a high potential of Pt to interact with developmental processes in this species. In response to Pt

treatment 29.9 ± 32.78% of surviving *M. cornuarietis* juveniles continuously exposed to 74.2 μg/L Pt (85.1 ± 9.41% survival) did not form an external shell, whereas at exposure to 163.4 μg/L Pt (84.4 ± 6.23% survival), all surviving animals were 'shell-less' (100 ± 0%). To detect the most sensitive stage in embryogenesis in which Pt interferes with the formation of the shell, we conducted two separate runs of a pulse-exposure experiment. These experiments included pulses of 200 μg/L $PtCl_2$ with a duration of either 1 day or 2 days. Data varied between the two experimental runs but indicated the embryonic stages at days 4 and 5 postfertilization to be most susceptible to Pt action on shell formation (Fig. 1).

We repeatedly raised large numbers of *M. cornuarietis* embryos without external shell by pulse exposure to nominal concentrations of 200 μg/L $PtCl_2$ at days 4 and 5 postfertilization. Subsequently, the embryos in their egg capsules were transferred to uncontaminated water and cultivated at 26 °C. We never obtained reversal of the Pt pulse-induced body plan changes under these conditions and, thus, none of these individuals ever developed an external shell. Without exception, all juveniles shared the following alterations relative to the nontreated snails (Fig. 2a): no mantle cavity was formed at all and hence the gill, which remained posterior to the heart at the hind part of the visceral sac, protruded from the visceral sac into the surrounding water (Fig. 2b). Nevertheless, as indicated by the deflected intestine, the position of the anus at the lower right side (Fig. 2b), and by a slight movement of the gill from hind left to hind right, part of developmental processes associated with torsion was accomplished in all individuals. The hepatopancreas, as usual, surrounds the mid part of the intestine. Dorsal of the hepatopancreas, the hindgut bends to the front. In addition, the visceral sac surface of these snails bloats and blisters to varying degree, forming hemocoel cavities of different sizes (Fig. 2, b, d, and f). An operculum was present (Fig. 2c) and the morphology of the head and ventral part of the body, including the operculum, did not differ from the archetypical body plan (Fig. 2, a, b, and e).

Up to now, *M. cornuarietis* individuals with induced body plan changes due to Pt exposure reached a maximum age of 7 months and a maximum

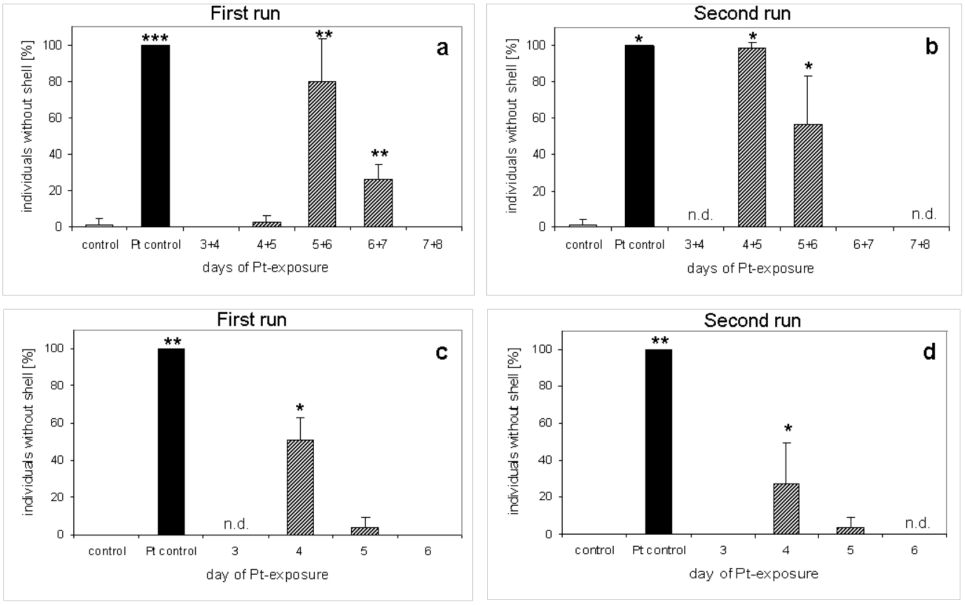

Fig. 1[2]: Pulsed Pt-exposure of *M. cornuarietis* to 200 μg/L $PtCl_2$ at different days of embryonic development. Percentages of surviving individuals without external shell at day 11 post fertilization (means ± SD). (a) and (b) Two-days-pulses. (c) and (d) One-day-pulses. For each experiment and run, n = 4 replicates with 20 individuals per replicate (except for control and Pt-control in the first run of two-days-pulses n = 8). Control: water exposure; Pt control: continuous exposure to $PtCl_2$ during the entire embryonic phase; n.d.: not determined. Significance vs. control: $***$ p $\leq$ 0.001, $**$ p $\leq$ 0.01, $*$ p $\leq$ 0.05.

length of about 1.5 cm. During their lifetime, the animals steadily grew and gained mass but did not change their outer appearance. So far, the only known way to partly protect embryos from the action of Pt is to supplement the Pt solution with equimolar concentrations of bivalent calcium ions. In experiments with *M. cornuarietis* embryos exposed to 200 μg/L $PtCl_2$ plus 0.54 g/L $CaCl_2 \times 2H_2O$ (equimolar Pt^{2+} and Ca^{2+} concentrations) for 9 days postfertilization, 84 ± 12% of the individuals formed an external shell and 16 ± 12% did not. However, a considerable number of the shelled animals in this experiment only developed a small, cap-like external shell, which was not sufficiently large to cover completely the gill (Fig. 3a).

[2]Die Graphen wurden von Raphaela Osterauer erstellt und zu einer Bildtafel zusammengefügt.

[3]Die Bildtafel wurde von Raphaela Osterauer erstellt. Die Abbildungen 2a,b,d,e und f stammen von Raphaela Osterauer.

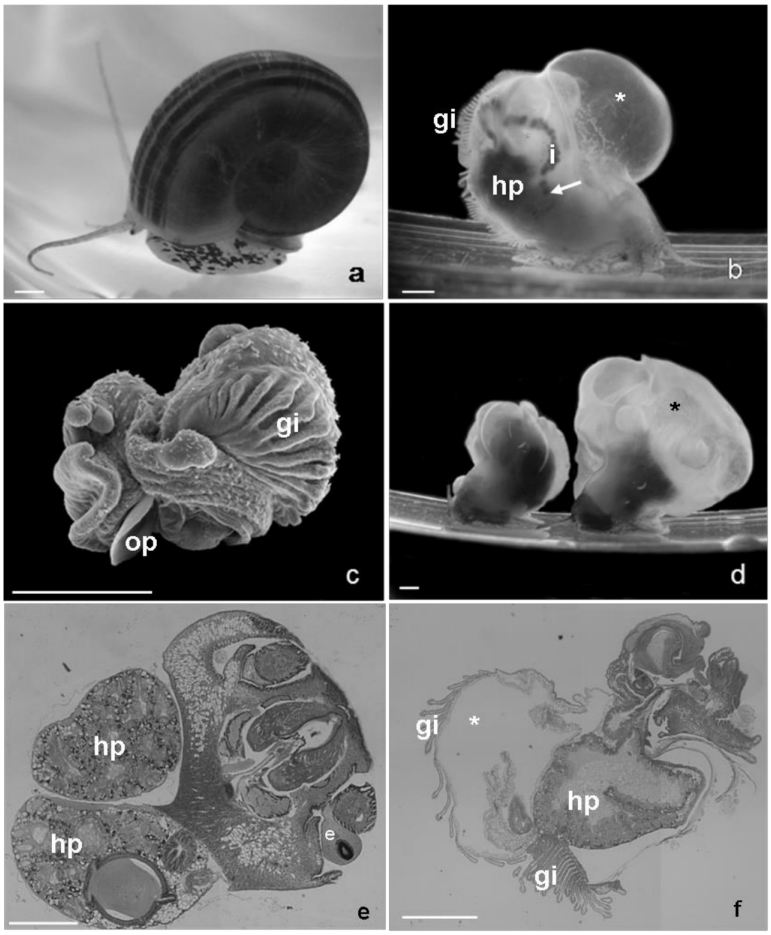

Fig. 2^3: Images of *M. cornuarietis* exposed to 200 μg/L $PtCl_2$ without external shell and control. (a) Control, 3 months old. (b) and (d) Pt-exposed snails without external shell, 2 months old. Arrow indicates position of the anus. (c) Scanning electron micrograph of an embryo without external shell, 14 days post fertilization. (e) Horizontal section of a control animal, 26 days post fertilization, ventral part of the body. (f) Sagittal section of a Pt-exposed animal, 26 days post fertilization, median part of the body. gi: gill, i: intestine, hp: hepatopancreas, op: operculum, asterisks: bloats and blisters of the hemocoel. Scale bars are 500 μm.

Ca supplements did not diminish Pt uptake: snails without an external shell exposed to 200 μg/L $PtCl_2$ accumulated 90.3 $\pm$ 9.9 mg/g Pt, snails without an external shell exposed to Pt and equimolar concentrations of Ca accumulated 115 $\pm$ 28.1 μg/g Pt, and snails exposed to Pt and equimolar concentrations of Ca, which developed an external shell accumulated 82.5 $\pm$

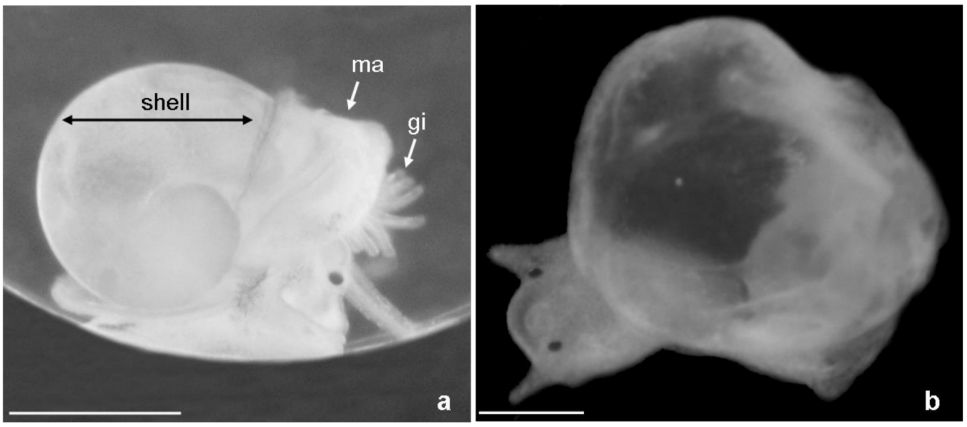

Fig. 3: Pt effect in Ca-supplemented *Marisa cornuarietis* and in *Planorbarius corneus*. (a) *M. cornuarietis* with a small, external shell, 11 days post fertilization, exposed to 200 μg/L $PtCl_2$ and equimolar concentrations of Ca^{2+}, ma: mantle, gi: gills. (b) *P. corneus* without external shell, 23 days post fertilization, exposed to 300 μg/L $PtCl_2$. Scale bars are 500 μm.

26.4 μg/g Pt. In contrast to Pt^{2+}, the physicochemical similar ion Pd^{2+} did not affect shell formation during embryogenesis. Only occasionally were we able to induce shell-less *M. cornuarietis* embryos with high concentrations of Li^{+}: 2.5 mg/L LiCl caused 10.0 $\pm$ 6.0% shell-less snails and 3 mg/L LiCl caused 20.0 $\pm$ 9.5% shell-less snails.

The fate of the shell secreting edge of the mantle fold and the formation of an internal shell

Since we found DAB to specifically stain the shell-secreting peripheral edge of the mantle fold, we were able to follow the fate of the tissue, which usually forms the mantle fold edge during embryogenesis and to visualize the presumably shell-secreting region of Pt-exposed *M. cornuarietis*. In contrast to the controls, the tissue archetypically designated to form the mantle edge did neither evaginate nor overgrow the visceral sac but remained at the posterior end of the embryo and invaginated into the body (Fig. 4, c–f), thus closing the aperture of the shell gland.

Using SEM, the morphology of the shell gland and the initial protoconch of continuously Pt-exposed embryos and water controls did not differ sub-

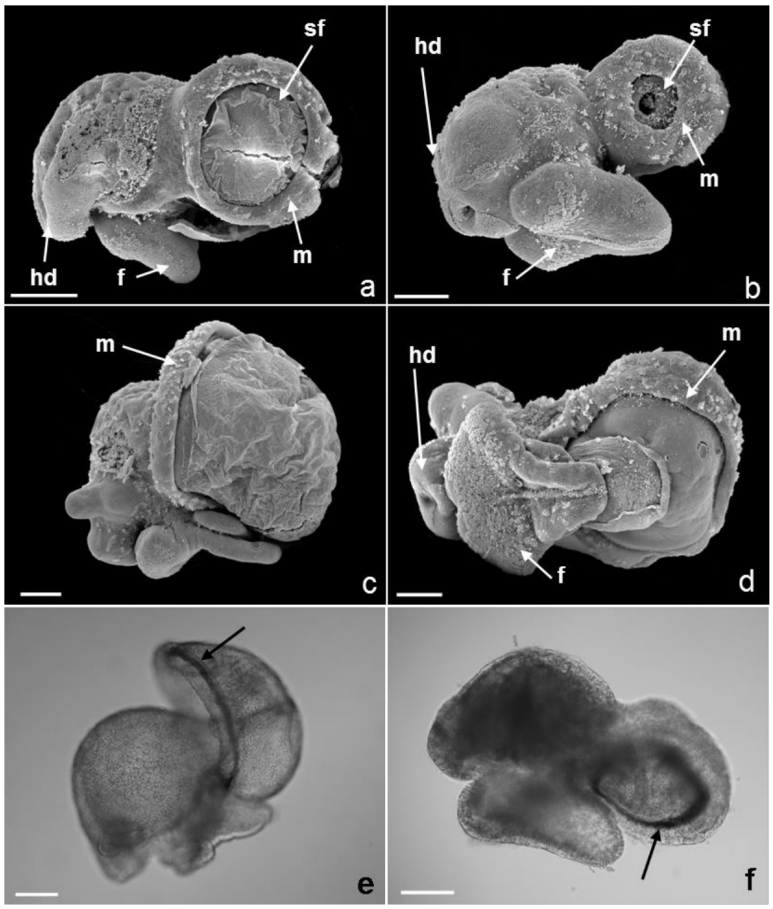

Fig. 4[4]: Location of the shell-secreting peripheral edge of the mantle fold in *Marisa cornuarietis* exposed to 200 μg/L PtCl2 and in controls. Scanning electron micrographs of Pt-exposed (200 μg/L PtCl2) *M. cornuarietis* and controls. (a) Control, 3 days post fertilization. (b) Pt-exposed M*M. cornuarietis*, 4 days post fertilization. (c) Control, 5 days post fertilization. (d) Pt-exposed *M. cornuarietis*, 6 days post fertilization. DAB staining (arrows) of the shell-secreting mantle edge of a control individual (e) and a Pt-exposed individual (f), both 5 days post fertilization. Scale bars are 100 μm.

stantially (Fig. 4, a and b). However, while the shell grows rapidly during the subsequent days of embryogenesis in controls, the opening of the shell gland of Pt-exposed individuals was reduced in size. To test whether this effect and the subsequent lack of an external shell was possibly based on a lack or a drastic diminution of biomineralization activity during the days

[4]Die Abbildungen 4e und f stammen von Raphaela Osterauer, die Bildtafel wurde von Raphaela Osterauer erstellt.

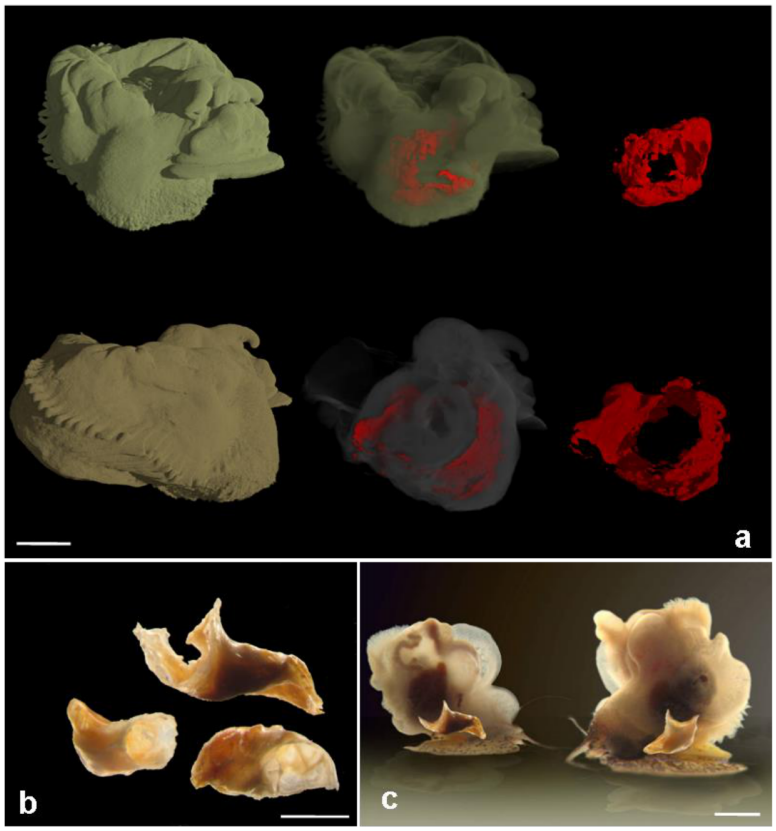

Fig. 5[5]: Internal shells of Pt-exposed *Marisa cornuarietis*. (a) Synchrotron X-ray phase-contrast microtomographs of snails exposed to 100 μg/L $PtCl_2$, 26 days post fertilization. Upper row: view from the right, ahead; lower row: view from the left, rear. Respective left pictures: whole body; pictures in the middle: semi-transparent view of the body; respective right pictures: internal shell fragment. Scale bar is 500 μm. (b) Three examples of internal shells of snails exposed to 200 μg/L $PtCl_2$, about 2 months old. Scale bar is 500 μm. (c) Approximate position of the internal shell in *M. cornuarietis* exposed to 200 μg/L $PtCl_2$, about 2 months old, photo editing. Scale bar is 1 mm.

subsequent to the Pt-sensitive stages, CA activity was measured in embryos continuously exposed to 200 μg/L $PtCl_2$ at day 10 postfertilization. Even though Pt exposure decreased CA activity from 13.8 $\pm$ 2.6/mg in controls to 8.5 $\pm$ 3.6/mg in shell-less *M. cornuarietis* embryos, this difference was not significant ($p = 0.107$). Synchrotron X-ray phase-contrast microtomography applied on a 26 dpf old Pt-exposed juvenile revealed the formation of an

[5]Die Abbildungen stammen von Raphaela Osterauer.

internal solid circular structure in the ventral part of the visceral sac, right at the position of the invaginated ectodermal tissue that has been formed the shell gland (Fig. 5a). Starting from this solid structure, with increasing age the snails developed an internal calcareous shell in the shape of a hollow, nonsegmented cone, which surrounds the hepatopancreas in its ventralmost part (Fig. 5).

The phenomenon of Pt-induced body plan changes is not restricted to *M. cornuarietis* but could also be observed in embryos of the pulmonate snail *P. corneus* exposed to nominal concentrations of $\geq$ 300 μg/L $PtCl_2$ from fertilization until hatch. Also shell-less *P. corneus* did not form a mantle cavity (Fig. 3b). In contrast to *M. cornuarietis*, the longevity of unshelled *P. corneus* was restricted to a maximum of about 2 weeks postfertilization.

Discussion

The present study describes and investigates artificially induced shell internalization in *Marisa cornuarietis* due to Pt exposure, which corresponds with fundamental body plan changes.

In contrast to Pt^{2+}, the physicochemical similar ion Pd^{2+} and other bivalent metals (Zn^{2+}, Ni^{2+}, Cd^{2+}; Schirling *et al.*, 2006; Sawasdee and Köhler, 2009) did not interfere with shell formation during embryogenesis. Only occasionally high concentrations of Li^{+} (2.5 and 3 mg/L LiCl2), a metal which has been shown to interact with the positional system of predominantly ectodermal tissue in *Xenopus* and *Loligo* (Kao *et al.*, 1986; Crawford, 2003), prevented the formation of an external shell in *M. cornuarietis*. So far, solely the heavy metal Pt seems to specifically interact with key processes during early embryonic development, which inhibits the mantle to evaginate and to overgrow the visceral sac, hence, leading to the growth of an internal shell as it could be traced by the staining of the mantle edge.

Pulse experiments revealed days 4 and 5 postfertilization to be most susceptible to Pt action on shell formation. Data probably varied due to slight variation in culture temperature (26 $\pm$ 1 °C) and depending on the exact time of fertilization during the night. During these days of embryonic de-

velopment the initial stages of the embryonic shell are formed (Demian and Yousif, 1973a). One hypothetical approach to explain the Pt-induced internalization of the shell relies on a possible interaction of Pt with the Ca metabolism and its uptake via Ca trans-membrane transport. Because Ca supplements did not diminish Pt uptake, we conclude that Pt likely interacts with Ca signalling pathways involved in the positional system, which may be stabilized by increasing intracellular levels of Ca. Some heavy metals have been shown to act as inhibitors of the ezyme CA (Christensen and Tucker, 1976; Morgan *et al.*, 1997; Vitale *et al.*, 1999) or to reduce shell mass in snails (Beeby *et al.*, 2002). We therefore tested the CA activity in Pt exposed *M. cornuarietis*. The results indicated a diminuation but no significant difference of the activity in Pt exposed snails. Hence, the mechanisms of the internal shell production seem to be almost as effective as those involved in the growth of the external shell, and the reduction in shell size could probably only be attributed to a compressed shape due to the limited space inside the gastropod's body.

The effect of body plan changes due to Pt exposure could also be observed in embryos of the pulmonate snail *P. corneus*. Also shell-less *P. corneus* did not form a mantle cavity which might indicate that Pt action on the re-direction of presumptive mantle tissue is likely universal in gastropods. In contrast to prosobranch gastropods, however, pulmonates lack a gill but use their mantle cavity to form a lung. A re-direction of mantle tissue here consequently leads to a lack of any respiratory organ and, therefore, to a short life span in *P. corneus* embryos.

Descriptions of various authors about the time span of torsion (from about 2 min until about 200 h) and its main cause(s) (muscular activity, differential growth, hydraulic activity) in different groups of gastropods vary to a high degree (for detailed informations see Wanninger *et al.*, 2000). Therefore, it can be assumed that ontogenetic torsion of gastropods has been highly modified within different groups subsequent to its rise in early phylogeny.

Because no external shell is formed after exposure to Pt, torsion occurs independently from retractor muscle action on the larval shell in *M. cornuar-*

ietis as it was shown for other gastropod species in earlier studies of Hickman and Hadfield (2001) and Page (2002) who provided evidence for this view. As shown for other organisms (for an overview see Wanninger *et al.*, 2000), our results provide additional independent evidence that several processes are involved in the ontogenetic process of torsion, in contrast to Garstang (1929) and Crofts (1937, 1955) who proclaimed contraction of asymetric larval retractor mussels to be the cause of developmental rotation. We could show that at least two of the processes associated with torsion can be uncoupled during the development of *M. cornuarietis*. That is, the anus of the treated snails is located anteriorly, but the mantle tissue and gill remains in a posterior location. Hence, the process of torsion is neither inevitably connected to mantle cavity formation nor to the translocation of its aperture together with the gill into a frontal position but rather developmentally separated from the distal outgrowth of the mantle epithelium, which is also the prerequisite for an external shell. Both freshwater model species, *M. cornuarietis* and *P. corneus*, go through a "direct development" lacking a trochophora or veliger larva. Therefore, differential growth may play a crucial role in torsion because muscles are differentiated after the torsion process only.

The fact that only the position of the mantle tissue and the gills but not the anus in Pt-treated *M. cornuarietis* can be uncoupled from torsion processes compared to nontreated animals, might be due to the observations made by Demian and Yousif (1973b) who described that the intestine of this species is entirely endodermal and opens into the mantle cavity at a relatively late stage.

This is the first report on snail–slug conversion and experimentally induced shell internalization in gastropods. Even though the morphological similarity of these artificial internal shells with internal shell derivatives in extant or fossil molluscan taxa is striking, we do not claim to be able physiologically to trigger exactly what has evolved in cephalopods, nudibranchs, and pulmonate slugs. The mechanisms of shell–mantle interactions in the formation of internal shell derivatives in extant molluscs are manifold and do not follow exactly the same developmental pattern, even though, in all cases and also

in our experiments, a shell precursor is overgrown by ectodermal (mantle) tissue (Kniprath, 1981; Page, 2000; Gibson, 2003). Particularly in extant taxa of opisthobranchs, there is evidence for a stepwise reduction of the shell (Wägele and Klussmann-Kolb, 2005) which is contradicting a hypothesis of "macromutation"- based radical developmental shifts underlying body plan modifications such as detorsion in these heterobranch gastropods. Nevertheless, it is evident from our study that minimal changes in the blueprint for molluscan ontogeny (or the corresponding signal transduction machinery of the positional system) may lead to sudden body plan shifts. This observation is consistent with the notion of modularity, the idea that a subset of variables in a system may be changed independent of the remaining variables in the system (Lipson *et al.*, 2002) – in this case Pt leads to a drastic change during early development to one part of the body without lethal consequences to the whole organism.

We cannot exclude that similar, mutation-based body plan alterations have contributed to the evolution of shell internalizations in several molluscan taxa as we know them today.

Acknowledgements

The authors thank K.-H. Hellmer for technical assistance with the SEM, J. Oehlmann for initially providing a *M. cornuarietis* stock, A. Dieterich for help with tomography imaging, and R. Paxton and two anonymous reviewers for critical comments on the manuscript. Studienstiftung des deutschen Volkes and Landesgraduiertenförderung Baden-Württemberg are highly acknowledged for financial support.

References

Beeby, A., Richmond, L. and Herpé, F., 2002. Lead reduces shell mass in juvenile garden snails (*Helix aspersa*). *Environ. Pollut.* 120:283–288.

Bradford, M.M., 1976. A rapid and sensitive method for the quantitation of microgram quantities of protein utilizing the principle of protein-dye binding. *Anal. Biochem.* 72:248–254.

Burnett, L.E., Woodson, P.B.J., Rietow, M.G. and Vilicich, V.C., 1981. Crab gill intra-epithelial carbonic anhydrase plays a major role in haemolymph CO_2 and chloride ion regulation. *J. Exp. Biol.* 92:243–254.

Christensen, G.M. and Tucker, J.H., 1976. Effects of selected water toxicants on the in vitro activity of fish carbonic anhydrase. *Chem.Biol. Interact.* 13:181–192.

Costlow, J.D., 1959. Effects of carbonic anhydrase inhibitors on shell development and growth of *Balanus improvisus* Darwin. *Physiol. Zool.* 32:177–189.

Crawford, K., 2003. Lithium chloride inhibits development along the animal vegetal axis and anterior midline of the squid embryo. *Biol. Bull.* 205:181–182.

Crofts, D.R., 1937. The development of *Haliotis tuberculata* with special reference to organogenesis during torsion. *Philos. Trans. R. Soc. Lond. B* 228:219–268.

Crofts, D.R., 1955. Muscle morphogenesis in primitive gastropods and its relation to torsion. *Proc. Zool. Soc. Lond.* 125:711–750.

Demian, E.S. and Yousif, F., 1973a. Embryonic development and organogenesis in the snail *Marisa cornuarietis* (Mesogastropoda: Ampullariidae). I. General outlines of development. *Malacologia* 12:123–150.

Demian, E.S. and Yousif, F., 1973b. Embryonic development and organogenesis in the snail *Marisa cornuarietis* (Mesogastropoda: Ampullariidae). II. Development of the alimentary system. *Malacologia* 12:151–174.

Demian, E.S. and Yousif, F., 1973c. Embryonic development and organogenesis in the snail *Marisa cornuarietis* (Mesogastropoda: Ampullariidae). III. Development of the circulatory and renal systems. *Malacologia* 12:175–194.

Demian, E.S. and Yousif, F., 1973d. Embryonic development and organogenesis in the snail *Marisa cornuarietis* (Mesogastropoda: Ampullariidae). IV. Development of the shell gland, mantle and respiratory organs. *Malacologia* 12:195–211.

Demian, E.S. and Yousif, F., 1975. Embryonic development and organogenesis in the snail *Marisa cornuarietis* (Mesogastropoda: Ampullariidae). V. Development of the nervous system. *Malacologia* 15:29–42.

Furbish, D.R. and Furbish, W.J., 1984. Structure, crystallography, and morphogenesis of the cryptic shell of the terrestrial slug *Limax maximus* (Mollusca, Gastropoda). *J. Morphol.* 180:195–212.

Garstang, W., 1929. The origin and evolution of larval forms. *Rep. Brit. Assoc. Adv. Sci. Section* D:77–98.

Gibson GD., 2003. Larval development and metamorphosis in *Pleurobranchaea maculata*, with a review of development in the notaspidea (Opisthobranchia). *Biol. Bull.* 205:121–132.

Giraud, M.M., 1981. Carbonic anhydrase activity in the integument of the crab *Carcinus maenas* during the intermold cycle. *Comp. Biochem. Physiol.* 69A:381–387.

Heethoff, M. and Cloetens, P.A., 2008. Comparison of synchrotron X-ray phase contrast tomography and holotomography for non-invasive investigations of the internal anatomy of mites. *Soil Organisms* 80:205–215.

Henry, R.P., 1991. Techniques for measuring carbonic anhydrase activity in vitro: the electrometric delta pH and pH stat methods. In: Dodgson, S.J., Tashien, R.E., Gros, G., Carter, N.D. (eds). *The Carbonic Anhydrases: Cell. Physiol. Mol. Gen.* New York: Plenum Press. pp. 119–125.

Hickman, C.S., and Hadfield, M.G., 2001. Larval Muscle Contraction Fails to Produce Torsion in a Trochoidean Gastropod. *Biol Bull* 200:257-260.

Kao, K.R., Masui, Y. and Elinson, R.P., 1986. Lithium-induced respecification of pattern in *Xenopus laevis* embryos.*Nature* (Lond.) 322 371–373.

Kniprath, E. 1981. Ontogeny of the molluscan shell field: a review: *Zool. Scr.* 10:61–79.

Lipson, H., Pollack, J.B., Suh, N.P., 2002. On the origin of modular variation. *Evolution* 56:1549–1556.

Maren, T.H., 1967. Carbonic anhydrase: chemistry, physiology, and inhibition. *Physiol. Rev.* 47:595–781.

Morgan, I.J., Henry, R.P. and Wood, C.M., 1997. The mechanism of acute silver nitrate toxicity in freshwater rainbow trout (*Oncorhynchus mykiss*) is inhibition of Na- and Cl- transport. *Aquat. Toxicol.* 39:145–163.

OECD Guideline for Testing of Chemicals, 1992. *Test Guideline 203: Fish, Acute Toxicity Test.*

Osterauer, R., Haus, N., Sures, B. and Köhler, H.-R., 2009. Uptake of platinum by zebrafish (*Danio rerio*) and ramshorn snail (*Marisa cornuarietis*) and resulting effects on early embryogenesis. *Chemosphere* 77:975–982.

Osterauer, R., Köhler, H.-R. and Triebskorn, R., 2010. Histopathological alterations and induction of stress proteins in ramshorn snail (*Marisa cornuarietis*) and zebrafish (*Danio rerio*) after exposure to $PtCl_2$ during embryogenesis. *Aquat. Toxicol.* 99:100–107.

Page, L.R., 2000. Inflated protoconchs and internally dissolved, coiled protoconchs of nudibranch larvae: different developmental trajectories achieve the same morphological result. *Invertebrate Biol.* 119:278–286.

Page, L.R., 2002. Ontogenetic torsion in two basal gastropods occurs without shell attachments for larval retractor muscles.*Evol. Dev.* 4: 212–222.

Rousseau, M., Plouguerne, E., Wan, G., Wan, R., Lopez, E. and Fouchereau-Peron, M., 2003. Biomineralization markers during a phase of active growth in *Pinctada margaritifera*. *Comp. Biochem. Physiol.* 135:271–278.

Sawasdee, B. and Köhler, H.-R., 2009. Embryo toxicity of pesticides and heavy metals to the ramshorn snail, *Marisa cornuarietis* (Prosobranchia). *Chemosphere* 75:1539–1547.

Scheltema, A. H. and Schander, C., 2006. Exoskeletons: Tracing molluscan evolution. *Venus* 65: 19–26.

Schirling, M., Bohlen, A., Triebskorn, R. and Köhler, H.-R., 2006. An invertebrate embryo test with the apple snail *Marisa cornuarietis* to assess effects of potential developmental and endocrine disruptors. *Chemosphere* 64: 1730–1738.

Sures, B., Taraschewski, H. and Haug, C., 1995. Determination of trace metals (Cd, Pb) in fish by electrothermal atomic absorption spectrometry after microwave digestion. *Anal. Chim. Acta* 311:135–139.

Takaichi, S., Mizuhira, V., Hasegawa, H., Suzaki, T., Notoya, M., Ejiri, S., Ozawa, H. and Van Wyk, J.H., 2003. Ultrastructure and early embryonic shell formation in the terrestrial pulmonate snail, *Euhadra hickonis*. *J. Moll. Stud.* 69: 229–244.

Triebskorn, R., Bader, K., Linder, B. and Köhler, H.-R., 2005. Snails and slugs as non-targets for environmental chemicals. *IOBC Bull.* 28:1–9.

Vitale, A.M., Monserrat, J.M., Castilho, P. and Rodriguez, E.M., 1999. Inhibitory effects of cadmium on carbonic anhydrase activity and ionic regulation of the estuarine crab *Chasmagnathus granulata* (Decapoda, Grapsidae). *Comp. Biochem. Physiol. C* 122:121–129.

Wägele, H. and Klussmann-Kolb A., 2005. Opisthobranchia (Mollusca, Gastropoda) – more than just slimy slugs. Shell reduction and its implications on defence and foraging. *Frontiers in Zoology* 2:1-18.

Waller, T.R., 1981. Functional morphology and development of veliger larvae of the European Oyster, *Ostrea edulis* Linné. *Smithsonian Contrib. Zool.* 328:1–70.

Wanninger, A., Ruthensteiner, B. and Haszprunar, G., 2000. Torsion in Patella caerulea (Mollusca, Patellogastropoda): ontogenetic process, timing, and mechanisms. *Invert. Biol.* 119:177–187.

Wilbur, K.M. and Saleuddin, A.S.M., 1983. Shell formation. In: Saleuddin, A.S.M., Wilbur, K.M. (Eds.), *The Mollusca* 4. Academic Press, New York. Pp. 235–287.

Zimmermann, S., Menzel, C.M., Berner, Z., Eckhardt, J.D., Stuben, D., Alt, F., Messerschmidt, J., Taraschewski, H. and Sures, B., 2001. Trace analysis of platinum in biological samples: a

comparison between sector field ICP-MS and adsorptive cathodic stripping voltammetry following different digestion procedures. *Anal. Chim. Acta* 439:203–209.

Zimmermann, S., Messerschmidt, J., von Bohlen, A. and Sures, B., 2003. Determination of Pt, Pd and Rh in biological samples by electrothermal atomic absorption spectromety as compared with adsorptive cathodic stripping voltammetry and total-reflexion X-ray fluorescence analysis. *Anal. Chim. Acta* 498:93–104.

Kapitel 2: Arresting mantle formation and redirecting embryonic shell gland tissue by Platinum^{2+} leads to body plan modifications in *Marisa cornuarietis* (Gastropoda, Ampullariidae)[6]

Leonie Marschner[1], Rita Triebskorn[1,2] ,Heinz-R. Köhler[1]

[1] *Animal Physiological Ecology, Institute of Evolution and Ecology, Biology Department, University of Tübingen, Tübingen D-72072, Germany*

[2] *Transfer Center for Ecotoxicology and Ecophysiology, Rottenburg 72108, Germany*

Abstract

To evaluate the threat that anthropogenic substances pose to animals when they are emitted into the environment, tests like the invertebrate embryo toxicity test with the ramshorn snail *Marisa cornuarietis* have been developed. These tests are used to investigate substances like the heavy metal platinum (Pt) that is used in catalytic converters and is gradually released in car exhausts. In 2010, our group reported that high Pt concentrations cause body plan alterations in snails and prevent the formation of an external shell during *M. cornuarietis* embryogenesis. Now, this study presents scanning-electron micrographs and histological sections of platinum^{2+} (Pt^{2+})-treated and untreated *M. cornuarietis* embryos and compares "normally" developing and "shell-less" embryos during embryogenesis, to reveal the exact course of

[6] J. Morphol. 273:830–841, 2012,

events that lead to this body plan shift. Both groups showed similar development until the onset of torsion 70- to 82-h postfertilization. In the Pt^{2+}-exposed embryos, the rudimentary shell gland (=anlage of both shell gland and mantle, which usually evaginates, grows, and eventually covers the visceral sac) does not spread across the visceral sac but remains on its ventral side. Without the excessive growth of the shell gland, a horizontal rotation of the visceral sac relative to head and foot does not occur, as being normal during the process of torsion. J. Morphol. 273:830–841, 2012.

Key words: *Marisa cornuarietis*; platinum; embryogenesis; mantle formation; torsion

Introduction

Numerous reports document how heavy metals affect embryonic development of vertebrates and invertebrates: they can block or alter development in polychaetes (Gopalakrishnan *et al.*, 2008), induce developmental anomalies in sea urchin embryos (Kobayashi and Okamura, 2004), and delay, alter, or arrest development in fish (Jezierska *et al.*, 2008).

Consequently, several heavy metals have also been tested on embryos of the ramshorn snail *Marisa cornuarietis*, and the effects ranged from early hatching (copper and lead) to delayed development (nickel, zinc, copper, palladium, lithium, and lead) and increased mortality (zinc and copper; Sawasdee and Köhler, 2009, 2010). The induced developmental changes are rarely as spectacular as the effect of platinum on *M. cornuarietis* embryogenesis. Osterauer *et al.* (2010b) showed that exposure to high platinum concentrations during embryogenesis reproducibly prevents the formation of the external shell in *Marisa* and redirects the formation of the "shell" to the snail's interior. In addition, a mantle is not present in the transformed snails, which also show alterations in the position of organs that deviate from the conventional arrangement defined by the process of torsion. The term torsion describes a morphogenetic process that is unique to the gas-

tropods (Crofts, 1937, summarized by Page, 2006a). During this process, the visceropallium, which includes most of the visceral organs, rotates 180° anticlockwise relative to the cephalopodium (head and foot), leading to a reorganization of tissues and organs. The post-torsional state is characterized by an anterior mantle cavity with anus and ctenidium and the crossing of the pleurovisceral nerve connectives, which is known as streptoneury. This horizontal, anticlockwise rotation by 180° can be observed in developing embryos of patellogastropods and some vetigastropods ("ontogenetic torsion"). Such a rotation can also be observed in our test animal, *M. cornuarietis* (Demian and Yousif, 1973a), although it undergoes a direct development inside a capsule instead of the indirect development with a veliger larva like vetigastropods and patellogastropods. In contrast to extant gastropods, the molluscan archetype is hypothesized to have a posterior mantle cavity with posterior ctenidium and anus as well as uncrossed pleurovisceral nerve cords (Garstang, 1929, summarized by Page, 2006a) and, thus, could be described as untorted.

Two different mechanisms have been discussed as possible causes for torsion in gastropods. Crofts (1937, 1955) suggested a process involving larval retractor muscles attached to the protoconch, whereas Haszprunar (1988) and Ponder and Lindberg (1997) suggested differential growth to be the cause for torsion. In the case of *M. cornuarietis*, Demian and Yousif (1973a) reported that the rotation of the visceral sac must be the result of differential growth of the two sides of the embryo, as it has not yet developed any muscles on the onset of this rotation.

Subsequent to the description of conditions causing the mentioned body plan shift (Osterauer *et al.*, 2010b), this article gives details of the platinum-induced alteration of developmental processes in *M. cornuarietis* embryos. It presents scanning-electron micrographs and histological sections of both normal and "shell-less" embryos and compares the morphology and anatomy of the developmental stages of platinum-treated embryos with untreated ones.

Methods

The experiments were conducted on the basis of the *M. cornuarietis* embryo test (MariETT) developed by Schirling *et al.* (2006) and modified as described below. For a detailed description of material, techniques and keeping of *M. cornuarietis* in aquaria see Osterauer *et al.* (2009, 2010a) and Sawasdee and Köhler (2009, 2010). Scanning-electron micrographs and histological sections were compared to the light microscopic observations of *M. cornuarietis* embryonic development as analyzed in detail by Demian and Yousif (1973a–d, 1975). All experiments were conducted in the laboratories of the Institute of Evolution and Ecology, Tubingen University, between 17 June 2008 and 24 July 2008 (SEM) and 14 January 2010 and 3 August 2010 (histology). All animal care regulations and legal requirements were adhered to.

Rearing of shell-less *M. cornuarietis*

On the first day of the experiment, all freshly deposited egg clutches were carefully removed from the aquaria; the single eggs were separated from each other using a razor blade and were then distributed into Petri dishes in a way that all Petri dishes received 30 eggs. Petri dishes were made from polystyrol and had a diameter of 94 mm. They were filled with the test solution, or, for the water control, aquarium water.

For platinum^{2+} exposure, a solution of nominally 200 μg/l platinum chloride (corresponding to a real concentration of 163.4 $\pm$ 2.7 μg Pt/l, Osterauer *et al.*, 2010b) was used, made from one liter aquarium water and 200 μl platinum chloride standard solution (platinum standard, Ultra Scientific, Wesel, Germany, 1,000 μg/ml, Matrix: 98% water, 2% HCl). The Petri dishes were kept at 26 °C in a climate chamber at a light–dark regime of 12:12 h. The test solutions were changed daily. Some shell-less embryos were transferred to aquarium water after completion of embryonic development, and raised.

Pictures taken of living shell-less *M. cornuarietis* were edited in GIMP (scaling, rotating, and cropping), labeling was added in Inkscape.

Scanning electron microscopy

All Petri dishes received eggs from at least three different clutches. Embryos were fixed at different stages of their development. Every day, beginning with the first day of the experiment (age 0 day), 10–12 embryos were removed from their eggs and transferred into fixative (2% glutaraldehyde (VWR-Merck) dissolved in 0.01 mol l^{-1} cacodylate buffer (VWR-Merck), pH 7.4). For each timepoint, two specific Petri dishes were used, one for the control and one for the platinum exposure. As the eggs were taken from different clutches, slight differences in age were possible. Used Petri dishes were discarded.

The eggs were opened with two syringes, and the embryos were removed and then transferred into snap-cap vials using an Eppendorff pipette. The snap-cap vials were filled with the mentioned fixative. Until further processing the samples were kept at 4 °C.

Processing started with rinsing the embryos in 0.01 mol l^{-1} cacodylate buffer (three times for 10 min each). The embryos were then stained overnight with reduced osmium tetroxide and dehydrated successively with 75%, 80%, 85%, 95% and absolute ethanol (three times 15 min for each concentration). The specimens were then critical point dried, mounted on stubs, and sputtered with gold. They were examined with a scanning electron microscope (Cambridge Stereoscan 250 Mk2, Cambridge Scientific, Cambridge, UK), and pictures were taken. The images were edited with Adobe Photoshop CS2 (Adobe Systems; converting, cropping, and background color), GIMP 2.6 (converting, cropping, and scaling), and Inkscape 0.48 (converting and labeling) and examined visually.

Histology

Every day, beginning with the first day of the experiment, between six and fifteen embryos from both control and the platinum group were removed from the egg capsules (description see earlier) and fixed in Bouin's solution overnight or for several days. The embryos fixed on a given day all derived from the same clutch, assuring that control and platinum embryos were all of exactly the same age. After fixation, the embryos were washed

three times for 10 min with 70% ethanol containing one drop of 32% NH_3, dehydrated in a graded series of ethanol (70, 80, 90, 96, and 100%, three times for 10 min each) and embedded in Technovit (Heraeus Kulzer, Germany). An automatic microtome (2050 Supercut, Reichert-Jung, Germany) was used to cut serial sections of 2- to 5-μm thickness, which were mounted on microscope slides and stained with hematoxylin/eosin or methylene blue. The slides were covered with Histokitt (Roth, Germany) and examined and photographed with a light microscope (Axioskop 2, Zeiss, Germany). GIMP was used for image editing (converting, scaling, rotating, white balancing, color adjustment, and sharpening). Some SEM-images were vectorized with Inkscape and these scetches were then inserted into the pictures. Labeling was also done with Inkscape.

Results

The "normal" development will only be described briefly (for more detailed descriptions see Demian and Yousif, 1973a–d, 1975) and compared to the embryonic development under the influence of platinum. To make comparisons easier, we used the terminology and abbreviations that were introduced by Demian and Yousif (1973a) and added some new ones to better describe the anatomy of platinum^{2+} (Pt^{2+})-exposed snails. In this context, the term "rudimentary shell gland" indicates the tissue that is in fact the common anlage of the mantle and the shell gland, which spread over the visceral sac in control snails.

In Stage VI (according to the classification by Demian and Yousif (1973a,c)) the rudimentary shell gland has bulged up and its peripheral cells form a thickened ridge that will develop into the adult's shell gland. For this circular thickening the term "shell gland" is used. This nomenclature deviates from Eyster (1986) and Kniprath (1977) who both used the term "shell field" for the whole shell-secreting tissue and the term shell gland for the invaginated shell field only.

The central, bulged up part of the rudimentary shell gland that is encircled by the shell gland will develop into the outer mantle epithelium and will be

called “mantle anlage”.

One-day-old embryos

Figure 1A shows an embryo from the water control in the gastrula stage. In 1-day-old embryos, there is no visible difference between Pt-exposed embryos and the control.

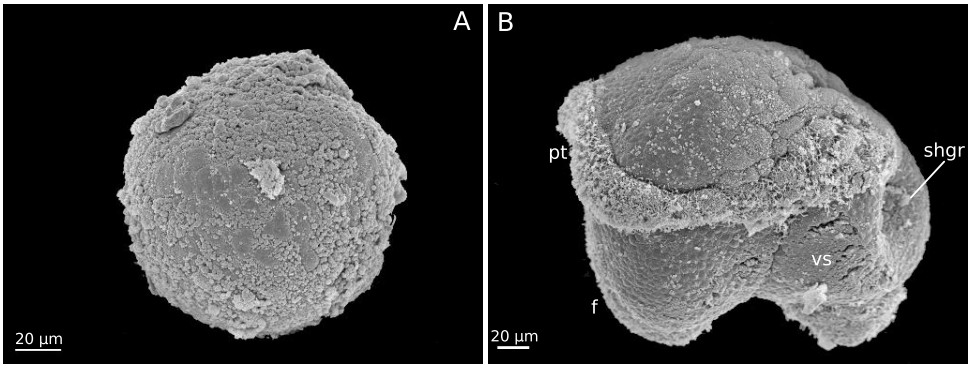

Fig. 1: *M. cornuarietis*, 1- and 2-day-old embryos; A: control embryo in gastrula stage; B: Pt-exposed embryo in Stage IV, left lateral view. f, foot; pt, prototroch; shgr, rudimentary shell gland; vs, visceral sac.

Two-day-old embryos

Figure 1B shows a 2-day-old embryo from the platinum exposure group. It matches the description given by Demian and Yousif (1973a) for embryos at about 48 h after oviposition (Stage IV). The foot rudiment and the developing visceral sac are clearly distinguishable. The rudimentary shell gland forms a depression on the visceral sac. The prototroch marks the region where the head will develop. Up to this timepoint, the embryos from the platinum exposure do not differ from those from the water control (not shown).

Three-day-old embryos

After 3 days of development, the control embryo in Figure 2A matches what Demian and Yousif (1973a) named Stage VII: head, foot, and visceral sac can clearly be distinguished. The foot has elongated, and the visceral sac

has become flattened laterally. The rudimentary shell gland enlarges and has shifted to the left of the visceral sac. Its central part, the mantle anlage, has grown excessively and, also according to Demian and Yousif (1973a), induces an anticlockwise rotation of the visceral sac (by an extremely imbalanced growth of both lateral sides) and the formation of the mantle.

In contrast, embryos exposed to platinum correspond to Stage V or VI after 3 days of development (Fig. 2C). The prototroch is still clearly visible, and the visceral sac is only slightly enlarged. The rudimentary shell gland still forms a depression on the visceral sac, and the mantle edge is not enlarged as well. Figure 2B,D depicts histological sections of the visceral sac showing the similarity in the anatomy of differently treated embryos.

Embryos both from the control (Fig. 2B) and the platinum group (Fig. 2D) resemble normally developing *M. cornuarietis* embryos in Demian and Yousif 's Stage VI. In both groups, the rudimentary shell gland has enlarged in comparison to earlier stages. Its center, the mantle anlage, has bulged up and is covered by a thin layer, the protoconch, or larval shell. Its peripheral cells have formed a thickened circle that is expected to become the adult's shell gland in the conventional body plan. In this stage, the mantle edge is a protruding fold that encircles the shell gland.

Four- and four-and-a-half-day-old embryos

At this stage of development, the embryo from the water control (Fig. 3A,B) can easily be recognized as a snail. The tentacles have started to be formed, and the mouth has developed. The foot has reached its final shape and position. Between foot and shell, the operculum has been formed. The shell covers almost all the visceral sac. The mantle edge, a thick ridge, limits the extension of the shell to the anterior.

Pt-exposed embryos (Fig. 3C,D) are clearly lagging behind in their development compared to controls. They resemble embryos in Stage VI or VII except for features of shell formation. In Stage VI, when the rudimentary shell gland usually enlarges, bulges outward, and thickens at the periphery (shell gland of the adult), platinum arrests outgrowth completely or right af-

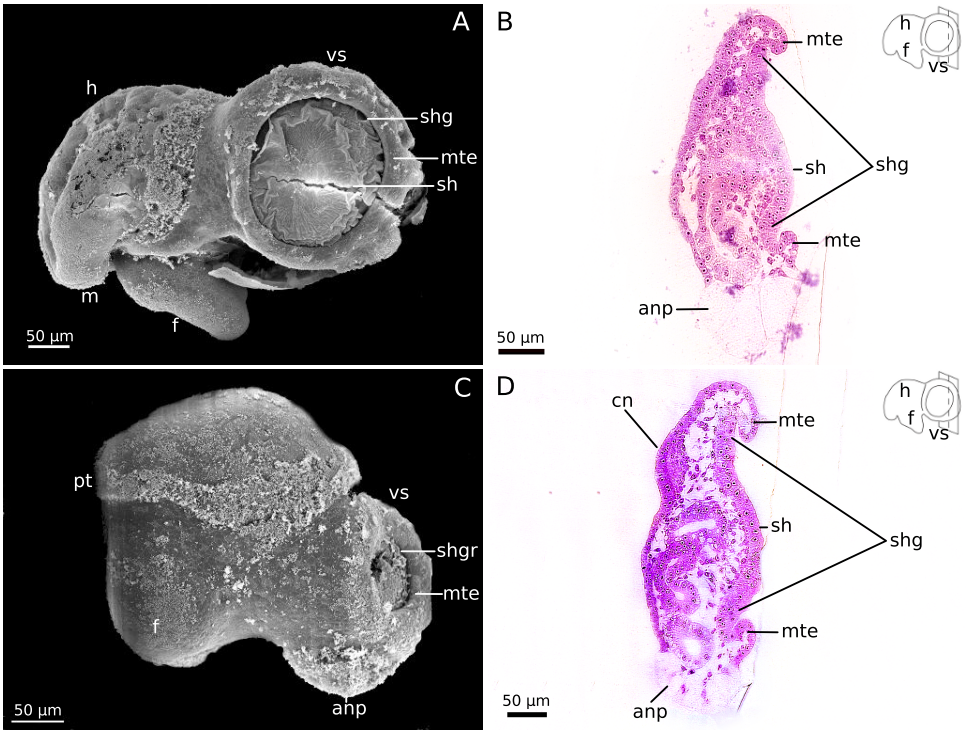

Fig. 2: *M. cornuarietis*, 3-day-old embryos; A: control embryo in Stage VII, left lateral view (from Osterauer *et al.*, Evol Dev, 2010, 12, 474–443, ©Wiley-Blackwell, reproduced by permission); B: histological transverse section of a control embryo, plane of section indicated by dashed line in sketch (left lateral view); C: Pt-exposed embryo, left lateral view; and D: histological transverse section of a Pt-exposed embryo, plane of section indicated by dashed line in sketch (left lateral view). anp, anal cell-plate; cn, ctenidium; f, foot; h, head; m, mouth; mte, mantle edge; pt, prototroch; sh, shell; shg, shell gland; shgr, rudimentary shell gland; vs, visceral sac. [Color figure can be viewed in the online issue, which is available at wileyonlinelibrary.com.]

ter the initial steps of evagination. Subsequently, the rudimentary shell gland does not evaginate further but invaginates into the body of the animals.

Figure 3B,D shows horizontal sections of embryos from both control and Pt-exposed groups. In both embryos, the anus can be recognized on the right side of the visceral sac. In the control, the visceral sac is covered by the mantle anlage, which, in turn, is covered by the shell. In the embryo from the platinum group, the mantle anlage has stopped growing and does not cover the visceral sac.

Comparing the horizontal sections in Figure 4A (control) and B (platinum

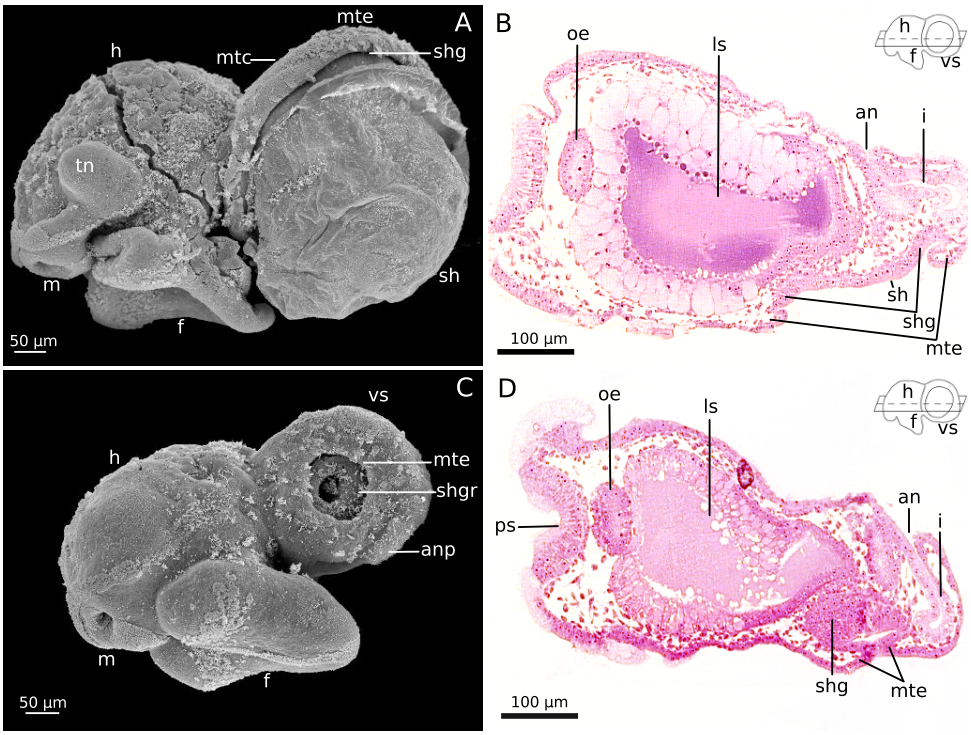

Fig. 3: *M. cornuarietis*, 4- and 4.5-day-old embryos; A: control embryo in Stage IX, 4-day old, left lateral view; B: histological horizontal section of a control embryo, 4-day old, plane of section indicated by dashed line in sketch (left lateral view), HE-staining; C: Pt-exposed embryo, 4-day old, left lateral view (from Osterauer *et al.*, Evol Dev, 2010, 12, 474–443, ©Wiley-Blackwell, reproduced by permission); and D: histological horizontal section of a Pt-exposed embryo, 4.5-day old, plane of section indicated by dashed line in sketch (left lateral view), HE-staining. an, anus; anp, anal cell-plate; f, foot; h, head; i, intestine; ls, larval stomach; m, mouth; mtc, mantle cavity; mte, mantle edge; oe, oesophagus; ps, peristome; sh, shell; shg, shell gland; shgr, rudimentary shell gland; tn; tentacle; vs, visceral sac. [Color figure can be viewed in the online issue, which is available at wileyonlinelibrary.com.]

exposure), it is obvious that a horizontal rotation of the visceral sac relative to head and foot does not take place in the platinum group. This can also be seen in Figure 4C,D. Figure 4C shows a transverse section through a control embryo. The mantle anlage (under the shell) has spread across the visceral sac, which leads to a rotation of the visceral sac while forming the outer epithelium of the mantle. During this process, the mantle cavity develops. In contrast, the embryo from the platinum group (Fig. 4D) neither develops a mantle cavity nor a mantle itself. The mantle anlage has stopped growing,

and the visceral sac remains uncovered. The ctenidium stays on the dorsal side of the visceral sac instead of being moved into the mantle cavity by the growing mantle.

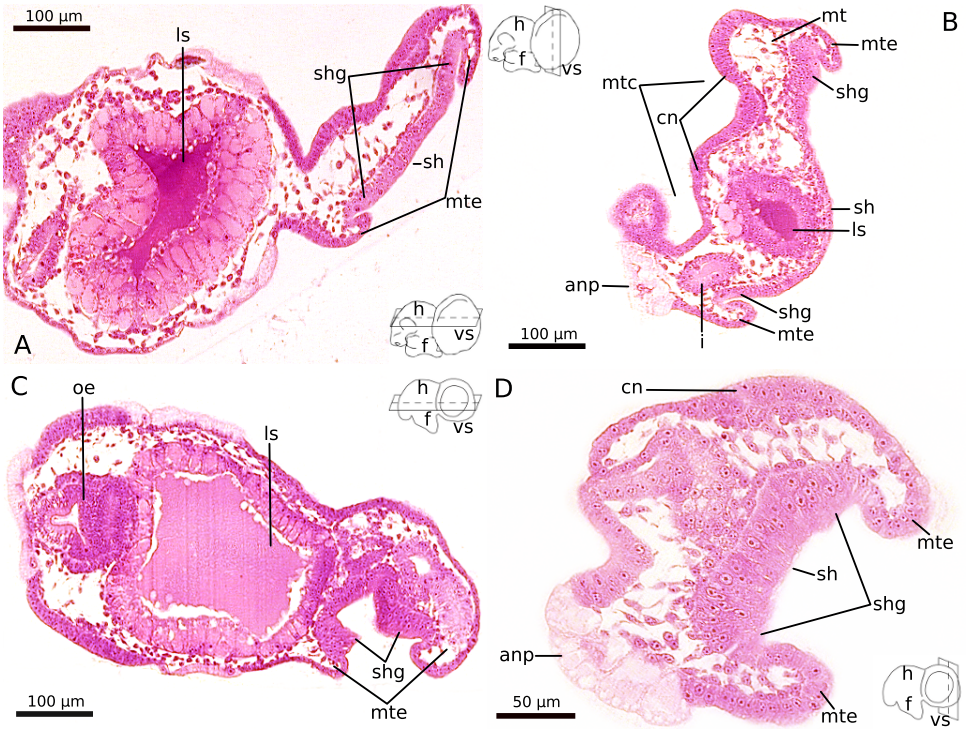

Fig. 4: *M. cornuarietis*, histological sections of 4.5-day-old embryos, planes of section indicated by dashed lines in sketches (all left lateral view), HE-staining; A: control embryo, horizontal section; B: control embryo, transverse section; C: Pt-exposed embryo, horizontal section; and D: Pt-exposed embryo, transverse section. anp, anal cell-plate; cn, ctenidium; f, foot; h, head; i, intestine; ls, larval stomach; mtc, mantle cavity; mt, mantle; mte, mantle edge; oe, oesophagus; sh, shell; shg, shell gland; vs, visceral sac. [Color figure can be viewed in the online issue, which is available at wileyonlinelibrary.com.]

Five-day-old embryos

Figure 5A,B shows 5-day-old control embryos. The rotation of the visceral sac has been completed, the tentacles have been elongated further,and the eyes can be recognized. As expected, the visceral sac is completely covered by the shell.

Embryos from the platinum exposure group (Fig. 5C,D) have also de-

veloped further: the foot is clearly formed, and the tentacles have started budding. These criteria correspond to what could be expected for a control embryo in Demian and Yousif 's Stage IX. This resemblance, however, does not include the visceral sac. The mantle anlage seems to have enlarged but not enough to cover a significant part of the visceral sac. Furthermore, it is still positioned in its initial position on the ventro-lateral side of the visceral sac, where a cap-like shell can now be seen. A horizontal, anticlockwise rotation of the visceral sac still does not occur.

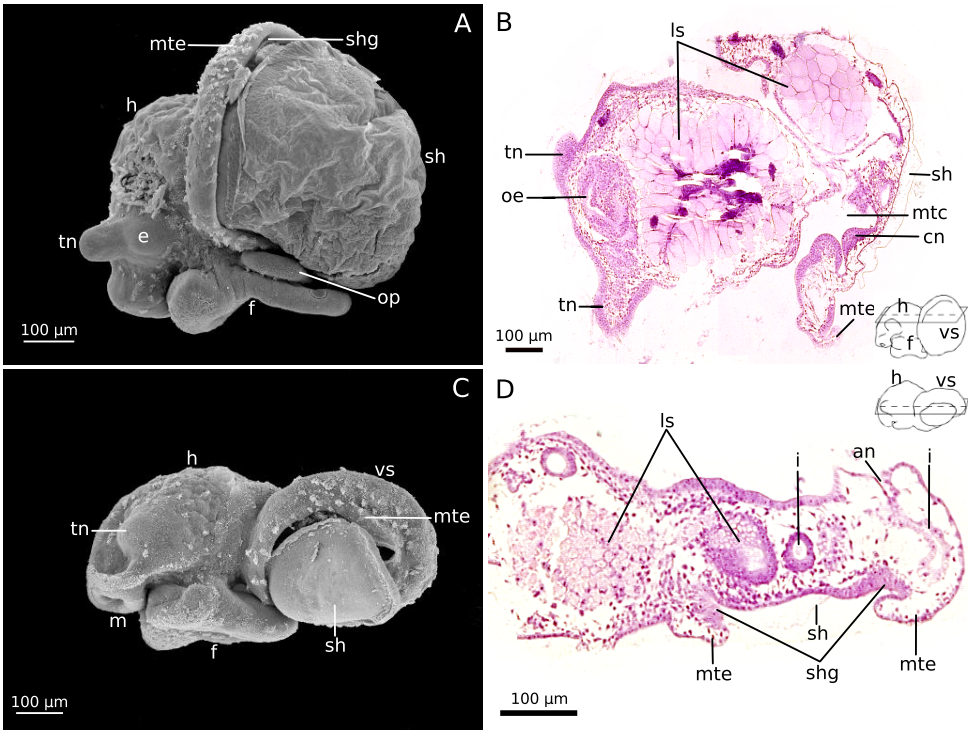

Fig. 5: *M. cornuarietis*, 5-day-old embryos; A: control embryo in Stage X, left lateral view (from Osterauer *et al.*, Evol Dev, 2010, 12, 474–443, ©Wiley-Blackwell, reproduced by permission); B: histological horizontal section of a control embryo, plane of section indicated by dashed line in sketch (left lateral view), HE-staining; C: Pt-exposed embryo, left lateral view; and D: histological horizontal section of a Pt-exposed embryo, plane of section indicated by dashed line in sketch (left lateral view), HE-staining. an, anus; cn, ctenidium; e, eye; f, foot; h, head; i, intestine; ls, larval stomach; m, mouth; mtc, mantle cavity; mte, mantle edge; oe, oesophagus; op, operculum; sh, shell; shg, shell gland; tn, tentacle; vs, visceral sac. [Color figure can be viewed in the online issue, which is available at wileyonlinelibrary.com.]

Seven-day-old embryos

At the age of 7 days, the embryos from the control almost completely resemble adult snails in shape (Fig. 6A). The tissue covering the dorsal side of the visceral sac usually forms the lining of the mantle cavity, whereas the tissue on its ventral side, the mantle anlage under the shell, covers the visceral sac. In contrast to this conventional anatomy, Figure 6B shows a sagittal section of the visceral sac of a Pt-exposed embryo. The distal parts of the mantle edge and shell gland shown in Figure 6B (Pt-exposed) correspond to the parts of the mantle edge and shell gland that are located above the head in controls (Fig. 6A). The proximal part of the shell gland in Pt-exposed animals (Fig. 6B) is found at exactly the same position right above the foot as in controls (Fig. 6A).

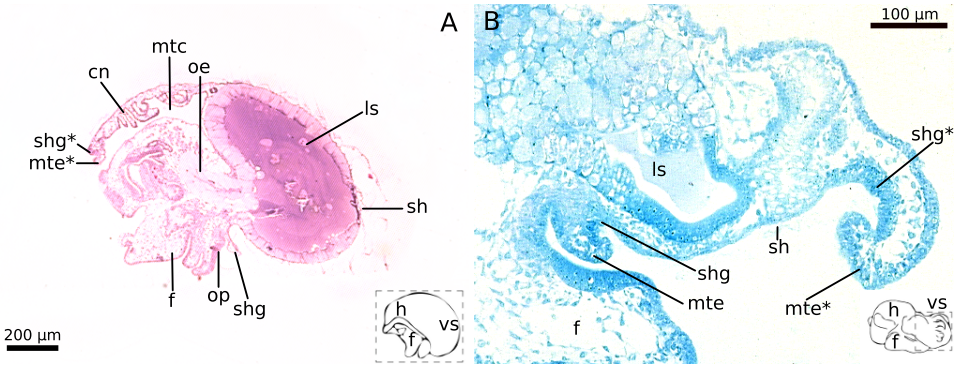

Fig. 6: *M. cornuarietis*, 7-day-old embryos, asterisks indicate corresponding structures; A: control embryo, sagittal section, plane of section indicated by dashed lines in sketch (left lateral view), HE-staining and B: Pt-exposed embryo, sagittal section through the visceral sac and foot; detail and plane of section indicated by dashed lines in sketch (left lateral view), methylene blue staining. cn, ctenidium; f, foot; h, head; ls, larval stomach; mtc, mantle cavity; mte, mantle edge; oe, oesophagus; op, operculum; sh, shell; shg, shell gland; vs, visceral sac. [Color figure can be viewed in the online issue, which is available at wileyonlinelibrary.com.]

Nine-day-old embryos

Figure 7A shows the shell of a 9-day-old control embryo. The soft tissue is not visible here, because the animal is completely retracted into its shell in response to the fixation procedure. In Figure 7B, a transverse section

through a control embryo is shown. Until hatching, the embryonic development of controls is completed (Demian and Yousif, 1973a). Also, the embryos from the platinum exposure group have developed further (Fig. 7C). The developmental state of tentacles, foot, and ctenidium now correspond well to control embryos in Stage XI, the stage that is usually reached in controls after 6 days postfertilization. The ctenidium has elongated and added ctenidial leaflets, but it is still located on the left side of the visceral sac. Neither mantle edge nor shell gland nor the mantle anlage have grown craniad but remain to be located on the ventral side of the visceral sac. This can also be seen in Figure 7D, which shows a transverse section through the visceral sac of a Pt- exposed embryo. The shell-secreting tissue (arrows in Fig. 7D) is positioned in a cavity on the ventral side of the visceral sac right above the foot.

The rotation of the visceropallium

Figure 8A shows an embryo from the control group 3-day postfertilization. The visceral sac has rotated approximately 20° anticlockwise (angle between dashed lines 1 and 2 in Fig. 8A). The arrow indicates the direction in which the distal part of the mantle edge and the shell gland will grow as a result of the growth of the mantle anlage and the outer mantle epithelium. In contrast to that, the 4-day-old embryo from the platinum group (Fig. 8) does not show any rotation at all. At the age of 5 days (Fig. 8C), the rotation has been completed in the control embryo, whereas in the embryo from the platinum group the visceral sac still lays on the same axis as head and foot (Fig. 8D). Figure 8D shows that mantle edge, shell gland, and mantle anlage have been shifted from their initial left lateral position to the ventral side of the visceral sac indicating that, instead of a horizontal rotation by 180°, a vertical rotation of the visceral sac by 90° has taken place.

Figure 8E,F displays the positions of intestine and anus in an adult shell-less snail (Fig. 8E, anus with feces) and in a 7-day old, partly dissected embryo from the platinum exposure group (Fig. 8F). A comparison with the description of the development of the alimentary tract by Demian and Yousif

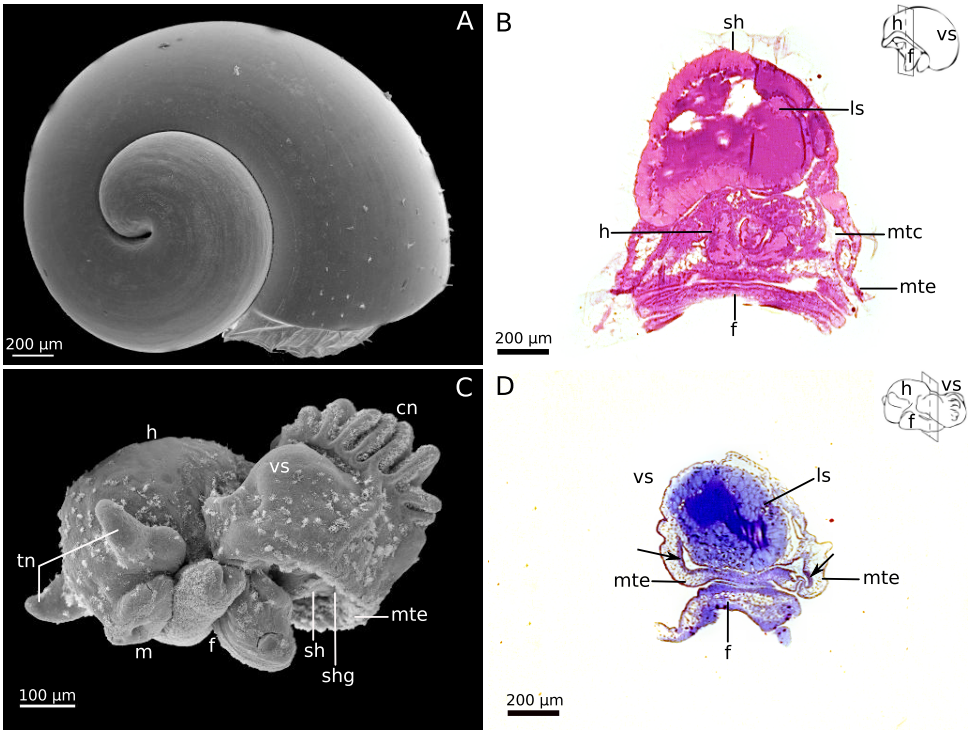

Fig. 7: *M. cornuarietis*, 9-day-old embryos; A: control embryo in Stage XII, right lateral view; B: histological transverse section of a control embryo, plane of section indicated by dashed line in sketch (left lateral view), HE staining; C: Pt-exposed embryo, left lateral view; and D: histological transverse section of a Pt-exposed embryo, arrows indicate shell-secreting tissue, plane of section indicated by dashed line in sketch (left lateral view), methylene blue staining. cn, ctenidium; f, foot; h, head; ls, larval stomach; m, mouth; mtc, mantle cavity; mte, mantle edge; sh, shell; shg, shell gland; tn, tentacle; vs, visceral sac. [Color figure can be viewed in the online issue, which is available at wileyonlinelibrary.com.]

(1973b) makes it evident that they have developed in the same position as in control animals. The shell-less individual in Figure 8E allows a close inspection of the intestine. Its shape resembles the form that was described by Demian and Yousif (1973b) for the usual arrangement of the intestine.

The fate of the mantle edge

Figure 9A–C illustrates the fate of the tissue equivalent to the mantle edge in a Pt-exposed *M. cornuarietis* individual. Figure 9A shows a transverse section of a part of the visceral sac and reveals the mantle edge to be posi-

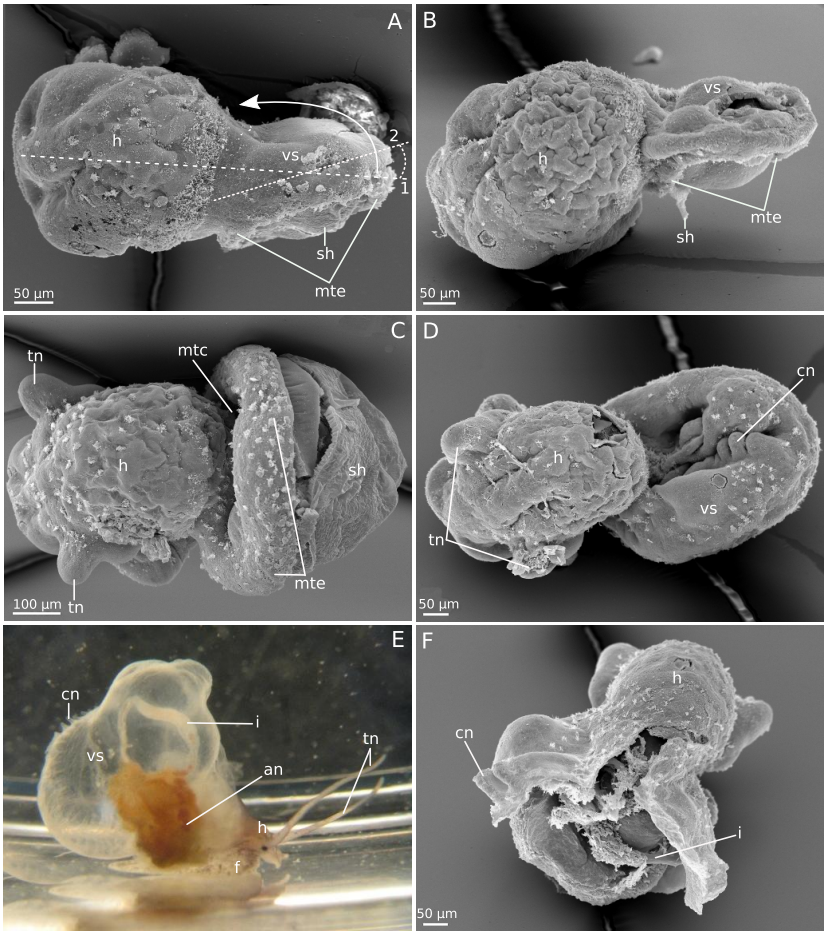

Fig. 8: *M. cornuarietis*, A: control animal, 3-day old, dorsal view, arrow indicates direction of growth of the mantle edge, dashed line 1 symbolizes the longitudinal body axis of head and foot, dashed line 2 symbolizes the longitudinal axis of the visceral sac, and the angle between these two lines indicates the rotation angle; B: animal from the platinum group, 4-day old, dorsal view; C: control animal, 5-day old, dorsal view; D: animal from the platinum group, 6-day old, dorsal view; E: shell-less snail, Pt-exposed, about 3 weeks after hatching, right lateral view; and F: animal from the platinum group, 7-day old, body cavity opened, dorsal view. an, anus; cn, ctenidium; h, head; i, intestine; mtc, mantle cavity; mte, mantle edge; sh, shell; tn, tentacle; vs, visceral sac. [Color figure can be viewed in the online issue, which is available at wileyonlinelibrary.com.]

tioned on the ventral side of the visceral sac. Secretions, forming an internal shell, can be detected in a quite deep cavity that is lined with the tissue that normally forms the mantle. This can also be seen in Figure 9B, which shows a 9-day-old embryo from the platinum group lying on its back. An investi-

gation of internal shells of adult shell-less snails showed that these internal shells consist of calcium carbonate (unpublished data of R. Osterauer and O. Eibl, University of Tubingen, Germany). Occasionally, adult individuals display internal shells bulging out of the snail during further growth (Fig.9C). As shown in this photograph, also in Pt-exposed snails, all organs and tissues that develop from the rudimentary shell gland (mantle with mantle edge and shell gland) become located and, later, remain on the ventral side of the visceral sac dorsal to the foot throughout the shell-less snail's life, and usually are concealed by both the visceral sac and the foot.

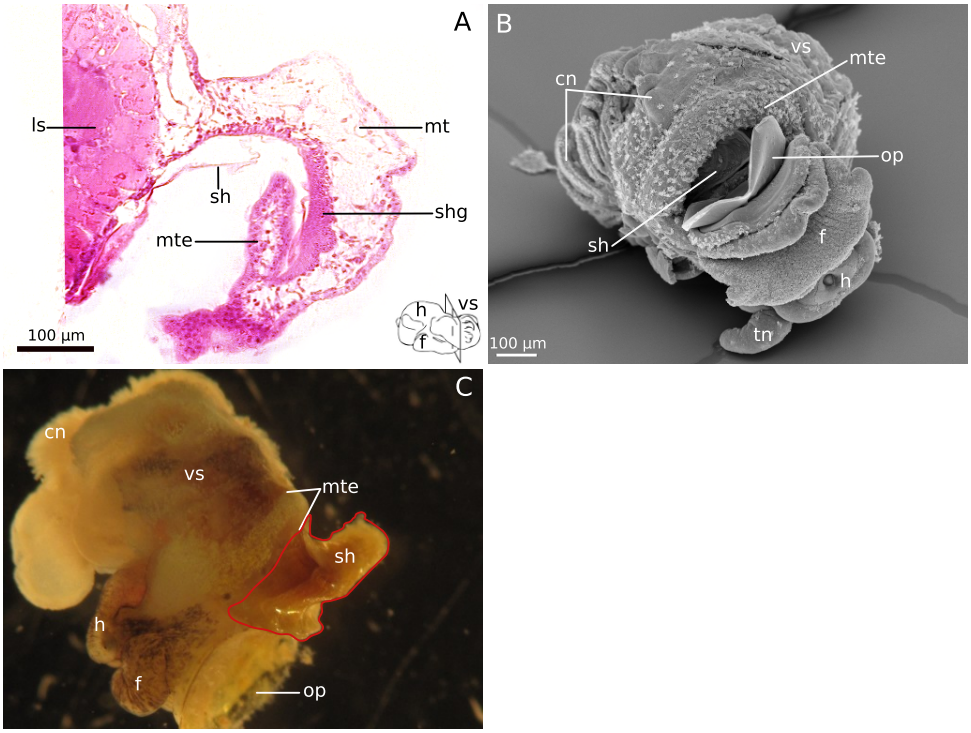

Fig. 9: *M. cornuarietis*, A: histological transverse section of a Pt-exposed embryo, 9-day old, HE staining; B: Pt-exposed embryo, 9-day old, ventral view; and C: adult shell-less *M. cornuarietis* individual (about 4-month old), shell encircled in red, left lateral view. cn, ctenidium; f, foot; h, head; ls, larval stomach; mt, mantle; mte, mantle edge; op, operculum; sh, shell; shg, shell gland; tn, tentacle; vs, visceral sac. [Color figure can be viewed in the online issue, which is available at wileyonlinelibrary.com.]

Discussion

As shown by scanning electron microscopy analysis, Pt^{2+}-treated and untreated *M. cornuarietis* embryos developed similarly until the onset of a torsion-like rotation of the visceral sac between Demian and Yousif 's Stages VI and VII (70–82 h postfertilization at 26 °C) although, generally, the Pt^{2+}-treated embryos developed slower. The severity of the slowing-down effect varied somewhat between the embryos, which accounts for observed variability in embryonic development between different Pt^{2+}-treated embryos of the same age. This retardation of embryonic development in gastropods as a consequence of platinum^{2+} exposure has already been described by Osterauer *et al.* (2009) and has also been shown for other heavy metals (e.g. Ravera, 1991; Gomot, 1998; Coeurdassier *et al.*, 2003; Sawasdee and Köhler, 2009). The slowing-down of embryonic development is not a unique feature of platinum^{2+} on gastropods, whereas its effect on morphogenesis definitely is. Osterauer *et al.* (2010b) reported maximum susceptibility of the embryos to platinum^{2+} at days 4 and 5 of their experiment. Considering the fact that the first day of the experiment in that study, and also in the present one, equals the day of fertilization, exposure on days 4 and 5 means the embryos were 3 and 4 days old, respectively (postfertilization). The most susceptible phase identified by Osterauer *et al.* (2010b) therefore corresponds well to the phase in embryonic development in which the rotation of the visceral sac should commence, and this is exactly the phase in which the first differences between the control and the platinum^{2+} group occurred in this study.

Based on these facts, it can be concluded that platinum^{2+} disrupts normal development just before the visceral sac normally starts rotating anticlockwise. Demian and Yousif (1973a) stated that in *M. cornuarietis* this rotation was caused by differential growth of the two sides of the visceral sac. During normal development, the mantle anlage (the tissue covered by the shell) overgrows the visceral sac and becomes the outer epithelium of the mantle, whereas the tissue that covers the right side of the visceral sac is enfolded into the mantle cavity.

In embryos exposed to bivalent platinum ions, the rudimentary shell gland

first tended to invaginate and its central portion tentatively evaginated, thus forming the mantle anlage. However, this anlage stopped growing before leading to a rotation of the visceral sac and to mantle formation. In older embryos, it could be observed that the whole complex associated with shell secretion and mantle formation (consisting of mantle edge, shell gland, and mantle anlage) did not remain on the lateral side of the embryo but moved to the ventral side of the visceral sac. This movement may be due to a redirection of the counter-clockwise rotation program of the visceral sac. Apparently, the body axis around which differential growth lets the tissues rotate had changed (Fig. 10) and caused the whole visceral sac to rotate vertically by 90°. The described movement alteration is also in accordance with an observation we made during our investigations of the internal anatomy of adult shell-less snails (not yet published): the osphradium, which originates on the right dorso-lateral side of the visceral sac, was finally located on the left ventro-lateral side of the visceral sac in Pt^{2+}- exposed *M. cornuarietis* (unpublished data). This is not a surprise if its anlage rotated vertically by 90° relative to its origin. The orientation of this altered rotation also explains why the ctenidium that differentiates next to the osphradium on the right dorso-lateral side shifted sinistrad relative to its origin.

As Osterauer *et al.* (2010b) described, the shell gland secreted calcium carbonate despite its abnormal position. This calcium carbonate precipitation, called "internal shell", was found to cup the digestive gland inside the snail's body. How these internal shells are secreted exactly is unknown. We also do not yet know about the future of the mantle anlage during postembryonic development. With time, the shell grows larger inside the snail, but shell gland and mantle edge do not expand much. Normally, it would not be possible for the shell to grow into the body because of the underlying tissue (mantle anlage). So for this to happen, the invaginated mantle anlage either followed the growth of the internal shell or it was torn by it as a result of shell growth, two possibilities one may speculate upon. Demian and Yousif (1973c) reported that the mantle first appeared in Stage VII, when the rotation of the visceral sac had begun, as a result of the excessive growth of the mantle anlage. Lacking this outgrowth, Pt^{2+}-exposed embryos neither de-

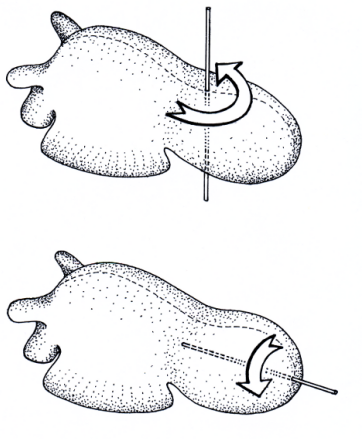

Fig. 10[7]: Hypothetical change in body axis around which the visceral sac rotates; upper sketch: control embryo and lower sketch: Pt-exposed embryo.

veloped a mantle nor a mantle cavity. As described, platinum^{2+} completely stopped mantle anlage growth and, thus, also prevented a physical horizontal rotation of the visceropallium relative to the cephalopodium.

Presuming that the horizontal rotation of the visceral sac in *M. cornuarietis* has similar effects on its body plan as the rotation in vetigastropods and patellogastropods called "torsion", and following the rotation hypothesis proposed by Garstang (1929), one would expect our experimentally modified snails to resemble the hypothetical ancestral mollusc (Page, 1997) and thus to have a posterior anus. However, this was not the case. On the contrary, the intestine seemed to be formed just like in embryos from the control group and the anus in shell-less snails was located at approximately the same position on the right side of the visceral sac just behind the head. At least the intestine ended up in a postrotational position even without the event of rotation itself, that is, the lacking of a horizontal rotation of the visceropallium by 180° relative to the cephalopodium, and despite a vertical rotation of the visceral sac by 90°.

This was not true for the ctenidium. Without the normal, disproportionate growth of the mantle epithelium that pushes the epithelium of the right

[7]Die Zeichnung wurde von Heinz-R. Köhler angefertigt.

side of the visceral sac forward and into the mantle cavity, this right-hand side epithelium in Pt^{2+}-exposed snails became the outer epithelium of the snail's visceropallium instead of just lining the mantle cavity. The ctenidium developed on the right-hand side of the visceral sac and should conventionally also be pushed into the mantle cavity by the growing mantle epithelium. Instead, in Pt^{2+}-exposed *M. cornuarietis*, it remained at the posterior end of the snail and even shifted a bit to the left.

All this suggests that in a shell-less and clearly "nonrotated" *M. cornuarietis* embryo characteristic traits of both "torted" and "untorted" (in the sense of the ancient mollusc type) gastropods could be found. Interpretations are difficult, because the concept of ontogenetic torsion was described in species with planktonic veliger larvae in which a horizontal rotation is clearly visible. Nevertheless, based on the facts that the *M. cornuarietis* visceropallium also shows a clearly visible horizontal rotation and that torsion was defined to be a common feature of all gastropods, we presume that the rotation of the visceral sac in *M. cornuarietis* corresponds at least to some extend to the conventional torsion in vetigastropods and patellogastropods. Our observations lead us to the conclusion hat this torsion-like rotation in *M. cornuarietis* is not a unitary process in one fell swoop and only partly a result of differential growth, as intestine and anus reached their normal positions without a horizontal anticlockwise rotation of the visceral sac (and, furthermore, in spite of a vertical rotation), and that this differential growth affects particularly the outer organs like the ctenidium.

There have been reports on several gastropod species, in which not all components of the visceropallium rotated synchronously (summarized by Page, 2003); and Page (1997) herself reported a "partial torsion" in *Haliotis kamtschatkana* due to a dislocation of pallial tissue which resulted in the mantle cavity and the anus being located on the right side of the embryo despite a full 1808 rotation of the shell. She also found this phenomenon in the gastropods *Trichotropis cancellata*, *Lacuna vincta*, *Haminoea vesicula*, *Pleurobranchea californica*, and *Diodora aspera* (Page, 2003). In *T. cancellata*, she also observed full streptoneury of the pleurovisceral connectives despite a rotation by mere 90° of the visceral sac. She proposed that torsion should

rather be considered a "conserved stage of anatomical organization rather than a conserved process of 180° rotation between two body division" (Page, 2003). In another study (Page, 2006b), she noticed a corotation of a mantle cell connected with the development of the nervous system together with the normally rotating cephalopodium. So, there is evidence that not all displacements of organs or tissues that are supposed to be triggered by torsion are directly caused by a horizontal rotation by 180° of the visceropallium relative to the cephalopodium but that they rather have, at least partly, been falsely attributed to the easily recognizable and simultaneously occurring event.

We regard our *Marisa* system a model to disrupt the torsion-like horizontal rotation of the visceral sac and to separate different, independent developmental modules which, in their entirety, lead to a post-torsional arrangement of organs commonly regarded to be typical for prosobranch snails.

Acknowledgments

The authors are grateful to Oliver Betz (Evolutionary Biology of Invertebrates, University of Tübingen) for the use of his SEM-equipment and to Karl-Heinz Hellmer for technical help. Furthermore, they thank Irene Gust and Matthias Hannig for their help with image editing.

Literature cited

Coeurdassier M, De Vaufleury A, Badot P-M. 2003. Bioconcentration of cadmium and toxic effects on life-history traits of pond snails (*Lymnaea palustris* and *Lymnaea stagnalis*) in laboratory bioassays. *Arch Environ Contam Toxicol* 45:102–109.

Crofts DR. 1937. The development of *Haliotis tuberculata*, with special reference to organogenesis during torsion. Philos Trans R Soc Lond Ser B: Biol Sci 228:219–268.

Crofts DR. 1955. Muscle morphogenesis in primitive gastropods and its relation to torsion. *Proc Zool Soc Lond* 125:711–750.

Demian ES, Yousif F. 1973a. Embryonic development and organogenesis in the snail *Marisa*

cornuarietis (Mesogastropoda: Ampullariidae). I. General outlines of development. *Malacologia* 12:123–150.

Demian ES, Yousif F. 1973b. Embryonic development and organogenesis in the snail *Marisa cornuarietis* (Mesogastropoda: Ampullariidae). II. Development of the alimentary system. *Malacologia* 12:151–174.

Demian ES, Yousif F. 1973c. Embryonic development and organogenesis in the snail *Marisa cornuarietis* (Mesogastropoda: Ampullariidae). IV. Development of the shell gland, mantle and respiratory organs. *Malacologia* 12:195–211.

Demian ES, Yousif F. 1973d. Embryonic development and organogenesis in the snail *Marisa cornuarietis* (Mesogastropoda: Ampullariidae). 3. Development of the circulatory and renal systems. *Malacologia* 12:175–194.

Demian ES, Yousif F. 1975. Embryonic development and organogenesis in the snail *Marisa cornuarietis* (Mesogastropoda: Ampullariidae). V. Development of the nervous system. *Malacologia* 15:29–42.

Eyster LS. 1986. Shell inorganic composition and onset of shell mineralization during bivalve and gastropod embryogenesis. *Biol Bull* 170:211–231.

Garstang W. 1929. The origin and evolution of larval forms. *Rep Br Assoc Adv Sci Sect D* 96:77–98.

Gomot A. 1998. Toxic effects of cadmium on reproduction, development, and hatching in the freshwater snail *Lymnaea stagnalis* for water quality monitoring. *Ecotoxicol Environ Saf* 41:288–297.

Gopalakrishnan S, Thilagam H, Raja PV. 2008. Comparison of heavy metal toxicity in life stages (spermiotoxicity, egg toxicity, embryotoxicity and larval toxicity) of *Hydroides elegans*. *Chemosphere* 71:515–528.

Haszprunar G. 1988. On the origin and evolution of major gastropod groups, with special reference to the streptoneura. *J Mollus Stud* 54:367–441.

Jezierska B, Lugowska K, Witeska M. 2008. The effects of heavy metals on embryonic development of fish (a review). *Fish Physiol Biochem* 35:625–640.

Kniprath E. 1977. Zur Ontogenese des Schalenfeldes von *Lymnaea stagnalis*. *Wilhelm Roux' Archiv* 181:11–30.

Kobayashi N, Okamura H. 2004. Effects of heavy metals on sea urchin embryo development. 1. Tracing the cause by the effects. *Chemosphere* 55:1403–1412.

Osterauer R, Haus N, Sures B, Köhler H-R. 2009. Uptake of platinum by zebrafish (*Danio rerio*) and ramshorn snail (*Marisa cornuarietis*) and resulting effects on early embryogenesis. *Chemo-*

sphere 77:975–982.

Osterauer R, Köhler H-R, Triebskorn R. 2010a. Histopathological alterations and induction of hsp70 in ramshorn snail (*Marisa cornuarietis*) and zebrafish (*Danio rerio*) embryos after exposure to $PtCl_2$. *Aquat Toxicol* 99:100–107.

Osterauer R, Marschner L, Betz O, Gerberding M, Sawasdee B, Cloetens P, Haus N, Sures B, Triebskorn R, Köhler H-R. 2010b. Turning snails into slugs: Induced body plan changes and formation of an internal shell. *Evol Dev* 12:474–483.

Page LR. 1997. Ontogenetic torsion and protoconch form in the archaeogastropod *Haliotis kamtschatkana*: *Evolutionary implications. Acta Zool* 78:227–245.

Page LR. 2003. Gastropod ontogenetic torsion: Developmental remnants of an ancient evolutionary change in body plan. *J Exp Zool* 297B:11–26.

Page LR. 2006a. Modern insights on gastropod development: Reevaluation of the evolution of a novel body plan. *Integr Comp Biol* 46:134–143.

Page LR. 2006b. Early differentiating neuron in larval abalone (*Haliotis kamtschatkana*) reveals the relationship between ontogenetic torsion and crossing of the pleurovisceral nerve cords. *Evol Dev* 8:458–467.

Ponder WF, Lindberg DR. 1997. Towards a phylogeny of gastropod molluscs: An analysis using morphological characters. *Zool J Linn Soc* 119:83–265.

Ravera O. 1991. Influence of heavy metals on the reproduction and embryonic development of freshwater pulmonates (Gastropoda; Mollusca) and cladocerans (Crustacea; Arthropoda). *Comp Biochem Physiol C* 100C:215–219.

Sawasdee B, Köhler H-R. 2009. Embryo toxicity of pesticides and heavy metals to the ramshorn snail, *Marisa cornuarietis* (Prosobranchia). *Chemosphere* 75:1539–1547.

Sawasdee B, Köhler H-R. 2010. Metal sensitivity of the embryonic development of the ramshorn snail *Marisa cornuarietis* (Prosobranchia). *Ecotoxicology* 19:1487–1495.

Schirling M, Bohlen A, Triebskorn R, Köhler H-R. 2006. An invertebrate embryo test with the apple snail *Marisa cornuarietis* to assess effects of potential developmental and endocrine disruptors. *Chemosphere* 64:1730–1738.

Kapitel 3: External and internal shell formation in the ramshorn snail *Marisa cornuarietis* are extremes in a continuum of gradual variation in development [8]

Leonie Marschner[1], Julian Staniek[1], Silke Schuster[1], Rita Triebskorn[1,2], Heinz-R. Köhler[1]

[1] *Animal Physiological Ecology, Institute of Evolution and Ecology, University of Tübingen, D-72072 Tübingen, Germany*

[2] *Transfer Center for Ecotoxicology and Ecophysiology, D-72108 Rottenburg, Germany*

Abstract

Background: Toxic substances like heavy metals can inhibit and disrupt the normal embryonic development of organisms. Exposure to platinum during embryogenesis has been shown to lead to a "one fell swoop" internalization of the shell in the ramshorn snail *Marisa cornuarietis*, an event which has been discussed to be possibly indicative of processes in evolution which may result in dramatic changes in body plans.

Results: Whereas at usual cultivation temperature, 26 °C, platinum inhibits the growth of both shell gland and mantle edge during embryogenesis leading to an internalization of the mantle and, thus, also of the shell, higher temperatures induce a re-start of the differential growth of the mantle edge and the shell gland after a period of inactivity. Here, developing embryos exhibit a broad spectrum of shell forms: in some individuals only the ven-

[8] BMC Developmental Biology. 2013, 13:22

tral part of the visceral sac is covered while others develop almost “normal” shells. Histological studies and scanning electron microscopy images revealed platinum to inhibit the differential growth of the shell gland and the mantle edge, and elevated temperature (28 - 30 °C) to mitigate this platinum effect with varying efficiency.

Conclusion: We could show that the formation of internal, external, and intermediate shells is realized within the continuum of a developmental gradient defined by the degree of differential growth of the embryonic mantle edge and shell gland. The artificially induced internal and intermediate shells are first external and then partly internalized, similar to internal shells found in other molluscan groups.

Keywords: platinum, shell internalization, embryogenesis, mantle formation

Background

The phenotype of an organism is not only determined by its genotype but also by the regulation of gene activity. Gene regulation can be influenced by environmental factors like temperature or presence of chemicals and thus lead to the emergence of new phenotypic traits (West-Eberhard, 2003). Platinum, acting on the embryonic development of the ramshorn snail *Marisa cornuarietis* has been shown to induce severe changes in the body plan (Osterauer *et al.*, 2010b; Marschner *et al.*, 2012). As described by Marschner *et al.* (2012), mantle and shell gland, tissues that normally spread across the visceral sac and cover it, stop growing during embryogenesis and remain on the ventral side of the visceral sac which itself has rotated horizontally by 90°. There, calcium carbonate is formed inside of the snail’s body, thus forming an internal shell instead of an external one. Gastropods, in contrast to other molluscs, are characterized by an event called “torsion”, a horizontal rotation of the visceropallium relative to head and foot by 180°, leading to a change of their internal anatomy (Aktipis *et al.*, 2008; Crofts, 1937; Page, 2006). In *Marisa cornuarietis*, this torsion can actually be observed

during embryonic development as a rotation of the visceral sac due to the differential growth of the mantle tissue on its left side (Demian and Yousif, 1973b). However, under the influence of platinum, this differential growth is stopped and a rotation does not occur. Nevertheless, these platinum-exposed individuals display several traits that are usually attributed to the process of torsion. They show an anterior anus, the ctenidium, however, is positioned on the posterior part of the visceral sac and not above the head. Both the ctenidium and the osphradium are even further displaced by the vertical rotation of the visceropallium. Those organs rotate sinistrad and the ctenidium in these snails becomes positioned on the left dorso-lateral side of the visceral sac. The osphradium, which normally can be found in the mantle cavity, is even shifted to the left ventro-lateral side of the visceral sac. Platinum-exposed embryos do not have an external mantle and a mantle cavity does not develop. Despite its new position, the shell-secreting tissue on the ventral side of the visceral sac secretes calcium carbonate which forms an internal shell cupping the digestive gland. These "sluggish" snails show traits of both "torted" (anterior anus) and "untorted" (no horizontal rotation of the visceropallium, posterior ctenidium) molluscs (Garstang, 1928; Page, 2003). Assuming that the rotation in *Marisa* is similar to the ontogenetic torsion that can be observed in other gastropods, it seems that gastropod characteristics that are supposedly caused by a torsion-like rotation of the visceropallium, at least in *Marisa*, might be independent from a rotation and, consequently, from each other.

However, the mechanism behind this platinum-induced developmental aberration is not yet known, but since platinum obviously affects development-controlling processes, we investigated whether platinum interacts with elevated temperature which is known to influence development as well, particularly in ectotherms. We exposed *Marisa cornuarietis* embryos to both platinum and elevated temperatures 2 to 4 °C higher than in previous experiments with this species (Osterauer *et al.*, 2009; 2010a; 2010b; Sawasdee and Köhler, 2009; 2010; Marschner *et al.*, 2012). In the first preliminary studies with combinations of platinum and elevated temperature we observed a new kind of developmental aberration which, at first sight, seems to be

an “intermediate” between the already described “sluggish” snails which develop internal shells after platinum exposure and “normal” control snails. We called these animals “partly-shelled”, since they developed a partial external shell, covering the ventral part of the visceral sac but which often do not extend to the dorsal part.

In order to elucidate the differences in the development of the “partly-shelled” animals and those with internal shells, we investigated adult “sluggish” and control individuals as well as “partly-shelled” and normally developing embryos histologically. As well, the course of development of platinum-plus-heat-exposed embryos was studied by scanning electron microscopy.

Results

Figure 1 shows selected individuals which have developed the different types of shells that we found in our experiments, ranging from completely “shell-less” or “sluggish”, i.e. snails with fully internal shells (Figure 1A), and “partly-shelled” individuals with small external shells, covering varying parts of the visceral sac (Figures 1B-D), to normally shelled animals (Figure 1E).

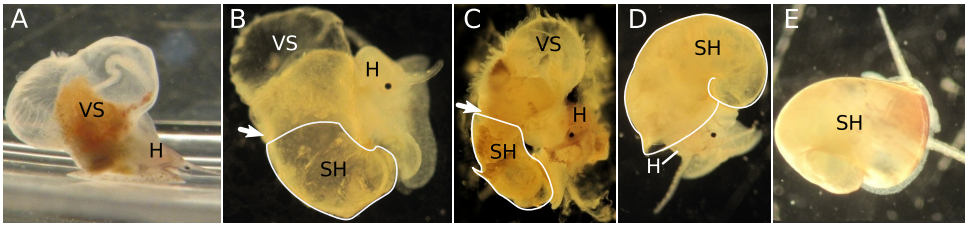

Fig. 1: *Marisa cornuarietis* individuals after hatching with different types of shells. Arrows indicate the mantle edge, “partial” shells are encircled in white; A: “sluggish” snail without an external mantle and with an internal shell (about 3 weeks old); B, C: snails with “partial” shells, D: snail with an almost normally developed “partial” shell; E: normally developed snail from the control; H: head, SH: shell, VS: visceral sac.

The normal embryonic development of *Marisa cornuarietis* has been thoroughly described by Demian and Yousif (1973a,b,c,d, 1975). An analysis of the embryonic development of platinum-exposed “sluggish” snails can be found in Marschner *et al.* (2012). All this work will be used to compare the development of “partly-shelled” snails with.

Differential growth of mantle anlage, mantle edge, and shell gland in "sluggish" snails

Figure 2 displays sections of Pt-exposed embryos from the study of Marschner *et al.* (2012) and sketches of these sections to illustrate development. Pt-exposed embryos develop similarly to control embryos until the onset of torsion. However, when torsion is supposed to begin by differential growth of the mantle anlage (i.e. tissue proximate to the protoconch in "sluggish" individuals), mantle edge, and shell gland, no differential growth of these tissues is visible after Pt-exposure. In contrast, these structures at first remain on the left side of the visceral sac and do not grow much (Figures 2A, B) but then shift to the ventral side of the visceral sac due to a vertical rotation of the visceral sac by 90° (Figures 2C, D) (Marschner *et al.*, 2012). In this position, the shell gland continues to secrete calcium carbonate. A closer examination of the developmental states shown in Figure 2 makes evident that, at the beginning, the shell gland is located on the visceral sac itself (Figures 2A, B). As can be taken from Demian and Yousif's (1973d) description of the "normal" development of shell gland and mantle, the shell gland remains on the surface of the visceral sac, encircling the mantle. The mantle edge is a fold that partially covers the shell gland. In Pt-exposed, "sluggish" embryos, however, the shell gland moves from the visceral sac's surface to the proximal side of a lobe protruding from the visceral sac (Figures 2C, D). In this process a "mantle gap" between lobe and the shell-secreting tissue covering the digestive gland develops.

During further growth this lobe increases in length, and both mantle edge and shell gland move further away from the visceral sac (Figures 2E, F). This affects also the position of mantle edge and shell gland which become located on the inner side of the lobe (Figure 2). These observations suggest that the mantle anlage does not actually stop growing. It is solely the complex of shell gland and mantle edge that does not increase in diameter. The tissue that is encircled by mantle edge and shell gland is in fact the tissue that would normally cover the visceral sac forming the mantle in the conventional way. The direction of growth of this mantle tissue, however, is restricted in the

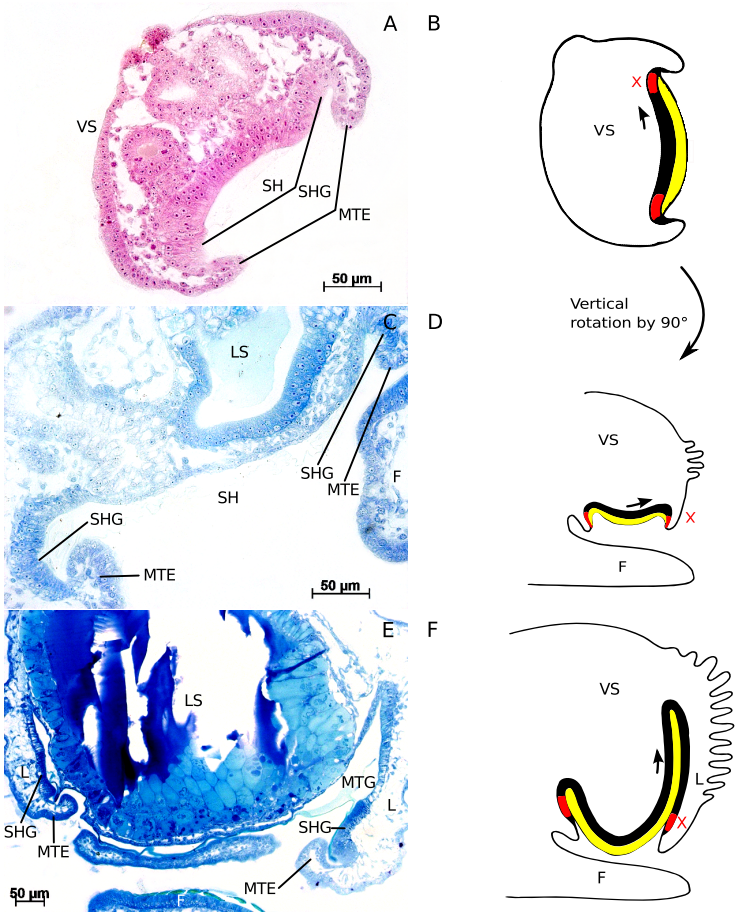

Fig. 2: Histological sections of Pt-exposed embryos and respective sketches explaining derection of tissue growth. Arrows indicate directional growth of a tissue, X indicates stop of growth of the respective tissue; black: mantle tissue, red: shell gland, yellow: shell; A: 3-day-old embryo, transverse section through the visceral sac; B: sketch of Figure 2A, frontal view; C: 7-day-old embryo, sagittal section; D: sketch of Figure 2C, left lateral view; E: 9-day-old embryo, transverse section through the visceral sac; F: sketch of Figure 2E, left lateral view; F: foot; L: lobe; LS: larval stomach; MTE: mantle edge; MTG: mantle gap; SH: shell; SHG: shell gland; VS: visceral sac.

"sluggish" individuals and directed by the unyielding tissues of mantle edge and shell gland which form a kind of inflexible ring around the growing mantle tissue, forcing it to fold inwards (Figures 2E, F). These diverging forms of development are also illustrated in Figure 3, which shows a control snail (Figure 3A) with the shell gland in its usual position on the visceral

sac, facing away from the snail's body. In contrast, Figure 3B shows an adult "sluggish" snail whose shell gland faces the interior of the mantle gap. In the case of Pt-exposed snails, it forms a part of the inner lining of the lobe where it encircles the mantle tissue which also forms the lining of the lobe and covers the visceral sac's surface distal of the digestive gland. Those snails do not only possess an internal shell as was first noticed by Osterauer *et al.* (2010b), they also have an internal mantle.

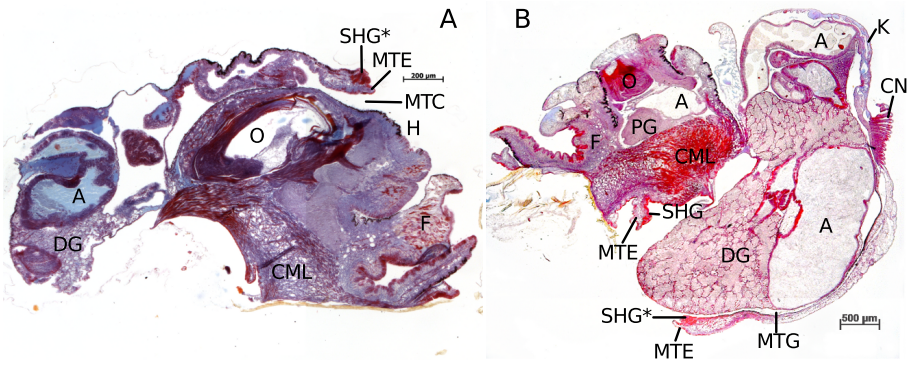

Fig. 3: Sagittal sections of adult *M. cornuarietis*. Asterisks indicate corresponding structures; A: snail from the control, six weeks after oviposition, right lateral view; B: Pt-exposed snail, several months old, left lateral view; A: alimentary tract; CML: columellar muscle; CN: ctenidium; DG: digestive gland; F: foot; K: kidney; MTC: mantle cavity; MTE: mantle edge; MTG: mantle gap; O: odontophor; PG: pedal ganglion; SHG: shell gland.

Embryonic development of "partly-shelled" snails

The embryonic development of *M. cornuarietis* in the presence of platinum and at elevated temperature is shown in Figure 4. All embryos, except for the one shown in Figure 4F, derive from the same clutch. Since they were fixed on subsequent days, Figures 4A-E show a developmental sequence. The sequence starts with an embryo at the age of 7 days (Figure 4A). This embryo resembles the appearance of the "sluggish" embryos that have been described by Marschner *et al.* (2012) at approximately the same developmental stage as "sluggish" embryos of similar age, although it is a bit further developed due to the higher cultivation temperature. Subsequently, however, their development begins to differ from the development of platinum-exposed embryos at 26° C. At lower temperatures, morphogenesis is completed as soon as shell

gland and mantle edge have stopped growing and the visceral sac has rotated horizontally. In contrast to this, the snails that are exposed to platinum at higher temperatures experience a new growth impulse that leads to a gradual covering of the visceral sac by a cap-like external shell while mantle edge and shell gland slowly grow craniad (Figures 4B-E). The onset of this new growth impulse can vary slightly between different clutches as shown in Figure 4F which displays a nine-day-old embryo that does not yet exhibit any signs of a formation of a "partial-shell" unlike its contemporary in Figure 4C.

Although shell gland and mantle edge do not grow much in "sluggish" embryos, calcium carbonate nevertheless is secreted (Marschner *et al.*, 2012). While the shell gland is positioned on the ventral side of the visceral sac, it secretes calcium carbonate which accumulates on the mantle anlage roughly in the shape of a plate which is subsequently incorporated into the developing internal shell as the mantle tissue folds inwards. However, in Pt-exposed snails at higher temperatures, mantle edge and shell gland resume growth and, thus, an external shell is formed. On the distal part of the shell, the "plate" that was formed before the re-start of the differential growth, is still visible (Figures 5A, B). In the case of the "partly-shelled" snails, the "plate" becomes part of the external shell instead of the internal shell.

Histology of "partly-shelled" snails

In Figure 6 histological sections of a control snail (Figure 6A) and several "partly-shelled" animals are shown (Figures 6B-F). Figure 6B displays a 12-day-old "partly-shelled" individual. The visceral sac in this animal is almost completely covered by an external shell, and only the ctenidium remains uncovered. The ctenidium actually has moved craniad and is now positioned above the head, a position that cannot be found in "sluggish" snails but which is normal for prosobranch gastropods as displayed by the control individual in Figure 6A. The mantle gap is basically nonexistent, and there is only a very small lobe holding shell gland and mantle edge. Figure 6C shows an older individual (17 days after oviposition) which shows a smaller external shell and a larger mantle gap than the younger individual in Figure 6B. Figures

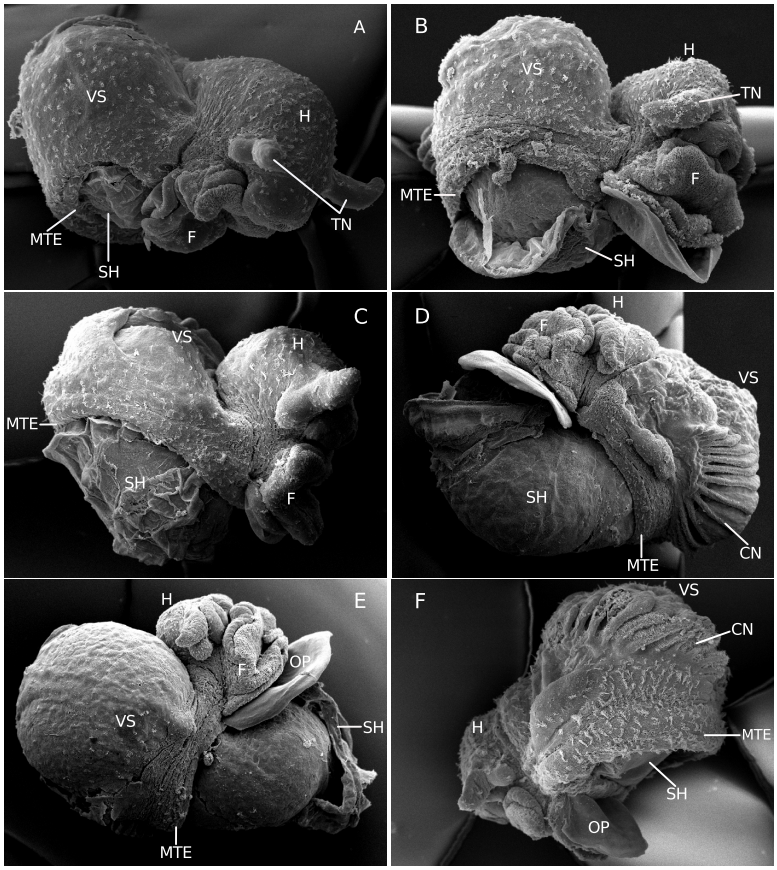

Fig. 4[9]: SEM-images of *M. cornuarietis* embryos from the same clutch (A-E) exposed to platinum and elevated temperature at different stages of development. A: seven-day-old embryo resembling a stage of development present also in "sluggish" individuals as described in Marschner *et al.* (2012) , right lateral view; B: eight-day-old embryo, right lateral view; C: nine-day-old embryo, right lateral view; D: ten-day-old embryo, left lateral view; E:eleven-day-old embryo, right lateral view; F: nine-day-old embryo from a different clutch, left lateral view; CN: ctenidium; F: foot; H: head; MTE: mantle edge; OP: operculum; SH: shell; TN: tentacles; VS: visceral sac.

6D and E both display horizontal sections of the same snail. In Figure 6D a section through the head and the visceral sac is shown, the section plane was slightly tilted, and mantle edge, shell gland and uncovered part of the external shell are visible. The section in Figure 6E is located dorsal to the section in Figure 6D, showing the posterior part of the digestive gland to

[9]Die einzelnen Bilder stammen von Silke Schuster.
[10]Die einzelnen Bilder stammen von Silke Schuster.

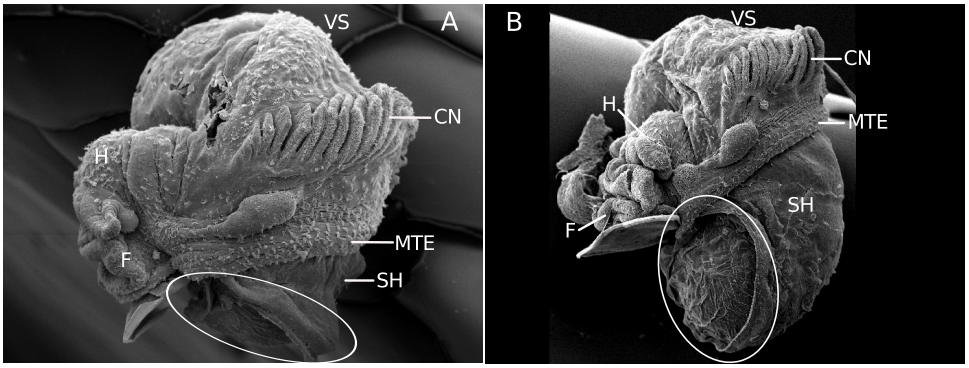

Fig. 5[10]: Images of platinum-plus-heat-exposed embryos. Left lateral views, circles highlight the portion of calcium carbonate that was secreted before the re-start of the differential growth of the shell gland-mantle edge-complex; A: 7-day-old embryo; B: 10-day-old embryo; CN: ctenidium; F: foot; H: head; MTE: mantle edge; SH: shell; VS: visceral sac.

be completely surrounded by the mantle gap and the lobe. The mantle gap also contains calcium carbonate, forming the part of the external shell that remains covered by the lobe. The "partly-shelled" snails do not only experience a new growth impuls, they also show some shell coiling (Figures 4D, E, Figure 6B, Figures 6B, C, F). However, the coils of these shells are not as tight as in control snails.

Comparison of embryogenesis in normal, "sluggish" and "partly-shelled" *M. cornuarietis*

In Figure 7 sketches of selected developmental stages of the differently treated snails are depicted. The top row shows the normal development (Marschner *et al.*, 2012). At the age of three days, the mantle anlage and the shell gland are positioned on the left side of the visceral sac. During further development, differential growth of the distal parts of the mantle anlage and the shell gland leads to an overgrowing of the visceral sac and an enfolding of the epidermal tissue of the right side of the visceral sac into the mantle cavity. Thus, the shell gland moves its orientation from being located parallel to the longitudinal body axis to being located perpendicular to the axis. After this rotation, mantle, shell gland, and mantle edge keep growing; the dorsal parts of the respective tissues grow to a greater extent than the ventral parts

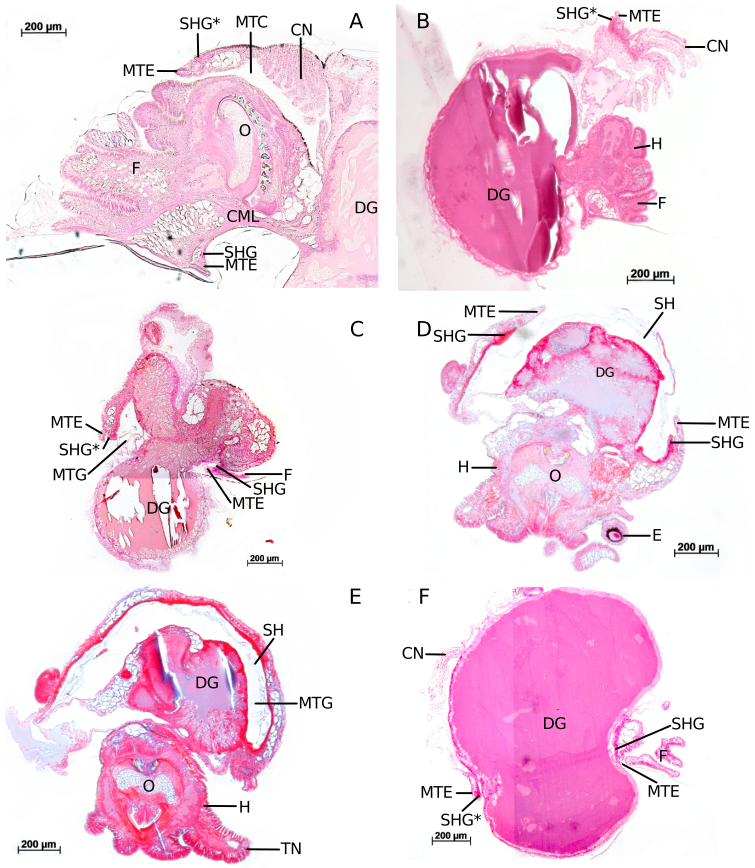

Fig. 6: Histological sections of *M. cornuarietis* embryos. Asterisks indicate corresponding structures; A: Sagittal section of a cephalopodium of a control snail, 12 days after oviposition, left lateral view; B: Sagittal section of a platinum-plus-heat-exposed snail, 12 days after oviposition, right lateral view; C: Sagittal section of a platinum-plus-heat-exposed snail, 17 days after oviposition, right lateral view; D: Horizontal section of a platinum-plus-heat-exposed snail, 17 days after oviposition; E: same individuum as in D, section more dorsal; F: Sagittal section of a platinum-plus-heat-exposed snail, 12 days after oviposition; CML: columellar muscle; CN: ctenidium; DG: digestive gland; E: eye; F: foot; H: head; MTC: mantle cavity; MTE: mantle edge; MTG: mantle gap; O: odontophor; SHG: shell gland.

and thus the animal coils. In "sluggish" snails, shown in the bottom row of the sketches in Figure 7, the differential growth is limited to the mantle anlage. Mantle edge and shell gland arrest growth and, therefore, do not overgrow the visceral sac. Simultaneously, however, the mantle anlage keeps growing and invaginates into the body. The arrested mantle edge and shell

gland form a kind of "inelastic ring" around the mantle anlage and thus facilitate the formation of an internal shell. The mantle moulds itself around the digestive gland and even folds in again on itself, forming a lobe and encircling a mantle gap. In the "partly-shelled" animals, displayed in the middle row of sketches, however, shell gland and mantle anlage resume their growth after several days of arrest. Their shells show a slight coiling but no real spiralling. Due to the temporary arrest of shell gland and mantle edge growth, the mantle anlage has started to invaginate into the body, forming a lobe like in the "sluggish" animals. As soon as the growth of the mantle edge and the shell gland resumes, the mantle tissue grows across the visceral sac, and only a small lobe and a small mantle gap remain which both are pushed craniad by the growing mantle. This revived growth is also differential, as the distal parts of shell gland and mantle edge grow more than the proximal parts. This differential growth results in the coiling of shell and visceral sac. Usually, the shell of the "partly-shelled" snails is only slightly coiled but, occasionally, almost normal shell coiling can be observed (Figure 8). The direction of the "revived" growth of mantle tissue, shell gland and mantle edge is parallel to the longitudinal body axis as it is in normally developing *M. cornuarietis* whose shells are planispiral. Figure 8B illustrates the respective directions of the differential growth of mantle tissue, shell gland and mantle edge in the differently treated snails. In the control, the first direction of differential growth is angular and results in a rotation of the visceral sac (ontogenetic torsion). After the completion of torsion, the differential growth vector shifts and now points parallel to the longitudinal body axis leading to the planispiral growth of the shell. In "sluggish" snails the outer tissues, mantle edge and shell gland, stop growing altogether, and the growth of the mantle anlage is restricted to the interior of the snail. Therefore, any directional or differential growth of the mantle tissue cannot be observed from the outside and is probably obscured due to lack of space in the snail's body. In "partly-shelled" animals, however, shell gland and mantle edge resume their growth and, since the exterior shell of these animals is also planispiral and slightly coiled, the growth vector in these animals is in line with the longitudinal body axis and not angular, starting from the ventral

side of the visceral sac after its vertical rotation by 90°.

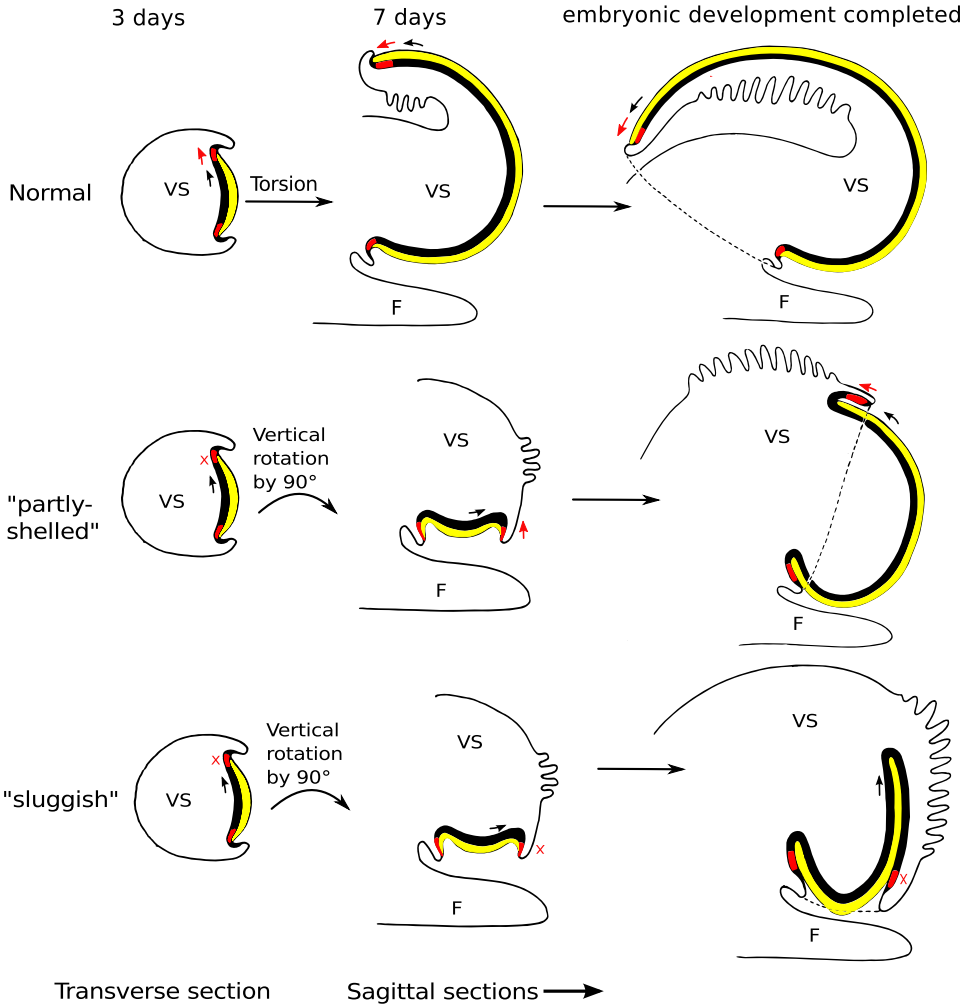

Fig. 7: Sketches of three different developmental stages (aged 3 (frontal view) and 7 days (left lateral view) and after completion of embryonic development (left lateral view)) of normal (top row), “partly-shelled” (middle row) and “sluggish” individuals (bottom row). Black: mantle tissue; red: shell gland; yellow: shell, direction of growth is indicated by an arrow, arrest of growth is indicated by X; F: foot; VS: visceral sac.

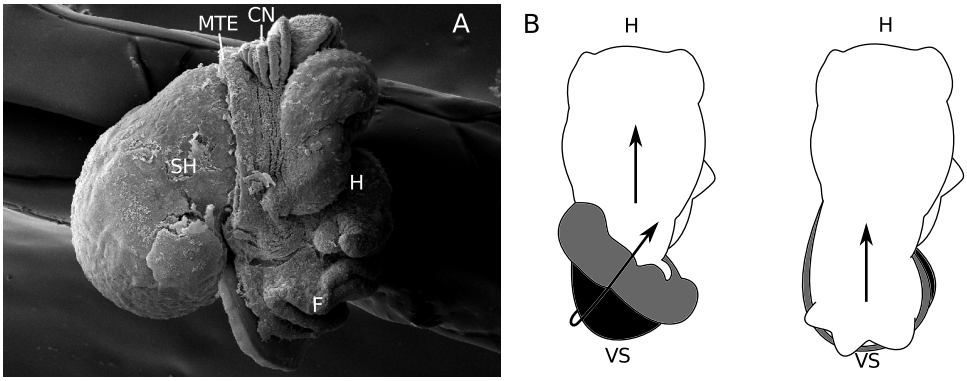

Fig. 8[11] Differential growth in "partly-shelled" snails. A: SEM-image of a 9-day-old platinum-plus-heat-exposed animal with a well developed shell whorl (right lateral view); B: sketches of a control animal (left) and a "partly-shelled" animal (right), dorsal view, black: mantle tissue; grey: mantle edge; arrows indicate the direction of differential growth; CN: ctenidium; F: foot; H: head; MTE: mantle edge; SH: shell; VS: visceral sac.

Discussion

There have been reports on artificially induced shell internalization before. Removal of distinct micromeres during early cleavage in *Ilyanassa obsoleta* can lead to veliger larvae that do not develop an exterior shell but in which an internal precipitate of calcium carbonate can be found (Cather, 1967; McCain, 1992). McCain (1992) suggested that the reason for the development of an internal shell in *Ilyanassa* embryos is a disruption of normal inductive interactions between the calcium carbonate precursor cells (cells that regulate shell and statocyst formation) in addition to the interactions between the 3D macromere and the micromeres. Dictus and Damen (1997) showed that the progeny of several micromeres contribute to the shell-secreting tissue of the larva in *Patella vulgata*. For *Marisa cornuarietis*, however, it is not known which micromeres contribute to which tissue (Demian and Yousif, 1973b) and, therefore, any speculation about a possible connection between a tissue's sensitivity to platinum and its progenitor cells is difficult. Besides, the induction of shell internalization by deletion of micromeres happens very early in embryonic development, whereas the platinum-induced shell internalization becomes feasible only in later stages of development, caused by a

[11] Abbildung 8a stammt von Silke Schuster.

different mechanism that affects tissue growth and not tissue formation.

In normally developing *Marisa* embryos two different directions of differential growth can be observed: first, the mantle anlage, the shell gland and the mantle edge overgrow the visceral sac in a way that leads to a horizontal rotation of the visceral sac by 180° (Demian and Yousif, 1973b). Subsequently, differential growth of the dorsal part of mantle, shell gland, and mantle edge, results in shell coiling (Ponder and Lindberg, 1997). Torsion and coiling are independent from each other (Haszprunar, 1988; Ponder and Lindberg, 1997). Marschner *et al.* (2012) showed that ontogenetic torsion does not take place in "sluggish" *Marisa* snails, however, it is not clear whether it is also absent in the "partly-shelled" individuals described here. A horizontal rotation cannot be observed in "partly-shelled" snails, although, in some specimens the ctenidium was positioned above the head which is a position which is supposed to be caused by ontogenetic torsion. In the "partly-shelled" snails the mantle anlage, the shell gland, and the mantle edge rotate vertically by 90° just like in the "sluggish" conspecifics. This rotation is unrelated to torsion and its cause is unknown. However, in contrast to the "sluggish" snails, the mantle tissue, the shell gland and the mantle edge resume growth in the "partly-shelled" animals. These tissues overgrow the visceral sac from a position on the ventral side of the visceral sac and thus the growth vector is not angular to the longitudinal body axis and no rotation of the visceral sac occurs. During this process, the tissue on the dorsal side of the visceral sac is pushed craniad, including the ctenidium which is drawn closer to its "normal" position above the snails' head. Due to the vertical rotation by 90°, the ctenidium starts its movement from the left side of the snail's body, and since the growth vector is parallel to the longitudinal body axis, the ctenidium ends up above the snail's head but is located still more to the left side instead of right as it is in controls. This way, a criterion that is usually attributed to torsion, the anterior ctenidium, can be formed without any horizontal rotation of the visceral sac. Comparing normally developing and exposed embryos, it can be concluded that platinum inhibits the differential growth of both shell gland and mantle edge. In the case of the Pt-exposed "sluggish" animals these tissues remain inactive and neither

angular nor straight differential growth takes place. In contrast, the combination of platinum and heat first leads to the described Pt-induced arrest of tissue growth but, some time later, heat reverses the effect. However, an angular growth does not take place, and straight differential growth leads to coiling. The platinum effect on the embryonic development of *Marisa cornuarietis* is obviously tissue-specific in the way that platinum specifically inhibits the growth of these tissues.

Growth of tissues and organs often occurs through cell proliferation which is usually, but not always, induced by growth factors (Wolpert, 2011). Grande and Patel (2008) investigated a signalling molecule of the growth factor β superfamily named Nodal. Nodal is involved in the development of chirality in snails and its inhibition by the chemical SB-431542 can lead to a loss of chirality that results in uncoiled shells. Disruption of the Nodal pathway obviously disrupts the differential growth that leads to coiling. The morphology of the resulting phenotype differs from the one induced by platinum, but is another example for body plan modification resulting from the inhibition of differential tissue growth by a single agent. Gene expression in the shell-secreting tissue has been investigated in *Haliotis asinina* (Jackson *et al.*, 2007) and *Patella vulgata* (Nederbragt *et al.*, 2002). Although many of these upregulated genes are probably involved in shell formation, the gene *dpp-BMP2/4*, that was traced by Nederbragt *et al.* (2002) in the ectodermal tissue surrounding the mantle edge, is known for its role in the specification of the dorsoventral axis in vertebrates and insects (Arendt and Nübler-Jung, 1997). Nederbragt *et al.* (2002) hypothesized that *engrailed*, which is expressed in the shell-secreting tissue, and *dpp-BMP2/4* together set up a compartment boundary between shell-secreting and non-secreting tissue. This hypothesis was supported by Baratte *et al.* (2007) who found engrailed proteins at the border of the mantle edge in the shell sac of *Sepia officinalis*, a cephalopod with an internal shell. These findings are especially interesting since dpp-BMP2/4, like Nodal, also belongs to the transforming growth factor β superfamily (Gilbert and Singer, 2006). Both *engrailed* and *dpp-BMP2/4* expression should therefore be investigated in control and platinum-exposed *Marisa cornuarietis* in the future, in order to find out,

whether the inhibition of the differential growth in platinum-exposed snails is also due to a disruption of a growth factor as it is in the case of inhibited shell coiling.

There are also several accounts on how heavy metals can influence tissue growth and development. Hanna *et al.* (1997) investigated several heavy metals and their impact on cell proliferation in embryos. They found that heavy metals could significantly reduce the number of cells in developing mouse embryos. Heavy metals can also act as carcinogens on different stages of carcinogenesis, including mutagenesis and altering gene expression (Snow, 1992).

Since some organoplatinum compounds are potent anticancer drugs, the genotoxicity of these chemicals has received reasonable attention. The genotoxicity of the different organoplatinum agents varies with their valency, structure, and conformation (Gebel *et al.*, 1997). While Gebel *et al.* (1997) did not observe any induction of micronuclei in human peripheral lymphocytes by $PtCl_2$, Migliore *et al.* (2002) found a significant increase of micronuclei in human lmyphocytes. According to Nordlind (1986), $PtCl_2$ inhibits the DNA synthesis of human lymphoid cells. Also, Osterauer *et al.* (2011) observed a significant increase in DNA damage induced by $PtCl_2$ in *Marisa cornuarietis*. It is, however, unlikely that genotoxicity alone can explain the highly tissue specific action of $PtCl_2$ observed in the present study.

It is striking that, while exposure to platinum alone results only in a single type of "sluggish" individuals, the combination of platinum and elevated temperature generates phenotypes displaying a whole continuum of shell forms ranging from completely internal shells to "partly-shelled" animals of different morphology, and normally shelled animals. Consequently, the higher temperature must be assigned to be responsible for the re-start of the differential growth of the mantle edge and the shell gland. The higher the temperature the faster is embryonic development in the exotherm species *Marisa cornuarietis* (Demian and Yousif, 1973b) - this effect could also be observed in our experiments. Actually, the animals exposed to platinum at higher temperatures (28 °C -30 °C) exhibited a lower mortality rate than at the lower temperature (26° C).

Heat stress, but also heavy metal exposure and other kinds of proteotoxic stress, induce stress protein synthesis (reviewed in Gupta *et al.*, 2010). However, constitutive levels of stress proteins are also important in stabilizing normal embryonic development (Rutherford and Lindquist, 1998; Queitsch *et al.*, 2002) but apparently need to be elevated under proteotoxic condition to enable a proper embryogenesis. Gunter and Degnan (2008) exposed embryos of *Haliotis asinina* to slightly elevated temperatures and observed larvae with abnormally located tissues, although the tissues themselves kept their unique stress protein expression patterns.

There are several examples showing that an induction of stress proteins during embryonic development can reduce the disrupting effect of teratogenic agents. In *Drosophila melanogaster* an elevated Hsp70 level either caused by a preceding heat shock or by genetic manipulation, mitigates the toxic effects of the mitotic poisons vinblastine and colchicine (Isaenko *et al.*, 2002). Hsp70 and Hsp90, and probably other stress-induced proteins as well, are involved in the cell cycle and in proliferating cells higher Hsp levels can be detected than in cells at another stage of the cell cycle (reviewed in Helmbrecht *et al.*, 2000). Hunter and Dix (2001) found that in mouse embryos stress-induced Hsp70 was able to decrease the incidence of neural-tube malformations induced by the metalloid arsenite. A further study on human cells by Barnes *et al.* (2002) revealed protection from arsenite-induced genotoxic effects by elevated Hsp70 levels. Osterauer *et al.* (2010a) investigated Hsp70-levels in juvenile platinum-exposed *Marisa cornuarietis* individuals. The highest concentration tested was 100 μg/L $PtCl_2$, half of the concentration that was used in this study and, although histological investigations showed histopathological tissue alterations, the Hsp70 level was not significantly elevated. Also own preliminary studies on the induction of stress protein in platinum- and platinum-plus-heat-exposed *Marisa* embryos did not reveal a consistend induction pattern so far which could have been indicative for a protective role of chaperones in the context of shell gland and mantle edge outgrowth. Thus, for the moment, the role of Hsps in the signalling cascade triggering differential growth in *Marisa* embryos remains unclear.

In *Marisa*, the evidently different phenotypes belong in fact to a con-

tinuum of gradual morphological variation and result from a more or less intense phenotypic expression of a single developmental trait: the formation and differential growth of an exterior mantle, and, consequently, an exterior shell. The further the exterior mantle is developed, the more "normal" is the development of the snail. This means, that, in this study, elevated temperatures, which are usually considered stressful, actually lead to a more normal development than lower temperatures when interacting with a developmental disruptor, platinum. Together with the observation that mortality in the platinum expositions was lower at higher temperatures than at 26 °C this leads to the conclusion that the increase in temperature in this case was not posing additional stress but actually protected development to some extent. There is also another group of stress-induced proteins that should be discussed regarding their possible interaction with platinum: metallothioneins, proteins that are involved in metal trafficking and detoxification. Serafim *et al.* (2002) observed that heavy metal-induced metallothionein levels were higher at higher temperatures in *Mytilus galloprovincialis*, and Piano *et al.* (2004) even found a temperature-induced increase of metallothionein levels in the absence of heavy metal exposure in the oyster *Ostrea edulis*. Metallothioneins have also received attention as possible cytosolic sinks for platinum-containing anticancer drugs (Knipp, 2009). Possibly, heat-induced metallothioneins may scavenge platinum in *Marisa* and thus decrease the internal concentration of "active" platinum. It is, however, unlikely that solely a quantitative reduction of "free" platinum is responsible for the formation of various "partial" shells, because these phenotypes never occurred in exposure experiments with lower platinum concentrations in the medium (Osterauer *et al.*, 2009).

Internal shells have evolved in a number of gastropod and other molluscan clades independently from one another. So the question arises, whether there are any similarities between *Marisa's* platinum-induced shell internalization and the formation of internal shells which have evolved in some molluscan taxa. In some groups (e.g. Naticidae), developing individuals start with an external shell which is then overgrown by extensions of the foot, the mantle, or both (Ponder *et al.*, 2008). In Opisthobranchia, shell-internalization and

reduction is very common and is theorized to have arisen independently in the different subgroups (Wägele and Klussmann-Kolb, 2005). In *Stylocheilus longicauda*, for example, the juvenile shell is overgrown by the parapodia and then shed (Switzer-Dunlap and Hadfield, 1977). The Nudibranchia all lose their juvenile shells and the visceral sac is overgrown by the mantle (Schmekel and Portmann, 1982), whereas the Saccoglossa are a heterogenous group with shell-bearing and non-shelled groups (Wägele and Klussmann-Kolb, 2005). However, in non-shelled Saccoglossa it is not the the mantle that overgrows the visceral sac, it is material of the foot that covers the naked visceral sac (Schmekel and Portmann, 1982). Another gastropod group without external shells is the group of terrestrial pulmonate slugs. In the slugs *Arion subfuscens* (Künkel, 1916) and *Limax maximus* (Simpson, 1901) the shell develops inside a shell sac which is located directly under the dorsal mantle region where it lies horizontally (Furbish and Furbish, 1984). Slugs, with occasional exceptions like the jumping-slugs of the genus *Hemphillia*, have a completely internal shell, but they have an external mantle unlike the "sluggish" phenotype of *Marisa cornuarietis*. Apart from pulmonate slugs, all gastropods have, at least at one time of their lives, external shells which may then be internalized during further development. In "sluggish" *Marisa* this is similar but less obvious: the first part of their shells, in this study called "plate", is secreted on the ventral part of the visceral sac and is never covered directly by any tissue but is only hidden from sight by the foot. Only the later formed part of the internal shell is covered by the lobe and calcium carbonate is secreted internally.

Gastropods are not the only molluscan group in which shell reduction and internalization have evolved convergently. Kröger *et al.* (2011) described several different reduction mechanisms in cephalopods, e.g. demineralisation of the shell or reduction of organic compounds. All these examples show that there is a phylogenetic continuum running between the two extrema - shell-bearing and non-shelled - and that different groups have evolved different mechanisms to reach their respective stages in this continuum independently from each other. While the presence or absence of an external shell is a very obvious trait in molluscs, it does not seem to be, mechanistically, a very con-

served one. However, there is also a similarity between the platinum-induced shell internalization in *Marisa* and the internal shell of cephalopods. In some coleoids a second layer of prismatic material is deposited on top of the original one (Nishiguchi and Mapes, 2008). According to Bandel (1989) mineralization of the primary shell occurs both inside and outside the shell and the calcium carbonate is attached to the periostracum from the exterior and the interior. This means that in these animals a part of the shell-producing tissue faces inwards just like it does in "sluggish" and "partly-shelled" *Marisa* individuals in which the shell gland is located on a lobe. Assuming, that the tissue of this lobe is in fact the tissue that would normally form the mantle, the shell in "sluggish" and "partly-shelled" *Marisa* individuals lies both on the mantle and is, at least partly, covered by it. This condition is similar to the one found in molluscs in which the mantle overgrows the shell, resulting in an inwardly facing shell-secreting tissue, like in almost all extant cephalopods.

Conclusion

In *Marisa*, manipulating the growth of the shell gland and the mantle edge during embryogenesis can induce the formation of normal, intermediate and internal shells. These intermediate and internal shells share characteristics with internal shells found in other molluscan groups: the first part of the shell is external and the shell is then partly overgrown. Also, the shell lies on the shell-secreting tissue and is partly covered by it like in many cephalopods. Our experiments with the ramshorn snail *Marisa cornuarietis* show that the transition from external shell to internal shell does not have to take place gradually via intermediate forms, although these exist, but that a full transition can be caused by a single trigger which specifically arrests differential growth of disctinct tissues.

Methods

"Sluggish" *M. cornuarietis* were reared according to the method described by Osterauer *et al.* (2010b) and Marschner *et al.* (2012). "Partly-shelled" *M. cornuarietis* were reared likewise, but at higher temperatures. All animal care regulations and legal requirements were adhered to.

Rearing of "sluggish" and "partly-shelled" *M. cornuarietis*

On the first day of the experiment, freshly deposited egg clutches were removed from aquaria of a *Marisa* laboratory hatchery and the single eggs were separated with a razor blade. The eggs were then transferred to Petri dishes in a way that all Petri dishes held between 20 and 30 eggs from at least three different clutches per dish. For the platinum exposure experiments, which lead to almost 100% "sluggish" individuals with internal shells, 200 μl platinum chloride standard solution (platinum standard, Ultra Scientific, Wesel, Germany, 1,000 μg/ml, Matrix: 98% water, 2% HCl) were mixed with 1 L tap water from the aquaria resulting in a concentration of 139 μg Pt^{2+}/L. For the controls tap water from the aquaria was used. Petri dishes were kept in a climate chamber at 26 °C at a light-dark regime of 12:12 h. To obtain "partly-shelled" animals, the Petri dishes with the platinum solution were kept at 28, 29 or 30 °C in climate chambers with a light-dark regime of 12:12 h. All test solutions were changed daily. A number of individuals from both the platinum-exposure and the control were transferred to aquarium water after completion of embryonic development, and raised to adulthood in glass Petri dishes and, later, in glass bowls. The water was changed every other day and the animals were fed small portions of Nutrafin Max flakes (Hagen, Germany) and, sometimes, small pieces of carrots. They were kept in a climate chamber at 26 °C. "Partly-shelled" animals from the platinum-plus-heat-exposure groups were also transferred to aquarium water after completion of their embryonic development and then kept at 26 °C. The development of the snails was photographically documented. All images were edited in Gimp (scaling, rotating, cropping, and color adjusting), labeling was added in Inkscape. Sketches were also done in Inkscape or drawn by

hand and modified in Inkscape.

Scanning Electron Microscopy

Three fresh egg clutches were selected, severed and distributed into 2 Petri dishes containing platinum solution and one Petri dish with aquarium water. Every Petri dish contained 25-30 eggs which were kept at 30 °C. Depending on the number of living embryos and the respective stages of development, embryos were removed from their egg capsules with two syringes and transferred into snap-cap vials filled with fixative (2% glutardialdehyde (VWR-Merck) dissolved in 0.01 M cacodylate buffer (VWR-Merck), pH 7.4). The embryos were selected in a way that for every clutch embryos from subsequent days of development could be obtained. Fixation took place between days 4 and 13 of embryonic development. This period had been identified as the time span in which the development from initially "sluggish" to "partly-shelled" individuals takes place. The embryos were then further processed for SEM imaging by rinsing them in 0.01 M cacodylate buffer (3 x 30 minutes). Subsequently, they were incubated overnight in a solution of reduced osmium tetroxide (2 mL of a solution of 1 g osmium tetroxide and 25 mL aqua dest + 2 mL aqua bidest + 4 mL of potassium ferrocyanide ($K_4[Fe(CN)_6]$*$3H_2O$, Merck) and rinsed again in 0.01 M cacodylate buffer (3 x 30 minutes). Samples were then successively dehydrated in 70%, 80%, 90%, 96%, and absolute ethanol (30 minutes for each concentration). Finally, animals were critical point dried, sputtered with gold, and mounted on stubs. Examination took place with a scanning electron microscope (Zeiss Evo LS10).

Histology

Embryos were removed from their egg capsules and transferred into snap-cap vials filled with fixative. The pictures of "sluggish" embryos in Figure 0.21 are unpublished data from experiments that have been described by Marschner *et al.* (2012). Embryos from the platinum exposures at 28 °C and 29 °C were removed at 12 and 17 days after oviposition. Both, embryos that remained "sluggish" and those with a clearly recognizable "partial" shell, were

selected and fixed in 2% glutardialdehyde dissolved in 0.01 M phosphate buffer (pH 7.4). They were then rinsed in phosphate buffer (2×30 minutes) and decalcified in 5% trichloroacetic acid in 37% formol ($3 \times$ within 24 h). Subsequently, the specimens were dehydrated in a graded series of ethanol (70% for 1 h, 80% for 1 h, 90% for 1 h, 96% for 30 minutes, and 100% for 2 h), and embedded in Technovit (Heraeus Kulzer, Germany). Serial sections of 3 to 3.5 μm thickness were cut with an automatic microtome (2050 Supercut, Reichert-Jung, Germany). Sections were mounted on microscopic slides and stained with hematoxylin/eosin or a modified Mallory's triple stain (Cason, 1950, modified for Technovit by staining for 1.5 h). A several months old "sluggish" snail and a six-week old control snail were fixed in 2% glutardialdehyde (VWR-Merck) in 0,01 M cacodylate buffer (VWR-Merck) at pH 7.4. Samples were rinsed $3 \times$ in 0.01 M cacodylate buffer (VWR-Merck), decalcified in a mixture of 37% formol and 70% ethanol (1:1) first for 30 minutes and again overnight. They were rinsed in 70% ethanol again and dehydrated in a graded series of 70% (30 minutes and 1.5 h), 80% (1 h), 90% (1 h), 96% (1 h), and 100% ethanol (2×1 h). Subsequently, samples were embedded in paraffin and cut in serial sections of 5 μm thickness using a microtome (Leica SM 2000R). The sections were mounted on slides and stained with Mallory's triple stain (Cason, 1950). All slides were examined with a light microscope (Axioskop 2, Zeiss, Germany).

Competing interests

The authors declare that they have no competing interests.

Authors' contributions

LM participated in the histological examinations of both adult snails and embryos, the scanning electron microscopy, the data analysis and prepared the manuscript. JS carried out the histological examinations of platinum-and-heat-exposed embryos and SS performed the scanning electron microscopy. RT participated in data analysis and helped draft the manuscript. HRK par-

ticipated in designing the study and helped with the data analysis and drafting of the manuscript. All authors read and approved the final manuscript.

Acknowledgements

Landesgraduiertenförderung Baden-Württemberg, Deutsche Forschungsgemeinschaft and the Open Access Publishing Fund of Tuebingen University are highly acknowledged for financial support. The authors wish to thank Diana Maier and Krisztina Vincze for their help with the laboratory work and Oliver Betz, Evolutionary Biology of Invertebrates, University of Tübingen for the use of his SEM-equipment and Monika Meinert for technical help.

References

Aktipis, S. W., Giribet, G., Lindberg, D. R., and Ponder, W. F. (2008). Gastropoda. In Ponder, W. F. and Lindberg, D. R., editors, *Phylogeny and evolution of the Mollusca*. University of California Press, Berkeley.

Arendt, D. and Nübler-Jung, K. (1997). Dorsal or ventral: Similarities in fate maps and gastrulation patterns in annelids, arthropods and chordates. *Mechanisms of Development*, 61(1–2):7–21.

Bandel, K. (1989). Cephalopod shell structure and general mechanisms of shell formation. *Short Courses in Geology*, 5:97–115.

Baratte, S., Andouche, A., and Bonnaud, L. (2007). Engrailed in cephalopods: a key gene related to the emergence of morphological novelties. *Development Genes and Evolution*, 217(5):353–362.

Barnes, J., Collins, B., Dix, D., and Allen, J. (2002). Effects of heat shock protein 70 (Hsp70) on arsenite-induced genotoxicity. *Environmental and Molecular Mutagenesis*, 40(4):236–242.

Cason, J. E. (1950). A rapid one-step Mallory-Heidenhain stain for connective tissue. *Biotechnic & Histochemistry*, 25(4):225–226.

Cather, J. N. (1967). Cellular interactions in the development of the shell gland of the Gastropod, *Ilyanassa*. *Journal of Experimental Zoology*, 166(2):205–223.

Crofts, D. R. (1937). The development of *Haliotis tuberculata*, with special reference to organogenesis during torsion. *Philosophical Transactions of the Royal Society of London. Series B, Biological Sciences*, 228(552):219–268.

Demian, E. S. and Yousif, F. (1973a). Embryonic development and organogenesis in the snail *Marisa cornuarietis* (Mesogastropoda: Ampullariidae). 3. Development of the circulatory and renal systems. *Malacologia*, 12(2):175–194.

Demian, E. S. and Yousif, F. (1973b). Embryonic development and organogenesis in the snail *Marisa cornuarietis* (Mesogastropoda: Ampullariidae). I. General outlines of development. *Malacologia*, 12(1):123–150.

Demian, E. S. and Yousif, F. (1973c). Embryonic development and organogenesis in the snail *Marisa cornuarietis* (Mesogastropoda: Ampullariidae). II. Development of the alimentary system. *Malacologia*, 12(1):151–174.

Demian, E. S. and Yousif, F. (1973d). Embryonic development and organogenesis in the snail *Marisa cornuarietis* (Mesogastropoda: Ampullariidae). IV. Development of the shell gland, mantle and respiratory organs. *Malacologia*, 12(2):195–211.

Demian, E. S. and Yousif, F. (1975). Embryonic development and organogenesis in the snail *Marisa cornuarietis* (Mesogastropoda: Ampullariidae). V. Development of the nervous system. *Malacologia*, 15(1):29–42.

Dictus, W. J. and Damen, P. (1997). Cell-lineage and clonal-contribution map of the trochophore larva of *Patella vulgata* (Mollusca). *Mechanisms of development*, 62(2):213–226.

Furbish, D. R. and Furbish, W. J. (1984). Structure, crystallography, and morphogenesis of the cryptic shell of the terrestrial slug *Limax maximus* (Mollusca, Gastropoda). *Journal of Morphology*, 180(3):195–211.

Garstang, W. (1928). The origin and evolution of larval forms. *Nature*, 122:366.

Gebel, T., Lantzsch, H., Pleßow, K., and Dunkelberg, H. (1997). Genotoxicity of platinum and palladium compounds in human and bacterial cells. *Mutation Research/Genetic Toxicology and Environmental Mutagenesis*, 389(2–3):183–190.

Gilbert, S. F. and Singer, S. R. (2006). *Developmental Biology*. Palgrave Macmillan, 8th rev. ed. edition.

Grande, C. and Patel, N. H. (2008). Nodal signalling is involved in left–right asymmetry in snails. *Nature*, 457(7232):1007–1011.

Gunter, H. M. and Degnan, B. M. (2008). Impact of ecologically relevant heat shocks on Hsp developmental function in the vetigastropod *Haliotis asinina*. *Journal of Experimental Zoology. Part B, Molecular and Developmental Evolution*, 310(5):450–464.

Gupta, S. C., Sharma, A., Mishra, M., Mishra, R. K., and Chowdhuri, D. K. (2010). Heat shock proteins in toxicology: How close and how far? *Life Sciences*, 86(11–12):377–384.

Hanna, L. A., Peters, J. M., Wiley, L. M., Clegg, M. S., and Keen, C. L. (1997). Comparative effects of essential and nonessential metals on preimplantation mouse embryo development in vitro. *Toxicology*, 116(1-3):123–131.

Haszprunar, G. (1988). On the origin and evolution of major gastropod groups, with special reference to the Streptoneura. *Journal of Molluscan Studies*, 54(4):367–441.

Helmbrecht, K., Zeise, E., and Rensing, L. (2000). Chaperones in cell cycle regulation and mitogenic signal transduction: a review. *Cell proliferation*, 33(6):341–365.

Hunter, E. S. and Dix, D. J. (2001). Heat shock proteins Hsp70-1 and Hsp70-3 are necessary and sufficient to prevent arsenite-induced dysmorphology in mouse embryos. *Molecular Reproduction and Development*, 59(3):285–293.

Isaenko, O. A., Karr, T. L., and Feder, M. E. (2002). Hsp70 and thermal pretreatment mitigate developmental damage caused by mitotic poisons in *Drosophila*. *Cell Stress & Chaperones*, 7(3):297–308.

Jackson, D. J., Wörheide, G., and Degnan, B. M. (2007). Dynamic expression of ancient and novel molluscan shell genes during ecological transitions. *BMC Evolutionary Biology*, 7(1):160.

Knipp, M. (2009). Metallothioneins and platinum(II) anti-tumor compounds. *Current Medicinal Chemistry*, 16(5):522–537.

Kröger, B., Vinther, J., and Fuchs, D. (2011). Cephalopod origin and evolution: A congruent picture emerging from fossils, development and molecules. *BioEssays*, 33(8):602–613.

Künkel, K. (1916). *Zur Biologie der Lungenschnecken: Ergebnisse vieljähriger Züchtungen und Experimente*. Winter, Heidelberg.

Marschner, L., Triebskorn, R., and Köhler, H.-R. (2012). Arresting mantle formation and redirecting embryonic shell gland tissue by platinum^{2+} leads to body plan modifications in *Marisa cornuarietis* (Gastropoda, Ampullariidae). *Journal of Morphology*, 273(8):830–841.

McCain, E. R. (1992). Cell interactions influence the pattern of biomineralization in the *Ilyanassa obsoleta* (Mollusca) embryo. *Developmental dynamics: an official publication of the American Association of Anatomists*, 195(3):188–200.

Migliore, L., Frenzilli, G., Nesti, C., Fortaner, S., and Sabbioni, E. (2002). Cytogenetic and oxidative damage induced in human lymphocytes by platinum, rhodium and palladium compounds. *Mutagenesis*, 17(5):411–417.

Nederbragt, A. J., van Loon, A. E., and Dictus, W. J. (2002). Expression of *Patella vulgata* orthologs of engrailed and dpp-BMP2/4 in adjacent domains during molluscan shell development suggests a conserved compartment boundary mechanism. *Developmental Biology*, 246(2):341–355.

Nishiguchi, M. K. and Mapes, R. H. (2008). Cephalopoda. In Ponder, W. F. and Lindberg, D. R., editors, *Phylogeny and evolution of the Mollusca*. University of California Press, Berkeley.

Nordlind, K. (1986). Further studies on the ability of different metal salts to influence the DNA synthesis of human lymphoid cells. *International Archives of Allergy and Immunology*, 79(1):83–85.

Osterauer, R., Faßbender, C., Braunbeck, T., and Köhler, H.-R. (2011). Genotoxicity of platinum in embryos of zebrafish (*Danio rerio*) and ramshorn snail (*Marisa cornuarietis*). *Science of The Total Environment*, 409(11):2114–2119.

Osterauer, R., Haus, N., Sures, B., and Köhler, H.-R. (2009). Uptake of platinum by zebrafish (*Danio rerio*) and ramshorn snail (*Marisa cornuarietis*) and resulting effects on early embryogenesis. *Chemosphere*, 77(7):975–982.

Osterauer, R., Köhler, H.-R., and Triebskorn, R. (2010a). Histopathological alterations and induction of Hsp70 in ramshorn snail (*Marisa cornuarietis*) and zebrafish (*Danio rerio*) embryos after exposure to $PtCl_2$. *Aquatic Toxicology*, 99(1):100–107.

Osterauer, R., Marschner, L., Betz, O., Gerberding, M., Sawasdee, B., Cloetens, P., Haus, N., Sures, B., Triebskorn, R., and Köhler, H.-R. (2010b). Turning snails into slugs: induced body plan changes and formation of an internal shell. *Evolution & Development*, 12(5):474–483.

Page, L. R. (2003). Gastropod ontogenetic torsion: Developmental remnants of an ancient evolutionary change in body plan. *Journal of Experimental Zoology*, 297B(1):11–26.

Page, L. R. (2006). Modern insights on gastropod development: Reevaluation of the evolution of a novel body plan. *Integrative and Comparative Biology*, 46(2):134 –143.

Piano, A., Valbonesi, P., and Fabbri, E. (2004). Expression of cytoprotective proteins, heat shock protein 70and metallothioneins, in tissues of *Ostrea edulis* exposed to heat andheavy metals. *Cell Stress & Chaperones*, 9(2).

Ponder, W. F., Colgan, D. J., Healy, J. M., Nützel, A., Simone, L. R. L., and Strong, E. E. (2008). Caenogastropoda. In Ponder, W. F. and Lindberg, D. R., editors, *Phylogeny and evolution of the Mollusca*. University of California Press, Berkeley.

Ponder, W. F. and Lindberg, D. R. (1997). Towards a phylogeny of gastropod molluscs: an analysis using morphological characters. *Zoological Journal of the Linnean Society*, 119(2):83–265.

Queitsch, C., Sangster, T. A., and Lindquist, S. (2002). Hsp90 as a capacitor of phenotypic variation. *Nature*, 417(6889):618–624.

Rutherford, S. L. and Lindquist, S. (1998). Hsp90 as a capacitor for morphological evolution. *Nature*, 396(6709):336–342.

Sawasdee, B. and Köhler, H.-R. (2009). Embryo toxicity of pesticides and heavy metals to the ramshorn snail, *Marisa cornuarietis* (Prosobranchia). *Chemosphere*, 75(11):1539–1547.

Sawasdee, B. and Köhler, H.-R. (2010). Metal sensitivity of the embryonic development of the ramshorn snail *Marisa cornuarietis* (Prosobranchia). *Ecotoxicology*.

Schmekel, L. and Portmann, A. (1982). *Opisthobranchia des Mittelmeeres: Nudibranchia und Saccoglossa*. Springer-Verlag, Berlin.

Serafim, M., Company, R., Bebianno, M., and Langston, W. (2002). Effect of temperature and size on metallothionein synthesis in the gill of *Mytilus galloprovincialis* exposed to cadmium. *Marine Environmental Research*, 54(3–5):361–365.

Simpson, G. B. (1901). *Anatomy and physiology of Polygyra albolabris and Limax maximus and embryology of Limax maximus*. Albany: University of the State of New York.

Snow, E. T. (1992). Metal carcinogenesis: mechanistic implications. *Pharmacology & Therapeutics*, 53(1):31–65.

Switzer-Dunlap, M. and Hadfield, M. G. (1977). Observations on development, larval growth and metamorphosis of four species of Aplysiidae (Gastropoda: Opisthobranchia) in laboratory culture. *Journal of Experimental Marine Biology and Ecology*, 29(3):245–261.

West-Eberhard, M. J. (2003). *Developmental Plasticity and Evolution*. Oxford University Press.

Wolpert, L. (2011). *Principles of development*. Oxford University Press, New York; Oxford.

Wägele, H. and Klussmann-Kolb, A. (2005). Opisthobranchia (Mollusca, Gastropoda) – more than just slimy slugs. Shell reduction and its implications on defence and foraging. *Frontiers in Zoology*, 2.

Kapitel 4: No torsion required for streptoneury in the ampullariid snail *Marisa cornuarietis*[12]

Leonie Hannig[a], Simon Schwarz[a], Heinz-R. Köhler[a]

[a] *Animal Physiological Ecology, Institute of Evolution and Ecology, University of Tübingen, Konrad-Adenauer-Str. 20, D-72072 Tübingen, Germany*

Abstract

The hallmark feature that distinguishes the gastropods from all other molluscs is the horizontal rotation of the visceropallium, the so-called torsion. Torsion is considered to be the cause of the anterior position of anus and gills as well as the crossing of the pleurovisceral nerve connectives, a feature that is known as streptoneury. In earlier experiments, we observed that exposure of the caenogastropod *Marisa cornuarietis* to bivalent platinum ions during embryogenesis does not only prevent the formation of an external mantle and shell but also inhibits the horizontal rotation of the visceral sac. In Platinum^{2+}-exposed embryos, immunohistochemical labeling with anti-serotonin antibodies showed the embryonic development of the nervous system to deviate from the typical arrangement. Nevertheless, histological investigations and subsequent 3D modelling of the arrangement of the nervous system in adults revealed Platinum^{2+}-exposed individuals to exhibit a streptoneurous arrangement of their nervous system even though the horizontal rotation of the visceropallium had been experimentally suppressed.

[12] Unveröffentlichtes Manuskript

Herewith, we were able to show that torsion is not a prerequisite for the development of a streptoneurous arrangement of the nervous system in *M. cornuarietis*.

Introduction

Torsion in gastropods is a difficult topic although the theory behind it is simple enough. It is defined as an anti-clockwise rotation of the visceral sac and mantle by 180° relative to head and foot, and takes place during the ontogeny of all snails and slugs (e.g. Bieler, 1992) as the so-called "ontogenetic torsion". It is the common morphological feature of gastropods (e.g. Garstang, 1928) and supposed to be responsible for several anatomical conditions that can be found in snails, some of which are the anterior position of anus and mantle cavity as well as the crossing of the pleurovisceral nerve connectives known as streptoneury or chiastoneury (Bieler, 1992; Haszprunar, 1988; Page, 2006; Raven, 1966). According to the theory, extant gastropods are descendants of an untorted so-called "hypothetical primitive mollusc" (Yonge, 1947) in which the mantle cavity with gills and anus was positioned posteriorly (reviewed in Page, 2006). Supposedly, this untorted "hypothetical primitive mollusc" exhibited a rotation of the visceropallium by about 180°, leading to a twisting of the internal organs, including the nervous system and the intestine and thus became a torted gastropod (Raven, 1966). We recently reported that exposure to bivalent platinum ions during embryogenesis stops the growth of mantle edge and shell gland in *Marisa cornuarietis* embryos (Marschner *et al.*, 2012; 2013). As a result, these embryos do not only exhibit no exterior shell but do also not show a horizontal rotation of the visceral sac by 180°, as can be seen in "normally" developing *Marisa* embryos (Marschner *et al.*, 2012; 2013). However, the ensuing snails possess an anterior anus which is typical for the torted condition of gastropods while, at the same time, the gills can be found posteriorly on the visceral sac. These individuals both display characteristics typical for torted gastropods (anterior anus) and characteristics that are supposed to apply to the untorted hypothetical ancient mollusc. Another anatomical condition that is, by theory, supposedly

caused by torsion, streptoneury, is not so easily accessible. To determine, if the Pt^{2+}-exposed "sluggish" snails exhibit a "torted" or "untorted" nervous system, we investigated adult sluggish snails histologically and created 3D models of their anatomy. Additionally, we conducted immunohistochemical analyses of the nervous system during different stages of embryonic development of both Pt^{2+}-exposed and control embryos. To label nervous tissue we chose the two neurotransmitters, FMRFamide and serotonin, which have already been regularly used to investigate the development of the nervous system in gastropods (Croll, 2000; Croll and Voronezhskaya, 1996; Goldberg and Kater, 1989; Page, 2003, 2006a) and other molluscs (Voronezhskaya *et al.*, 2008; Wanninger and Haszprunar, 2003). Furthermore, we investigated acetylated alpha-tubulin which has been used several times in examinations of the nervous system in gastropods (Jackson *et al.*, 1995; Kempf and Page, 2005). Using an animal model which does not undergo ontogenetic torsion we aimed at elucidating the question whether (ontogenetic) torsion really is the prerequisite for the formation of streptoneury in *M. cornuarietis* snails.

Methods

The experiments were conducted on the basic of the *M. cornuarietis* embryo test (MariETT) developed by Schirling *et al.* (2006) and modified. For a detailed description of material, techniques and keeping of *M. cornuarietis* see Osterauer *et al.* (2010b) and Marschner *et al.* (2012; 2013). Freshly fertilized eggs were transferred into Petri dishes (20 eggs each) containing either aquarium water for the control or a 200 μg/l $PtCl_2$-solution made from one liter aquarium water and 200 μl $PtCl_2$ (Platinum Standard, Ultra Scientific, Wesel, Germany, 1000 μg/ml, Matrix: 98% water, 2% HCl). The Petri dishes were kept at 26 °C in a climate chamber at a light-dark regime of 12:12 h. The test solutions were changed on a daily basis.

Histology and 3D reconstruction

After nine days, embryos from both $PtCl_2$-exposure and control were transferred into separate glass Petri dishes and, later, small glass bowls depending on the size. The water was changed every other day and the young snails were fed with small amounts of Nutrafin Max flakes (Hagen, Germany) and, occasionally, small pieces of organic carrots. Petri dishes and glass bowls were cleaned with toothbrushes when necessary. Temperature and light-dark regime remained the same throughout the whole lifetime of the snails. To compare the anatomy of the nervous system of adult "sluggish" *M. cornuarietis* and normally developed snails, eight weeks after oviposition one animal from each group was fixed in 2% glutardialdehyde (VWR-Merck) in 0.01 M cacodylate buffer (VWR-Merck) at pH 7.4. The animal from the control will be referred as C1 whereas the sluggish snail will be referred to as P1. In addition, a second adult sluggish snail was investigated. This snail was older than C1 and P1. It will be referred to as P2. All three individuals were processed as follows: rinsing in 0.01 M cacodylate buffer at pH 7.6 (3 x 10 min) and decalcification in a mixture of formic acid and 70% ethanol (1:1) first for 30 minutes and again over night. On the next day, the specimens were rinsed 3 x 10 minutes in 70% ethanol and then dehydrated in a graded ethanol series: 2 x 70% ethanol (30 minutes, 1.5 h), 80% ethanol (1 h), 90% ethanol (1 h), 96% ethanol (1 h), 2 x 100% ethanol (1 h each). They were then immersed in isopropanol (2 x 1.5 h and 2 h, respectively) and in a mixture of isopropanol and paraffin (Paraplast, Leica) for 3 h. They were then infiltrated with pure paraffin, once for 3 h and once for 5 h. Afterwards, they were embedded in paraffin. Using a microtome (Leica SM 2000R), serial sections of 5 μm thickness were cut and mounted on slides. The sections were stained with Mallory's triple stain (modified after Cason, 1950). All sections were then viewed by light microscopy and photographed. The pictures were loaded into Amira 4.1 or 5.3, respectively (Visage Imaging) and 3D models were created. Pictures of the models were taken. Due to the fact that smaller structures can get lost in computer based processing, the models were again compared to the original sections and modified accordingly by hand in Inkscape (depicted

in the figures of this publication in blue lines). Additionally, we added nerve connections that were expected but could not be doubtlessly observed in the slices directly because some slices were artificially damaged or folded. These structures were added to the figures in black dashed lines to emphasize that they are only hypothetical. Image editing was accomplished in Gimp Image Editor (scaling, cropping, color adjustment) and in Inkscape (labeling).

Immunohistochemistry with *M. cornuarietis* embryos

After reaching the required age (5 and 6 days for the controls and 7 to 12 days for $PtCl_2$-exposure group), the embryos were removed from the egg capsules with syringes and transferred into small glass Petri dishes filled with acidulated water for relaxation for 10 to 15 minutes prior to fixation (Römerquelle medium, Göppingen, Germany, Ca: 604 mg/L, Mg: 47,3 mg/L, CHO^{3-}: 203 mg/L, Na: 20 mg/L, Cl^-: 6,3 mg/L, SO_2^{-4}: 1328 mg/L). The embryos were then fixed in 4% Triton-paraformaldehyde (0.1% Triton X diluted in 4% paraformaldehyde diluted in phosphate-buffered saline (PBS, 8.0 g/L NaCl, 0.2 g/L KCl, 1.78 g/L $Na_2HPO_4*2H_2O$ and 0.27 g/L KH_2PO_4 diluted in bidistilled water, pH=7.4)). Fixation lasted at least 12 hours and was conducted at 6 °C. The embryos were then washed 4 times à 5 minutes in PBZ (0.1% sodium azide in PBS) and then transferred into a blocking buffer for 4 to 5 hours at 6 °C (blocking buffer: 1% Triton X, 3% horse serum and 10% of 1% PBZ diluted in PBS). The specimens were then incubated with the first antibody with a concentration of 1:200 in blocking buffer at 6 °C (rabbit anti-serotonin whole antiserum (Sigma-Aldrich, St. Louis, MO, USA), polyclonal rabbit anti-FMRFamide antibody (ImmunoStar, Hudson, WI, USA) or monoclonal mouse anti-acetylated tubulin antibody (Sigma-Aldrich, St. Louis, MO, USA)). Preliminary tests showed that incubation times between 48 h and 96 h yielded the same results and we therefore used either 48 h, 72 h, or 96 h for incubation. Subsequently, the embryos were washed 8 times à 45 min in 0.1% PBZ and then incubated with the second antibody (goat anti-rabbit IgG antibody linked to the fluorophor Alexa 488® (Invitrogen, Eugene, OR, USA) with a concentration of 1:200 in blocking buffer for 48,

72 or 96 hours at 6 °C. The second incubation as well as all following steps were performed in the dark. After incubation, the embryos were washed 4 times à 30 minutes in PBS and then transferred to Sca*l*eB4 (8 M urea, 0.1% (wt/vol) Triton X and 10% (wt/vol) glycerol in double destilled water (Hama *et al.*, 2011) for at least a 5 weeks clearing of the samples at room temperature. Before data analysis, the clearing solution was exchanged by a mounting solution (Sca*l*eB4 with 2.4 ml glycerol). The embryos were then analyzed with a confocal laser scanning microscope (Leica TCS SPE, Leica Microsystems, with Leica Application Suite - Advanced Fluorescence (LAS-AF, Version 2.6.0.7266)) and evaluated with FIJI-ImageJ (fiji.sc). Image editing was done in Gimp Image Editor and in Inkscape. Additionally, the stained nervous structures were three-dimensionally modeled by using Amira 5.2.1.

Results

Histology and 3D-reconstruction of the anatomy of adults

Both the histological sections and the 3D models clearly showed how the lack of an external mantle and shell influences the whole anatomy of a snail. In Fig. 1A a sagittal section of the control, C1, is shown. The corresponding "sluggish" snail, P1, is displayed in Fig. 1B. The older snail, P2, is shown in Fig. 1C,D. The histological sections were the basis of the 3D models and provided additional information that facilitated the interpretation of the models. The anatomy of the specimens will be described using the 3D-reconstructions.

Fig. 2 shows complete 3D reconstructions of the three investigated snails. The control individual, C1, is depicted in the upper row viewed from the left (Fig. 2A) and from the right side (Fig. 2B). This individual represents a "normally" developed snail, it will not be described here in detail but mainly be used for comparisons. It is obvious that a large part of the snail's body is shaped by the shell (not shown in the reconstructions); especially the coiling of the digestive gland is conspicuous. In contrast, the two sluggish snails in

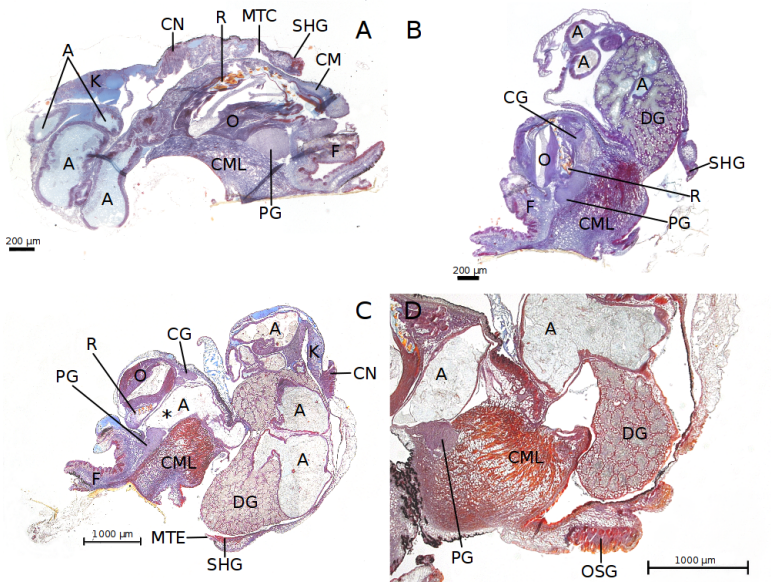

Fig. 1: Histological sections of C1, P1 and P2; A: C1, saggital section, right lateral view; B: P1, saggital section, left lateral view; C: Sagittal section of P2, left lateral view, asterisk indicates a protrusion of the alimentary system; D: P2, sagittal section of the visceral sac, same individual as in C; A, alimentary tract; CG: cerebral ganglion; CML, columellar muscle; CN: ctenidium; DG: digestive gland; F, foot; K, kidney; MTC, mantle cavity; MTE, mantle edge; O, odontophor; OSG, osphradial ganglion; PG, pedal ganglion; R, radula; SHG, shell gland

Fig. 2C-F are not restrained by a solid external structure that shapes their bodies. As snails are both soft and, to some extent, flexible, the relative positions of the organs and tissues can somewhat vary. Although this is the case, there are distinct common features that both sluggish snails share: compared to C1 they both seem to be compressed along the middle axis (see also Figs. 3 and 4) and the visceral sac does not have a distinct form at all but is simply bulky. Both snails do not show a mantle cavity and also a conventional ureter, as the kidney seems to open directly into the outer medium. As previously described (Marschner *et al.*, 2012), the shell secreting shell gland and the adjacent mantle edge (not indicated separately) remain on the ventral side of the visceral sac. This shell-secreting complex is ring-shaped and encircles the mantle rudiment and, later, the (internally located) mantle which secretes calcium carbonate. As can be seen in the histological sections and in the reconstructions, this ring-shaped complex is still posi-

tioned on the ventral side of the visceral sac. Previous studies showed that the mantle epithelium, encircled by shell gland and mantle edge, is enfolded into the inside of the snail (Marschner *et al.*, 2012; 2013). Furthermore, the 3D models of the $PtCl_2$ -exposed snails show that, during further growth, the digestive gland pushes the mantle epithelium ventrad until digestive gland, mantle, and internal shell (not shown in the models) protrude out of the ring formed by shell gland and mantle edge.

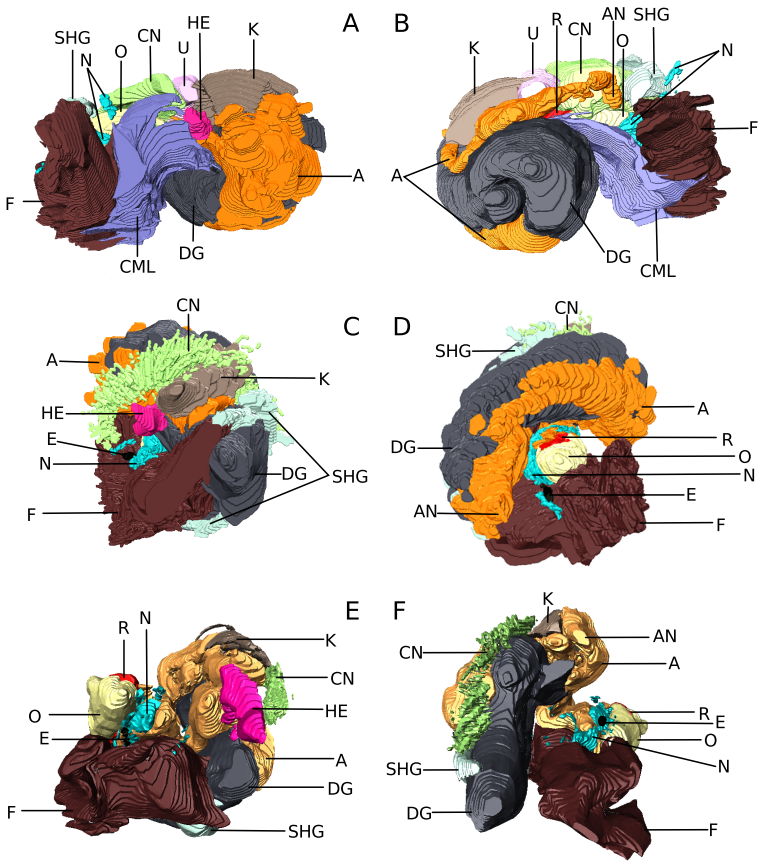

Fig. 2: Complete 3D models; A: C1, left lateral view; B: K1, right lateral view; C: P1, left lateral view; D: P1, right lateral view; E: P2, left lateral view; F: P2, right lateral view; A, alimentary tract; AN, anus; CML, columellar muscle; CN: ctenidium; DG: digestive gland; E, eye; F, foot; HE, heart; K, kidney; N, nervous tissue; O, odontophor; R, radula; SHG, shell gland; U, ureter

The nervous system of the adult

Fig. 3A,B shows two views of a submodel of C1 that focuses on the head and foot region. The columellar muscle follows the shape of the columella. The odontophor takes up a great part of the head and the radula curves slightly along the dorsal side of the head from the mouth to the transition to the visceral sac. This most distal part is the radular sac. The ganglia can easily be distinguished: the cerebral ganglion and pedal ganglion fuse to a large ganglionic mass on either side of the head. From the left cerebral ganglion a ganglionic streak emanates, but does not connect to the supraintestinal ganglion. The supraintestinal ganglion is connected to the pedal ganglion and the osphradial ganglion in the mantle cavity. In Fig. 3C,D a submodel of P1 is shown. All organs inside the head are compressed in a craniad direction. The odontophor is only about 1/3 of its usual size and the the curvature of the radula is increased. The supraintestinal ganglion is shoved craniad and now positioned laterally of the left cerebral ganglion. This compression seems to be caused by the columellar muscle which curves upward too much and thus takes up space that is usually occupied by nerves, radula, and odontophor. Unlike in C1, the osphradial ganglion in P1 is not positioned above the head. The osphradium and its ganglion originate on the right lateral side of the visceral sac. As was shown by Marschner *et al.* (2012; 2013), differential growth of shell gland and mantle edge stops and the visceral sac rotates vertically by about 90°. It is this rotation that makes the osphradium and its ganglion end up on the left lateral side of the visceral sac slightly above the mantle edge and shell gland. This kind of visceral sac rotation does not correspond to ontogenetic torsion - as mentioned, these snails remain untorted. P2, shown in Fig. 3E,F, is the older of the two sluggish snails. Here, the odontophor is also compressed and the radula is bent even stronger, crudely resembling the shape of a bass clef. The radula enwinds the odontophor in a way that the usually most distal part, the radular sac, is now positioned on the oral pole of the head and not on the aboral one. The odontophor in P2 is not surrounded by the ganglia like in C1 (Fig. 3A,B), but is pushed in front of them along with the radula. Like in P1, the columellar muscle in

P2 does not curve backwards but pushes the organs in the head forwards. This effect is amplified by a protrusion of the visceral sac (not shown in Fig. 3E,F, see histological section in Fig. 1C, protrustion marked by asterisk). Osphradium and osphradial ganglion are again positioned on the ventral side of the visceral sac like in P1, in this case even beneath the digestive gland (Fig. 1D).

Comparing Fig. 4A, depicting the control situation, and Fig. 4B, depicting the nervous system in the untorted individual, the difference between the two arrangements of this organ is quite striking. The nervous system of the sluggish snail is compressed along the middle axis in a way that visceral ganglion and supraintestinal ganglion are located in the same plane. However, a closer inspection reveals that the general bauplan of the two nervous systems is essentially the same. During embryogenesis of *M. cornuarietis* two intestinal ganglia develop on either side of the larval stomach (details will be explained in the following section of this paper). During torsion, these ganglia change sides and the one which has moved to the right side of the body, the subintestinal ganglion, fuses with the right pleuro-pedal ganglionic mass, later only called pedal ganglion. In Ampullariidae, this fusion leads to a loss of the connective between right pleuro-pedal ganglion and subintestinal ganglion, thus obscuring the crossing of the pleuro-visceral connectives and, therefore, the classical form of streptoneury even though streptoneury in its broadest sense has been established in this snail family (for a detailed description see Demian and Yousif, 1975). Because of this, only the supraintestinal nerve can be clearly seen, the subintestinal nerve is too closely associated with the pedal commissure. In both $PtCl_2$-exposed and control adult snails, P2 and C1, the seperate intestinal ganglia can be seen on the left side of the body and in both cases the connection between supraintestinal ganglion and right pedal ganglion, the supraintestinal nerve is present. The nervous system of P2 is in a "post-torsional" arrangement even though ontogenetic torsion was experimentally prevented. Views (from caudal to cranial) of the nervous systems of P1 and P2 are shown in Figs. 4C and D. Also here, the "post-torsional" and thus streptoneurous condition can be observed in both untorted individuals. Nevertheless, some individual

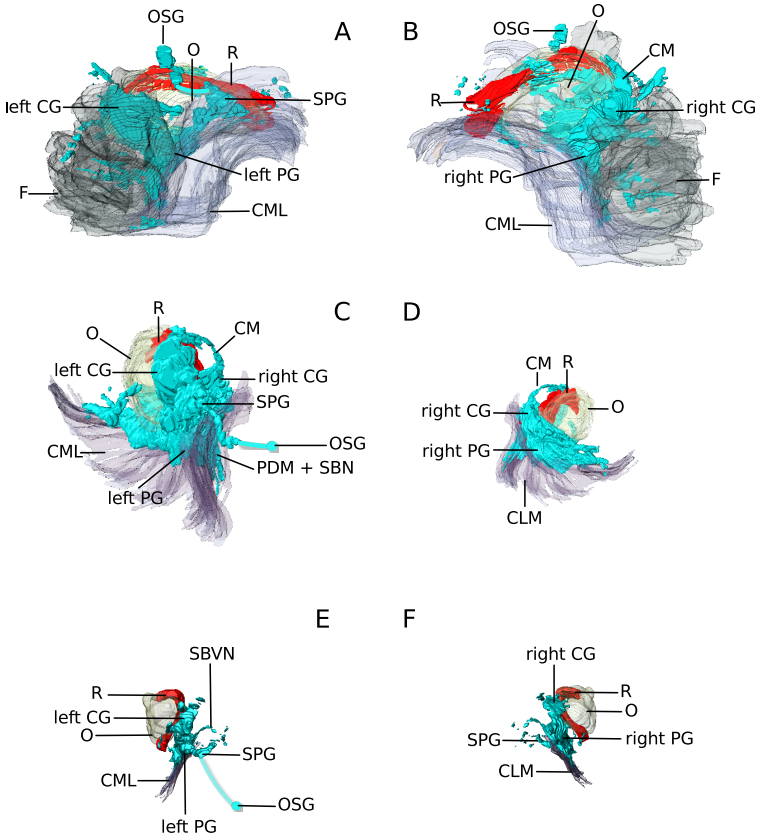

Fig. 3: Submodels of C1, P1 and P2 showing the odontophor, the radula, the columellar muscle, and the nervous system; A: C1, left lateral view, the connection between supraintestinal ganglion (SPG) and osphradial ganglion was added by hand on the basis of histological eidence; B: C1, right lateral view; C: P1, left lateral view, osphradial ganglion and its connection with the supraintestinal ganglion were added by hand; D: P1, right lateral view; E: P2, left lateral view, osphradial ganglion and its connection with the supraintestinal ganglion were added by hand; F: P2, right lateral view; CG, cerebral ganglion; CM, cerebral commissure; CML, columellar muscle; F, foot; O, odontophor; OSG, osphradial ganglion; PDM, pedal commissure; PG, pedal ganglion; SBN, subintestinal nerve; SBVN, subintestinal-visceral connective; SPG, supraintestinal ganglion; TN, tentacle

peculiarities exist. In P1 (Fig. 4C), the right cerebral ganglion is pushed behind and almost beneath the odontophor and thus shoved “into” the right pedal ganglion. This also is due to the undirected growth of the columellar muscle in this individual. In P2 (Fig. 4D), the supraintestinal nerve loops above the oesophagus but is pushed craniad which results in a position in

which this nerve is attached to the right cerebral ganglion. The location of fusion with the pedal ganglion is positioned only marginally proximal of the connection of the cerebral ganglion with the pedal ganglion. This connection between cerebral and pedal ganglion is marked with "Connection PG/CG" (in Fig. 4D). The large ganglionic mass on the right ventro-lateral side is indeed only the right pleuro-pedal ganglionic mass and the right cerebral ganglion remains rather small and compressed.

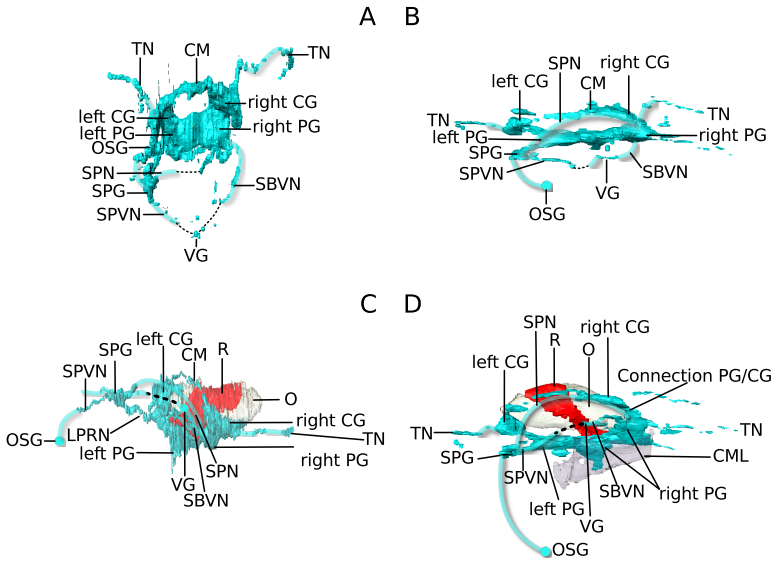

Fig. 4: Submodels of C1, P1 and P2 showing either the nervous system or the nervous system with odontophor and radula; A: Nervous system of C1, dorsal view; B: P2, dorsal view, tentacles, supraintestinal nerve, subintestinal-visceral connective, supraintestinal-visceral connective, osphradial ganglion and its connection to the supraintestinal ganglion were added by hand on the basis of histological evidence; C: Submodel of P1, cranial view, supraintestinal nerve, visceral ganglion, subintestinal-visceral connective, osphradial ganglion and its connection to the supraintestinal ganglion were corrected by hand on the basis of histological evidence; D: P2, cranial view, supraintestinal nerve, tentacle, supraintestinal-visceral and subintestinal-visceral connectives, visceral ganglion, osphradial ganglion and its connection to the supraintestinal ganglion were added by hand on the basis of histological evidence; CG, cerebral ganglion; CM, cerebral commissure; LPRN, left zygosis; O, odontophor; OSG, osphradial ganglion; PG, pedal ganglion; R, radula; SBVN, subintestinal-visceral connective; SPG, supraintestinal ganglion; SPVN, supraintestinal-visceral connective; TN, tentacle; VG, visceral ganglion

Development of the nervous system in untorted and "normal" *M. cornuarietis*

Examinations of embryos incubated with anti-FMRFamide and anti-tubulin antibodies showed little specific staining and the results are not shown. Thus, in the following, we exclusively focus on serotonin-like immunoreactivity in controls and Pt^{2+}-exposed embryos. The application of an extended clearing using the Sca*l*eB4-mixture proved to be essential for the visualization of the stained structures. Fig. 5 shows the 3D reconstructions of a control embryo (Fig. 5A,B) and a Pt^{2+}-exposed embryo (Fig. 5C,D).

The 3D reconstructions of the control embryo (Fig. 5 A,B) show almost all elements of the nervous system of *M. cornuarietis* that should be present at that age according to Demian and Yousif (1975). Both cerebral and pedal ganglia can be seen although the two connections between them, the cerebro-pedal connective and the cerebro-pleural connective, are only partially stained. There is also a gap between the subintestinal ganglion and the pleuro-pedal ganglionic mass and the fusion between these two ganglionic masses cannot be seen. The connection between the left pleuro-pedal ganglionic mass and the supraintestinal ganglion is also not stained. The connection between the supraintestinal ganglion and the right pleuro-pedal ganglionic mass, the supraintestinal nerve, which crosses from the left side to the right side, was only partially stained. This connective was added by hand in Fig. 5A to show the visceral loop more clearly. Fig. 5 C,D shows a nine days old platinum-exposed sluggish embryo and the structures that are labeled with an anti-serotonin antibody. The structure is much less clear than in the control. The only elements that can be distinctly identified are the pedal ganglia. The visceral ganglion can also be seen in the posterior region of the embryo although its position is not completely clear. On the right side of the embryo there is a second ganglionic mass associated with the pleuro-pedal ganglion: this is probably the subintestinal ganglion that is fused with this complex. This interpretation is supported by the presence of a connective between this ganglion and the pleuro-pedal ganglionic mass on the left side. This connective is most probably the subintestinal nerve

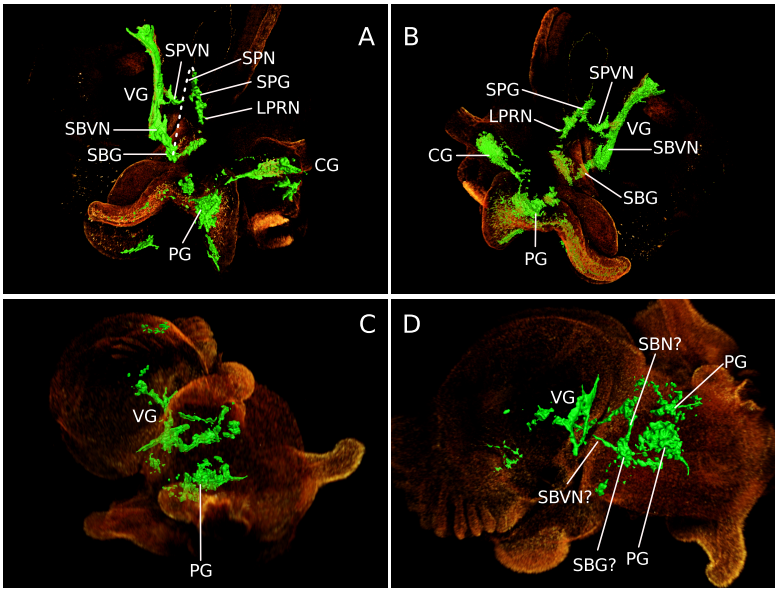

Fig. 5[13]: 3D reconstructions of *Marisa cornuarietis* embryos, anti-serotonin labeled structures are coloured green; A: Control embryo at the age of 5 days, right lateral view, theoretical position of the supraintestinal nerve was added by hand (white dotted line); B: same individual as in A, right lateral view; C: Pt^{2+}-exposed embryo at the age of 9 days, right dorso-lateral view; D: same individual as in C, left dorso-lateral view; CG, cerebral ganglion; LPRN, left zygosis; PG, pedal ganglion; SBG, subintestinal ganglion; SBN, subintestinal nerve; SBVN, subintestinal-visceral connective; SPG, supraintestinal ganglion; SPN, supraintestinal nerve; SPVN, supraintestinal-visceral connective; VG, visceral ganglion

that connects the subintestinal ganglion to the left pleuro-pedal ganglion. In our study we could thoroughly reconstruct the nervous system of the control embryos. As well, we were able to label the neural tissue in Pt^{2+}-exposed embryos but, due to the untypical mode of development, it was not possible to doubtlessly specify some of the ganglia.

Discussion

We have recently described how platinum can disrupt and alter the embryonic development of the ramshorn snail. Bivalent platinum regularly stop stop the growth of both shell gland and mantle edge and thus prevent the

[13]Die Bilder stammen von Simon Schwarz.

formation of an external mantle and an external shell (Marschner *et al.*, 2012; 2013). During these investigations we noticed that in Pt^{2+}-exposed snails a horizontal rotation of the visceral sac does not take place. However, our examinations of the nervous system of adult sluggish snails showed that, despite the lack of this horizontal rotation, undoubtedly a streptoneurous arrangement of the nervous system was established: on the left side of the body the supraintestinal ganglion can be seen as a distinct ganglionic mass from which emanates the supraintestinal nerve, which connects the supraintestinal ganglion with the right pleuro-pedal ganglionic mass. This is what has been described as the crossing of the pleurovisceral connectives (streptoneury, chiastoneury), i. e., the crossing of the nerves that connect the left pleural ganglion to the subintestinal ganglion on the right side and the right pleural ganglion to the supraintestinal ganglion on the left side (e.g. Raven, 1966). In *Marisa*, this crossing of the two nerves is obscured because the subintestinal ganglion is fused with the right pleuro-pedal ganglionic mass and the second part of this crossing, the subintestinal nerve, "disappears" (Demian and Yousif, 1975). What makes the interpretation of the 3D models difficult, is the deformation of not only the nervous system but of all internal organs caused by the undirected growth of the columellar muscle. This is especially spectacular in P2, the oldest snail, in which the radula is almost folded back on itself, nearly forming a loop.

However, despite this compression of the nervous system, the overall arrangement is clearly identifiable in adults. Unfortunately, the 3D models of the nervous systems of the embryos are not so easy to interpret. In the control, the structure of the nervous system can be seen quite well, although there are gaps in which there was no staining, maybe because serotonin was not expressed there in these life stages. Those gaps were even more numerous in the platinum-exposed embryos. In these specimens, only parts of the nervous system could be recognized and the overall structure is almost totally obscured. There are, however, structures that can be interpreted as a complex consisting of the subintestinal ganglion fused with the right pleuro-pedal ganglionic mass on the right side of the embryo. Despite all the gaps, this observation is indicative for an arrangement of the nervous

system in which the right intestinal ganglion is fused with the right pleuropedal ganglionic mass as it is normal for Ampulariidae (Demian and Yousif, 1975). Although the 3D models of the Pt^{2+}-exposed embryos are difficult to interpret, they definitely do not contradict the results of the investigations of the adult snails. Furthermore, it is likely that the position of ganglia has been influenced by the growth of the columellar muscle even in very young Pt^{2+}-exposed individuals. Despite the uncertainties remaining for early neurogenesis, in *Marisa* it has become clear that in adult non-torted snails both intestinal ganglia are in their "normal" positions, which means, that either this exchange of positions of the two intestinal ganglia can occur without the rotation of the visceral sac or the two ganglia do not exchange their positions but simply "assimilate" each other's identity, which is only defined on the basis of the ganglia's positions anyway. Whichever possibility is true, our results show that, at least in *Marisa*, ontogenetic torsion, the horizontal rotation of the visceral sac, is not necessary for the nervous system to establish a physical arrangement that is supposed to be caused by torsion (Haszprunar, 1988).

However, although the theory says that the crossing of the pleurovisceral connectives is caused by torsion, there are several accounts on embryonic development in snails showing that the situation is not so simple. Raven (1966) summarized the details of neurogenesis of different gastropods and stated that in *Acmaea*, *Haliotis*, *Trochus*, and *Littorina* the parietal and visceral ganglia were only formed after ontogenetic torsion and that the connections between the intestinal ganglia and the opposite pleural ganglia were emanated from their definite positions. Page (2003) investigated ontogenetic torsion in different species and did not only find that the visceropallium does not always rotate as a single unit, but that a full streptoneurous condition can be found in embryos of *Trichotropis cancellata*, in which the visceropallium has only rotated by 90°. The available data on ontogenetic torsion are rather scanty and show that there is a quite high degree in variability between different gastropod groups (Jenner, 2006) which caused Page (2006) to suggest an alternative hypothesis called "asymmetry hypothesis". This hypothesis explains the development of what is considered as the post-torsional

arrangement of the snails' nervous system, including streptoneury, without the need for a horizontal rotation.

Previous studies have shown that parts of the nervous system that the visceral loop consists of, may develop before, during, or after torsion. Additionally, in Pt^{2+}-exposed *M. cornuarietis* we find streptoneury in individuals whose visceropallium did not undergo any horizontal rotation at all. All these facts raise the question how the structure of the nervous system in gastropods is determined. Does the crossing of the pleurovisceral connectives necessarily have to be caused passively by a movement of their surrounding tissues? Or could the growth of the pleurovisceral connectives rather be directed by chemical signals independent from mechanical constraints? Haszprunar (1988) speculated that cytochemical markers might lead the growth of the pleurovisceral nerve connectives to their destinations although, in his opinion at that time, this mechanism would not influence the dependence of torsion and streptoneury. Indeed, chemical components, nerve growth factors, can influence the survival of neurons or induce and inhibit neurite outgrowth (Berg, 1984). Hermann *et al.* (2000) found a homolog of an epidermal growth factor in *Lymnaea stagnalis* that can induce neurite outgrowth in vitro and that may also play a role during the development of the nervous system. Another group of molecules that may act as morphogens and regulators of neurogenesis are neurotransmitters (Buznikov *et al.*, 1996). In isolated *Helisoma* nerve cells, serotonin can inhibit neurite outgrowth (Haydon *et al.*, 1987) and changing the serotonin content in developing *Helisoma* embryos leads to alterations in the development of specific neurons (Goldberg and Kater, 1989).

Croll and Voronezhskaya (1996) investigated neurogenesis in *Lymnaea* and observed very early appearing nerve cells, which are positioned in the posterior region of the body and that seem to serve as a scaffold for the developing ganglia and connectives. Dickinson *et al.* (1999; 2000) also observed very early developing nervous structures that may serve as "guidances" for the developing adult central nervous system in *Crepidula fornicata* (1999) and *Aplysia californica* (2000). In gastropods in which the pleurovisceral nerve connectives develop only after torsion, such nerve structures, which are al-

ready present during torsion, may preserve the streptoneurous structure for the adult central nervous system that develops later (Dickinson *et al.*, 2000). In our experiments with *M. cornuarietis*, the youngest embryos we investigated were four days old, but we did not observe similar staining patterns when we investigated FMRFamide. Whether this is due to the advanced age of the embryos compared to the stages in which such early neurons have been observed, however, is unclear: it is also possible that such early nervous structures are simply not present in *Marisa*.

Still, many unanswered questions remain regarding the development of the nervous system in experimentally untorted *M. cornuarietis*. However, our investigations have shown that a horizontal rotation of the visceral sac, the hallmark feature for ontogenetic torsion, is not necessary for a streptoneurous arrangement of the central nervous system to develop in adults. This shows, along with many other studies that have been conducted, that there is a need for alternative explanations for streptoneury, e.g. growth factors or other morphogens, that are expressed independently of the movements of other organs in ontogeny and that guide the connectives to their respective destinations.

References

Berg, D. K. (1984). New neuronal growth factors. *Annual Review of Neuroscience*, 7(1):149–170.

Bieler, R. (1992). Gastropod Phylogeny and Systematics. *Annual Review of Ecology and Systematics*, 23:311–338.

Buznikov, G. A., Shmukler, Y. B., and Lauder, J. M. (1996). From oocyte to neuron: Do neurotransmitters function in the same way throughout development? *Cellular and Molecular Neurobiology*, 16(5):533–559.

Cason, J. E. (1950). A rapid one-step Mallory-Heidenhain stain for connective tissue. *Biotechnic & Histochemistry*, 25(4):225–226.

Croll, R. and Voronezhskaya, E. E. (1996). Early elements in gastropod neurogenesis. *Developmental Biology*, 173(1):344–347.

Croll, R. P. (2000). Insights into early molluscan neuronal development through studies of transmitter phenotypes in embryonic pond snails. *Microscopy Research and Technique*, 49(6):570–578.

Demian, E. S. and Yousif, F. (1975). Embryonic development and organogenesis in the snail *Marisa cornuarietis* (Mesogastropoda: Ampullariidae). V. Development of the nervous system. *Malacologia*, 15(1):29–42.

Dickinson, A. J., Croll, R. P., and Voronezhskaya, E. E. (2000). Development of embryonic cells containing serotonin, catecholamines, and FMRFamide-related peptides in *Aplysia californica*. *The Biological Bulletin*, 199(3):305–315.

Dickinson, A. J. G., Nason, J., and Croll, R. P. (1999). Histochemical localization of FMRFamide, serotonin and catecholamines in embryonic *Crepidula fornicata* (Gastropoda, Prosobranchia). *Zoomorphology*, 119(1):49–62.

Garstang, W. (1928). The origin and evolution of larval forms. *Nature*, 122:366.

Goldberg, J. and Kater, S. (1989). Expression and function of the neurotransmitter serotonin during development of the *Helisoma* nervous system. *Developmental Biology*, 131(2):483–495.

Hama, H., Kurokawa, H., Kawano, H., Ando, R., Shimogori, T., Noda, H., Fukami, K., Sakaue-Sawano, A., and Miyawaki, A. (2011). Scale: a chemical approach for fluorescence imaging and reconstruction of transparent mouse brain. *Nature Neuroscience*, 14(11):1481–1488.

Haszprunar, G. (1988). On the origin and evolution of major gastropod groups, with special reference to the Streptoneura. *Journal of Molluscan Studies*, 54(4):367–441.

Haydon, P. G., McCobb, D. P., and Kater, S. B. (1987). The regulation of neurite outgrowth, growth cone motility, and electrical synaptogenesis by serotonin. *Journal of Neurobiology*, 18(2):197–215.

Hermann, P. M., Kesteren, R. E. v., Wildering, W. C., Painter, S. D., Reno, J. M., Smith, J. S., Kumar, S. B., Geraerts, W. P. M., Ericsson, L. H., Smit, A. B., Bulloch, A. G. M., and Nagle, G. T. (2000). Neurotrophic actions of a novel molluscan epidermal growth factor. *The Journal of Neuroscience*, 20(17):6355–6364.

Jackson, A. R., MacRae, T. H., and Croll, R. P. (1995). Unusual distribution of tubulin isoforms in the snail *Lymnaea stagnalis*. *Cell and Tissue Research*, 281(3):507–515.

Jenner, R. A. (2006). Challenging received wisdoms: Some contributions of the new microscopy to the new animal phylogeny. *Integrative and Comparative Biology*, 46(2):93–103.

Kempf, S. C. and Page, L. R. (2005). Anti-tubulin labeling reveals ampullary neuron ciliary bundles in opisthobranch larvae and a new putative neural structure associated with the apical ganglion. *The Biological Bulletin*, 208(3):169–182.

Marschner, L., Staniek, J., Schuster, S., Triebskorn, R., and Köhler, H.-R. (2013). External and internal shell formation in the ramshorn snail *Marisa cornuarietis* are extremes in a continuum of gradual variation in development. *BMC Developmental Biology*, 13(1):22.

Marschner, L., Triebskorn, R., and Köhler, H.-R. (2012). Arresting mantle formation and redirecting embryonic shell gland tissue by platinum^{2+} leads to body plan modifications in *Marisa cornuarietis* (Gastropoda, Ampullariidae). *Journal of Morphology*, 273(8):830–841.

Osterauer, R., Marschner, L., Betz, O., Gerberding, M., Sawasdee, B., Cloetens, P., Haus, N., Sures, B., Triebskorn, R., and Köhler, H.-R. (2010). Turning snails into slugs: induced body plan changes and formation of an internal shell. *Evolution & Development*, 12(5):474–483.

Page, L. R. (2003). Gastropod ontogenetic torsion: Developmental remnants of an ancient evolutionary change in body plan. *Journal of Experimental Zoology*, 297B(1):11–26.

Page, L. R. (2006a). Early differentiating neuron in larval abalone (*Haliotis kamtschatkana*) reveals the relationship between ontogenetic torsion and crossing of the pleurovisceral nerve cords. *Evolution & Development*, 8(5):458–467.

Page, L. R. (2006b). Modern insights on gastropod development: Reevaluation of the evolution of a novel body plan. *Integrative and Comparative Biology*, 46(2):134 –143.

Raven, C. P. (1966). *Morphogenesis - The analysis of molluscan development*. Pergamon Press, Oxford.

Schirling, M., Bohlen, A., Triebskorn, R., and Köhler, H.-R. (2006). An invertebrate embryo test with the apple snail *Marisa cornuarietis* to assess effects of potential developmental and endocrine disruptors. *Chemosphere*, 64(10):1730–1738.

Voronezhskaya, E. E., Nezlin, L. P., Odintsova, N. A., Plummer, J. T., and Croll, R. P. (2008). Neuronal development in larval mussel *Mytilus trossulus* (Mollusca: Bivalvia). *Zoomorphology*, 127(2):97–110.

Wanninger, A. and Haszprunar, G. (2003). The development of the serotonergic and FMRF-amidergic nervous system in *Antalis entalis* (Mollusca, Scaphopoda). *Zoomorphology*, 122(2):77–85.

Yonge, C. M. (1947). The pallial organs in the aspidobranch Gastropoda and their evolution throughout the Mollusca. *Philosophical Transactions of the Royal Society of London. Series B, Biological Sciences*, 232:443–518.

Kapitel 5: Quantifikation der Hsp70-Level von bei unter Normalbedingungen gehaltenen sowie gegenüber Platin^{2+} exponierten Embryonen von *Marisa cornuarietis* bei 26 °C und 29 °C[14]

Leonie Hannig, Heinz-R. Köhler

Einleitung

Stressproteine erfüllen im Organismus die wichtige Aufgabe, die korrekte Proteinfaltung zu unterstützen (Gething und Sambrook, 1992). Hitzestress, Schwermetalle und andere proteotoxische Bedingungen oder Substanzen führen daher zu einer Induktion von Stressproteinen (Gupta *et al.*, 2010). Stressproteine spielen jedoch auch eine bedeutende Rolle bei der Embryonalentwicklung von Organismen. Sie können die Entwicklung stabilisieren und dabei genetische Variabilität unterdrücken (Rutherford und Lindquist, 1998; Queitsch *et al.*, 2002). Eine Induktion von Stressproteinen, wie z.B. Hsp70, während der Embryonalentwicklung kann die Schädigung des sich entwickelnden Organismus durch teratogene Substanzen abmildern. Isaenko *et al.* (2002) konnten zeigen, dass eine Erhöhung des Hsp70-Gehalts bei *Drosophila melanogaster* die Wirkung der Spindelgifte Vinblastin and Colchicin reduzieren kann. Die protektive Wirkung eines erhöhten Hsp70-Gehalts konnte ebenfalls bei gegenüber Arsen exponierten Mausembryonen und menschlichen Zellen beobachtet werden (Hunter und Dix, 2001; Barnes *et al.*, 2002).

[14] Unveröffentlichte Daten

Embryotests mit *Marisa cornuarietis* konnten zeigen, dass die Wirkung von Platin^{2+} bei einer Temperaturerhöhung um $2-4\,^{\circ}$C deutlich schwächer ist, als bei der konventionell verwendeten Temperatur von $26\,^{\circ}$C. Bei leicht erhöhten Temperaturen traten Schnecken mit sogenannten „Teilschalen“ auf. Diese Teilschalen waren zum Teil internalisiert, also vom Mantel bedeckt, und zum Teil extern, also unbedeckt. Bei niedrigeren Platin^{2+}-Konzentrationen im Testmedium konnten solche Teilschalen nicht beobachtet werden (Osterauer *et al.*, 2010a). Um zu ermitteln, ob die beobachtete „Abschwächung“ der Platinwirkung bei erhöhten Temperaturen auf eine Induktion von Stressproteinen zurückzuführen ist, wurden Embryonen von *Marisa cornuarietis* bei $26\,^{\circ}$C und $29\,^{\circ}$C gegenüber Platin exponiert, der Gehalt an Hsp70 ermittelt und mit dem der jeweiligen Kontrollembryonen verglichen.

Material und Methoden

Um eine genügende Anzahl an Embryonen für die Stressproteinanalyse zu gewinnen, wurden für die beiden Kontrollen (bei $26\,^{\circ}$C bzw. $29\,^{\circ}$C) jeweils 4 Petrischalen mit Aquarienwasser gefüllt und je 25 frisch abgelegte Eier eingesetzt. Für die Platinexposition bei $29\,^{\circ}$C wurden 8 Petrischalen und für die Platinexposition bei $26\,^{\circ}$C 12 Petrischalen mit Platinchloridlösung (200 μL/L) gefüllt und jeweils 30 Eier eingesetzt. Die Petrischalen wurden bei den jeweiligen Temperaturen in Klimaschränken bei einem Hell-Dunkel-Rhythmus von 12:12 Stunden aufbewahrt. Nach 9 Tagen wurde die Embryonen mit Kanülen aus den Eihüllen entfernt und in mit Extratktionsgemisch aus 980 μl konzentriertem Extraktionspuffer gefüllte Reaktionsgefäße überführt (80mM Kaliumacetat, 5mM Magnesiumacetat, 20mM Hepes, aufgefüllt auf 500 ml mit Aqua bidest) + 20 μl Proteasehemmer, wobei 40 μl für die Kontrollen und $29\,^{\circ}$C Platin und 30 μl bei der $26\,^{\circ}$C Platin- Exposition verwendet wurden. Hierbei wurden die Embryonen gepoolt ($26\,^{\circ}$C Kontrolle: 8 Embryonen, $26\,^{\circ}$C Platin: 30 Embryonen, $29\,^{\circ}$C Kontrolle: 8 Embryonen, $29\,^{\circ}$C Platin: 18 Embryonen). Die Embryonen wurden dann auf Eis mit einem Ultraschallgerät homogenisiert und das Homogenat danach 10 Minuten bei $4\,^{\circ}$C und 20000g abzentrifugiert.

Die Gesamtproteinmenge wurde nach Bradford (1976) ermittelt. Jeweils 40 μg Protein wurden auf ein Polyacrylamidgel gegeben und die Proteine elektrophoretisch aufgetrennt sowie auf Nitrocellulosemembranen transferiert. Im Anschluss wurden die Nitrocellulosemembranen mit dem ersten Antikörper (monoklonaler Maus anti-human Hsp70 Antikörper (1 μl Antikörperlösung, 0,5 ml Pferdeserum, 4,5 ml TBS)) inkubiert, gespült und mit einem zweiten, Peroxidase-konjugierten Antikörper inkubiert. Die Banden wurden durch eine Peroxidasefärbereaktion sichtbar gemacht und densitometrisch ausgewertet. Eine detaillierte Beschreibung der Stressproteinanalyse ist bei Osterauer *et al.* (2010a) zu finden.

Ergebnisse

Abb. 1 zeigt die relativen Hsp70-Level der Kontroll-Individuen bei 26 °C und bei 29 °C sowie der gegenüber $Platin^{2+}$ exponierten Embryonen bei ebenfalls 26 °C und 29 °C. Den höchsten Hsp70-Gehalt wiesen die Individuen mit interner Schale, bei 26 °C gegenüber $Platin^{2+}$ exponierten Embryonen auf. Die Kontrollen bei 29 °C zeigten den zweithöchsten Wert, gefolgt von den Kontrollen bei 26 °C. Den niedrigsten Hsp70-Gehalt wiesen die bei 29 °C gegenüber $Platin^{2+}$ exponierten Embryonen mit Teilschalen auf.

Diskussion

Bei 26 °C führt eine Exposition gegenüber $Platin^{2+}$ bei Embryonen von *Marisa cornuarietis* zu einer deutlichen und starken Fehlbildung. Diese Tiere bilden keine äußere, sondern nur eine innere Schale (Osterauer *et al.*, 2010b; Marschner *et al.*, 2012). Exponiert man die Embryonen jedoch bei einer leicht erhöhten Temperatur, so wird die drastische Wirkung dieses Edelmetalls abgemildert und die Schnecken bilden eine Teilschale, d.h. sie entwickeln sich „normaler“ als bei niedrigeren Temperaturen unter $Platin^{2+}$-Einfluss (Marschner *et al.*, 2013). Die Analyse der jeweiligen Stressproteinlevels ergab jedoch, dass diese Embryonen nicht nur einen weitaus niedrigeren Hsp70-

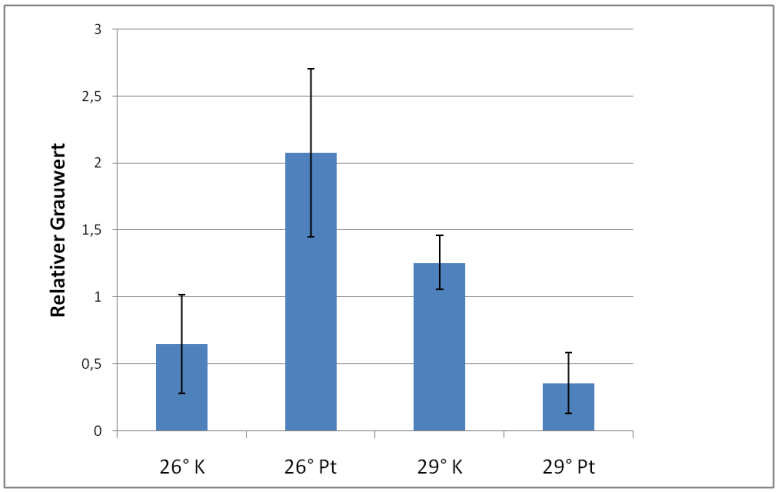

Fig. 1: Relative Hsp70-Gehalte der verschiedenen Testgruppen, Mittlerer Grauwert ± Standardabweichung

Gehalt besaßen als die gegenüber Platin exponierten Embryonen bei 26 °C, sondern sogar den niedrigsten Wert von allen Expositionsgruppen. Die „weniger aberrante“ Schalenentwicklung der bei 29 °C gegenüber Platin^{2+} exponierten Tiere kann also nicht auf einen durch die leichte Temperaturerhöhung induzierten Anstieg des Hsp70-Levels zurückzuführen sein.

Bei den Kontrollen hingegen war eine deutlich erhöhte Hsp70-Induktion bei 29 °C im Vergleich zur Kontrolle bei 26 °C festzustellen. Vergleicht man die Kontrollen mit den Platinexpositionen bei den jeweiligen Temperaturen, so sieht man, dass bei der niedrigeren Temperatur die Schwermetallbelastung zu einer deutlichen Erhöhung des Hsp70-Levels führt, bei der höheren Temperatur jedoch zu einer Erniedrigung. Stressproteine können durch Schwermetalle und Temperaturerhöhungen induziert werden (Gupta *et al.*, 2010; Kiang und Tsokos 1998). Exponiert man die Embryonen gegenüber zwei proteotoxischen Stressoren, sollte der Theorie nach eine deutliche Erhöhung des Hsp70-Gehalts zu beobachten sein. Es ist jedoch oftmals das Gegenteil der Fall, sodass eine Belastung von Organismen durch mehrere Stressoren gleichzeitig wie im vorliegenden Fall zum geringsten Hsp70-Gehalt von allen Expositionsgruppen führt. Es ist jedoch bekannt, dass die Hsp70 Antwort auf Stress einer Optimumskurve folgt (Köhler *et al.*, 2001). Der Hsp70-Gehalt

steigt mit steigendem proteotoxischen Stress an, nimmt jedoch bei zu starker Belastung wieder ab. Betrachtet man jedoch die gegenüber erhöhter Temperatur plus Platin^{2+} exponierten Embryonen, so ist festzustellen, dass der geringe Hsp70-Gehalt nicht auf eine Überlastung des Stressprotein-Systems zurückzuführen sein kann, da sich die Embryonen nicht nur besser entwickeln als bei 26 °C, sondern auch die Mortalität geringer ist. Warum jedoch bei 29 °C, im Gegensatz zu 26 °C, der Hsp70-Gehalt bei Schwermetallbelastung niedriger ist als bei der Kontrolle, lässt sich ohne weitere Untersuchungen nicht erklären.

Neben Hsp70 gibt es noch weitere induzierbare Stressproteine. Hsp90 stabiliert Entwicklungsprozesse (Rutherford und Lindquist, 1998; Queitsch *et al.*, 2002) und kann daher ebenfalls verantwortlich für die Abschwächung der Platin^{2+}-Wirkung bei erhöhter Temperatur sein. Ein weiterer möglicher Mechanismus ist die Entgiftung von Platin durch Metallothioneine, die ebenfalls durch Temperaturerhöhungen induziert werden können (Serafim *et al.*, 2002; Piano *et al.*, 2004). Auch zu diesem Diskussionspunkt sind weitere Untersuchungen zur abschließenden Klärung der Frage nötig.

Literatur

Barnes, J., Collins, B., Dix, D., und Allen, J. (2002). Effects of heat shock protein 70 (Hsp70) on arsenite-induced genotoxicity. *Environmental and Molecular Mutagenesis*, 40(4):236–242.

Bradford, M. M. (1976). A rapid and sensitive method for the quantitation of microgram quantities of protein utilizing the principle of protein-dye binding. *Analytical Biochemistry*, 72(1–2):248–254.

Gething, M.-J. und Sambrook, J. (1992). Protein folding in the cell. *Nature*, 355(6355):33–45.

Gupta, S. C., Sharma, A., Mishra, M., Mishra, R. K., und Chowdhuri, D. K. (2010). Heat shock proteins in toxicology: How close and how far? *Life Sciences*, 86(11–12):377–384.

Hunter, E. S. und Dix, D. J. (2001). Heat shock proteins Hsp70-1 and Hsp70-3 are necessary and sufficient to prevent arsenite-induced dysmorphology in mouse embryos. *Molecular Reproduction and Development*, 59(3):285–293.

Isaenko, O. A., Karr, T. L., und Feder, M. E. (2002). Hsp70 and thermal pretreatment mitigate developmental damage caused by mitotic poisons in *Drosophila*. *Cell Stress & Chaperones*, 7(3):297–308.

Kiang, J. G. und Tsokos, G. C. (1998). Heat shock protein 70 kDa: molecular biology, biochemistry, and physiology. *Pharmacology & Therapeutics*, 80(2):183–201.

Köhler, H.-R., Bartussek, C., Eckwert, H., Farian, K., Gränzer, S., Knigge, T., und Kunz, N. (2001). The hepatic stress protein (hsp70) response to interacting abiotic parameters in fish exposed to various levels of pollution. *Journal of Aquatic Ecosystem Stress and Recovery*, 8(3-4):261–279.

Marschner, L., Staniek, J., Schuster, S., Triebskorn, R., und Köhler, H.-R. (2013). External and internal shell formation in the ramshorn snail *Marisa cornuarietis* are extremes in a continuum of gradual variation in development. *BMC Developmental Biology*, 13(1):22.

Marschner, L., Triebskorn, R., und Köhler, H.-R. (2012). Arresting mantle formation and redirecting embryonic shell gland tissue by platinum^{2+} leads to body plan modifications in *Marisa cornuarietis* (Gastropoda, Ampullariidae). *Journal of Morphology*, 273(8):830–841.

Osterauer, R., Köhler, H.-R., und Triebskorn, R. (2010a). Histopathological alterations and induction of Hsp70 in ramshorn snail (*Marisa cornuarietis*) and zebrafish (*Danio rerio*) embryos after exposure to $PtCl_2$. *Aquatic Toxicology*, 99(1):100–107.

Osterauer, R., Marschner, L., Betz, O., Gerberding, M., Sawasdee, B., Cloetens, P., Haus, N., Sures, B., Triebskorn, R., und Köhler, H.-R. (2010b). Turning snails into slugs: induced body plan changes and formation of an internal shell. *Evolution & Development*, 12(5):474–483.

Piano, A., Valbonesi, P., und Fabbri, E. (2004). Expression of cytoprotective proteins, heat shock protein 70and metallothioneins, in tissues of *Ostrea edulis* exposed to heat andheavy metals. *Cell Stress & Chaperones*, 9(2).

Queitsch, C., Sangster, T. A., und Lindquist, S. (2002). Hsp90 as a capacitor of phenotypic variation. *Nature*, 417(6889):618–624.

Rutherford, S. L. und Lindquist, S. (1998). Hsp90 as a capacitor for morphological evolution. *Nature*, 396(6709):336–342.

Serafim, M., Company, R., Bebianno, M., und Langston, W. (2002). Effect of temperature and size on metallothionein synthesis in the gill of *Mytilus galloprovincialis* exposed to cadmium. *Marine Environmental Research*, 54(3–5):361–365.

Publikationsliste

Originalpublikationen in internationalen Fachzeitschriften

- Osterauer, R., **Marschner, L.**, Betz, O., Gerberding, M., Sawasdee, B., Cloetens, P., Haus, N., Sures, B., Triebskorn, R., Köhler, H.-R., 2010. Turning snails into slugs: induced body plan changes and formation of an internal shell. *Evol. Dev.* 12, 474–483

- **Marschner, L.**, Triebskorn, R., Köhler, H.-R., 2012. Arresting mantle formation and redirecting embryonic shell gland tissue by platinum^{2+} leads to body plan modifications in *Marisa cornuarietis* (Gastropoda, Ampullariidae). *J. Morphol.* 273, 830–841

- **Marschner, L.**, Staniek, J., Schuster, S., Triebskorn, R., Köhler, H.-R., 2013. External and internal shell formation in the ramshorn snail *Marisa cornuarietis* are extremes in a continuum of gradual variation in development. *BMC Dev. Biol.* 13, 22.

Unveröffentlichte Manuskripte

- **Hannig, L.**, Schwarz, S., Köhler, H.-R. No torsion required for streptoneury in the ampullariid snail *Marisa cornuarietis*. Geplante Einreichung bei *PNAS*

Vorträge

- **Marschner, L.** 2011. Arresting mantle formation and redirecting embryonic shell gland tissue by platinum^{2+} leads to body plan modifications in *Marisa cornuarietis* (Gastropoda, Ampullariidae). *Meeting of Students in Evolution and Ecology, Uni Tübingen*

- **Marschner, L.**, Staniek, J., Schuster, S., Triebskorn, R., Köhler, H.-R. 2013. Platinum-induced shell internalization in the ramshorn snail *Marisa cornuarietis* (Ampullariidae). *World Congress of Malacology, Azores*

- **Hannig, L.**, Schwarz, S., Köhler, H.-R. Die Streptoneuriebei Paradiesschnecken setzt keine ontogenetische Torsion voraus. *6. Graduiertentreffen der Fachgruppe Morphologie der Deutschen Zoologischen Gesellschaft*

Posterbeiträge

- **Marschner, L.**, Osterauer, R., Betz, O., Gerberding, M., Cloetens, P., Sures, B., Triebskorn, R., Köhler, HR. 2009. Platinum-induced internalization of shell formation in snails. *Comparative Biochemistry And Physiology A - Molecular & Integrative Physiology, 26th Congress of the European-Society-of-Comparative-Biochemistry-and-Physiology*

- Köhler, H. -R., Osterauer, R., **Marschner, L.**, Mckee, M., Betz, O., Gerberding, M., Sawasdee, B., Cloetens, P., Haus, N., Sures, B., Triebskorn, R. 2010. *Marisa* topless: What platinum may bring about. *Comparative Biochemistry And Physiology A - Molecular & Integrative Physiology, 27th Congress of the European-Society-of-Comparative-Biochemistry-and-Physiology*

Danksagung

Die hier vorliegende Arbeit wurde in der Abteilung Physiologische Ökologie der Tiere (POEDT) der Universität Tübingen durchgeführt.

Ich danke vor allem Prof Dr. Heinz-R. Köhler herzlichst für seine Unterstützung und Betreuung während der Durchführung und Erstellung dieser Arbeit.

Bei Prof. Dr. Rita Triebskorn und Prof. Dr. James Nebelsick bedanke ich mich für die Betreuung während meiner Arbeit und die Prüfungsabnahme. Für viele Diskussionen und Vorschläge möchte ich mich bedanken bei Prof. Dr. Katja Tielbörger, Prof. Dr. Michal Kucera und besonders bei Prof. Dr. Klaus Harter für die zusätzliche Bereitschaft zur Prüfungsabnahme.
Ich danke Prof. Dr. Oliver Betz für die Benutzung des Rasterelektronenmikroskops und die Möglichkeit Amira zu benutzen. Für die Unterstützung bei den 3D-Modellen bedanke ich mich bei Sebastian Schmelzle.
Allen Kollegen aus dem Graduiertenkolleg Morphologische Variabilität danke ich für die vielen wunderbaren Gesprächsrunden. Danke, DD, Manuel, Anne und Betty!
Ein ganz besonderer Dank geht an die Abteilung Physiologische Ökologie der Tiere, an alle gegenwärtigen und ehemaligen POEDTler, Zivis, Bufdis und Azubis. Ich danke Euch für die Unterstützung im Labor (Steffi, Anna, Andi, Diana), die Versorgung der Tiere (Zivis, Bufdis), Essen (Krisztina), Aufmunterung und Unterhaltung (Alex, Andi, Andrea, Anja, Diana, Irene, Katha, Katja, Krisztina, Lina, Lisa, Maddalena, Matthias, Paul, Raphaela, Sandra, Simon, Steffi und Volker)!

Ich danke meiner Familie und ganz besonders meinem Mann Matthias.